Functional analysis of septins in fission yeast sporulation

(分裂酵母の胞子形成におけるセプチンの機能解析)

Masayuki Onishi

大西雅之

Functional analysis of septins in fission yeast sporulation

（分裂酵母の胞子形成におけるセプチンの機能解析）

Masayuki Onishi

（大西雅之）

CONTENTS

CHAPTER I: GENERAL INTRODUCTIONS

Sporulation

Sporulation of *S. pombe* is a developmental process that includes a number of sequential events [1] (Fig. 1). There are two mating types (h^+ and h^-). When mixture of these cells containing the two mating types are shifted to the nitrogen starvation condition, cell fusion and karyogamy occurs in order to form diploid zygote, which then undergoes pre-meiotic DNA replication, two rounds of meiotic nuclear division, formation of the spore membrane, and maturation of spores [2-5] (Fig. 1). The intracellular cyclic AMP level decreases after nutrient starvation, which induces activation of Ste11p-Mei2p transcription cascade to start two rounds of meiosis to generate four haploid nuclei [6] [7] [8].

At the onset of meiosis II, intracellular double-layered membrane structures termed forespore membranes (FSMs), are formed by docking and fusion of vesicles at the cytoplasmic surface of spindle pole bodies (SPBs). FSMs grow and extend to encapsulate each of four divided nuclei [9] [4] [5] and other essential organelles and a portion of cytosol to become prespores (immature spores). Prespores maturate to spores as spore wall materials are synthesized and deposited into the lumen of the two layers of FSMs. The inner layer of the FSM forms a plasma membrane of the spore. Sporulation is an interesting phenomenon not only because it is an important step of gametogenesis but also because it is a good model for de novo formation of organella and membrane structure.

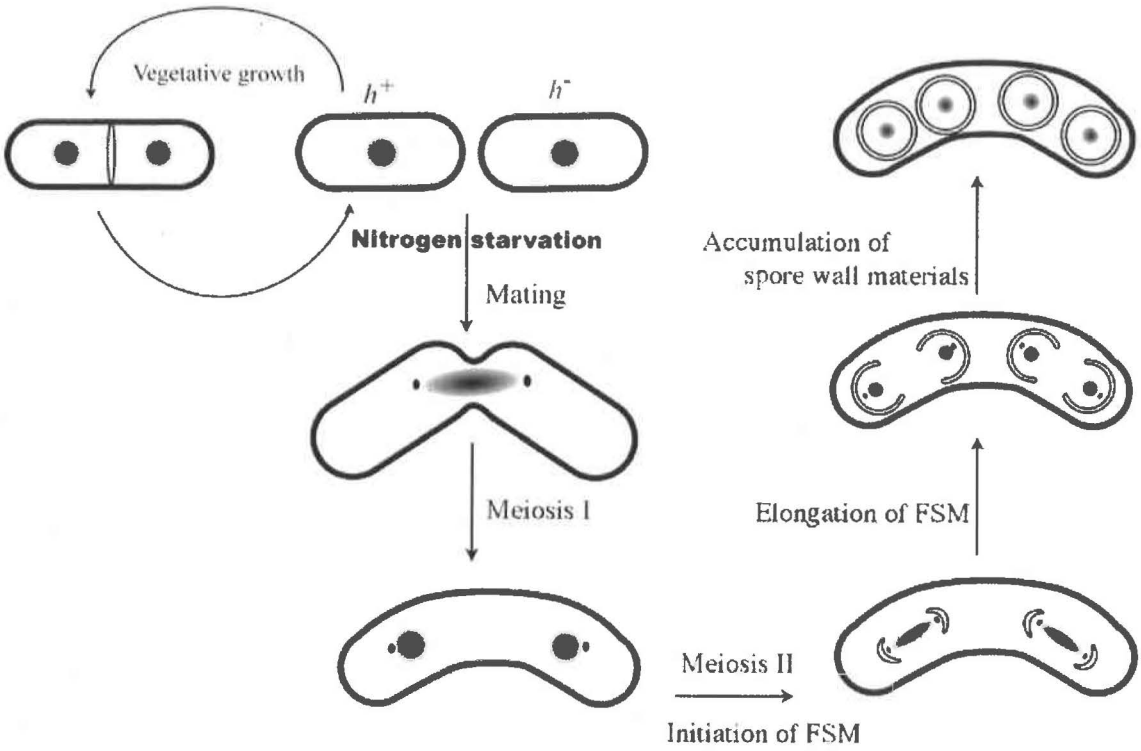

Figure 1 Sporulation of *Shizosaccharomyces pombe*

Formation of forespore membranes: importance of membrane traffic system

Among the sporulation procedure, spore membrane development is a key step to form even-sized spherical spore membranes, each of which correctly harboring a haploid nucleus. In this procedure, assembly, development, orientated extension, and closure of FSMs after engulfing the nuclei should be closely regulated. In FSM formation, it is well established that SPB modification and vesicle trafficking system play important roles. At the metaphase of meiosis II, SPB changes its shape from a compact dot to a crescent [5]. Outer plaque of SPB acquires meiosis specific components of *spo*$^{+}$ gene products, such as Spo13p and Spo15p [10] [1]. This modified outer plaque (MOP) is required for initiation of FSM assembly.

After the MOP formation, an FSM precursor assembles at the cytoplasmic surface of MOP, and then starts its extension. A number of genes in the vesicle trafficking system are known to be responsible for proper development of FSM. After exit from meiosis I, Psy1p, a t-SNARE protein, disappears from the plasma membrane and reappears at the FSM precursor [11]. Psy1p may mediate the docking/fusion of following vesicles containing v-SNAREs to develop the FSM probably in cooperation with a SNAP-25 Sec9p [12], because *psy1*$^{+}$ was identified as multicopy suppressor for *spo3*Δ, a strain defective in FSM development [11]. Several lines of evidence suggest that secretory pathway components are essential to supply vesicles to FSM. Shimoda and his co-workers (Osaka City University) have reported that *spo14*Δ and *spo20*Δ strains fail to deliver membrane from ER and Golgi to FSMs, respectively, resulting in sporulation defective phenotype [13] [14]. *S. cerevisiae* homologs of each gene (*SEC12* and *SEC14,* respectively) are known to be involved in protein transport through ER and Golgi apparatus, supporting the idea that these organelles are major origins of FSMs [15] [16] [17].

On the other hand, I have investigated the role of phosphatidylinositol (PtdIns) 3-kinase during sporulation and found that phosphoinositide-mediated membrane traffic system also contributes to formation and development of FSM [18]. Fission yeast *S. pombe* has a class III PtdIns(3)-kinase gene, *pik3*$^{+}$/*vps34*$^{+}$, that catalyzes PtdIns to produce PtdIns 3-phosphate (PtdIns(3)P) [19] [20]. By the fluorescence and electron micrographic analysis, I characterized *pik3*Δ strain to show defects in several steps of

FSM formation (Fig. 2 and Fig. 3): (i) In many of *pik3*Δ cells, FSMs fail to grow to form intact size of spore membranes, resulting in formation of small spheres nearby the nuclei (Fig. 2B, top panel, and Fig. 3B). (ii) Even when the FSMs grow, they frequently fail to close, resulting in formation of bubble-like structures at the leading edges of FSM (Fig. 2B, arrowheads, and Fig. 3C). (iii) In a few cases, FSMs extend in a disorientated manner, resulting in failure to engulf the nuclei (Fig. 3D). These results suggest that PtdIns 3-kinase and its substrate PtdIns(3)P have multiple functions in FSM formation.

My predecessor Dr. Takako Koga searched for the target protein for PtdIns(3)P by the screen of requirement of proteins containing putative PtdIns(3)P binding domain for sporulation. As a result, Vps5p and Vps17p, which contain PX domainas candidates for PtdIns(3)P binding domains, were found out to be candidates for target of PtdIns(3)P during sporulation [21]. Subsequently, I characterized the deletion mutants of these genes and found that both of *vps5*Δ and *vps17*Δ strains formed small spheres of aberrant FSMs as is the cases with *pik3*Δ (denoted above as (i)) [21] (Fig. 4). Thus, Vps5p and Vps17p were suggested to be the major downstream factors of PtdIns(3) kinase at the early stage of FSM development. It is well established in budding yeast that Vps5p and Vps17p form a complex called 'retromer' which mediates retrograde membrane traffic from early endosome to trans-Golgi apparatus by interaction with PtdIns(3)P on early endosome through their PX domains [22]. It is conceivable that *S. pombe* diverts 'retromer' to membrane/protein transport to FSMs, in order to mediate retrograde vesicle transport from endosome or FSM itself to trans-Golgi.

Another target of PtdIns(3)P was a FYVE domain containing protein, Vps27p. I found that *vps27*Δ formed FSMs with approximately wild-type sizes (Fig. 5A), however, FSMs in *vps27*Δ extended relatively slower than in wild-type and eventually failed to close (Fig. 5BC and D, arrows), forming bubble-like membranous structure at the leading edge (Fig. 5E). This phenotype was partly similar to that of *pik3*Δ (denoted above as (ii)), suggesting that Vps27p functions downstream of PtdIns 3-kinase. *S. cerevisiae* Vps27p is well established to mediate protein sorting to vacuole via endosome and multi-vesicular body (MVB) [23] [24]. Newly synthesized or endocytosed proteins targeted into the vacuolar lumen (such as carboxypeptidase S (CPS) or Ste6p) are mono-ubiquitinated at the early endosome. ScVps27p interact with these ubiquitins through two ubiquitin-interacting motifs (UIM), and with

PtdIns(3)P enriched on the endosomal membrane by PtdIns 3-kinase through its FYVE domain. ScVps27p subsequently recruits the ESCRT-I complex by the direct interaction with Vps23p, an ESCRT-I subunit, to trigger ESCRT-II/III mediated membrane invagination into the lumen of endosome to form MVB. My observations implicates that an analogous system in *S. pombe* contributes to the formation of FSMs and *vps27*Δ is defective in transport of unidentified mono-ubiquitinated protein to FSMs, which is required for the closure of FSM. Indeed, my colleague recently demonstrated that all the strains lacking proteins physically interact with Vps27p in this system, such as Vps23p, STAM-like Hse1p, and AMSH-like unnamed protein, accumulated the ubiquitinated proteins and showed essentially the same sporulation phenotype to *vps27*Δ (M. Iida, unpublished results).

Taken together, contribution of vesicle trafficking system to FSM formation has become somewhat clear [25] (Fig. 6). At the time of sporulation, *S. pombe* cells may transport vesicle to assemble to form FSM precursor through ER and Golgi using Spo14p and Spo20p (1-3). By these pathways, proteins newly synthesized after nitrogen starvation (such as Spo3p) may be transported to the FMS. Efficient vesicle traffic from trans-Golgi to FSMs or to endosome may require retrograde transport of membranes or receptors mediated by Vps5p/Vps17p (4, 5). On the other hand, proteins/vesicles from plasma membrane (such as Psy1p) may be transported via endosome and/or retrograde pathway, to which Vps27p and Vps5p/Vps17p may contribute (6 and 5). Relationship between these pathways should be studied in more detail to understand membrane trafficking to form FSMs.

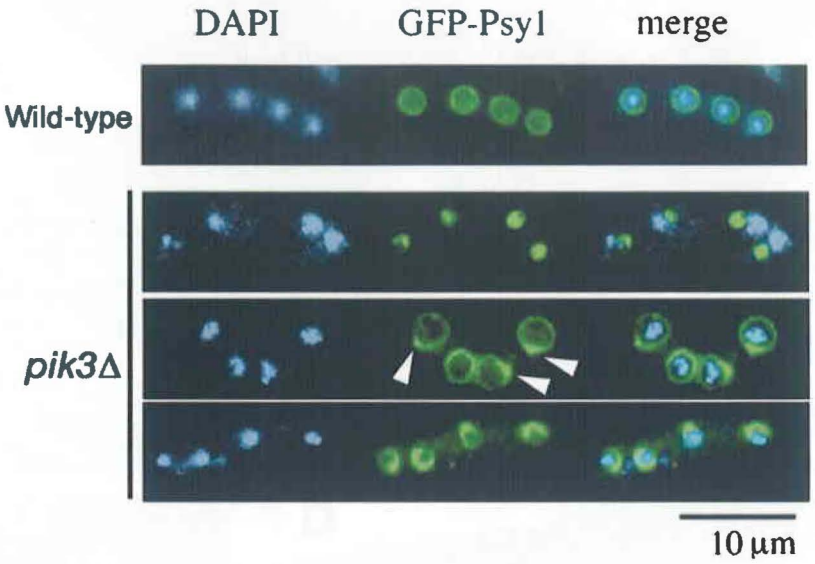

Figure 2 Fluorescence microscopic analysis of FSM in *pik*Δ cells

Sporulation of wild-type or *pik3*Δ haploid cells expressing GFP-Psy1p were induced on an SSA plate for 12 h, fixed, and stained with DAPI. (A) a wild-type cell with four FSMs enclosed each haploid nuclei. (B) *pik3*Δ cells with abnormal FSMs. Most cells formed FSM-like small membrane structure nearby the nuclei (top). Even when FSMs encapsulated the nuclei Signals of Spo3-GFP were uneven (middle, arrowheads) or small compared to the wild-type (bottom).

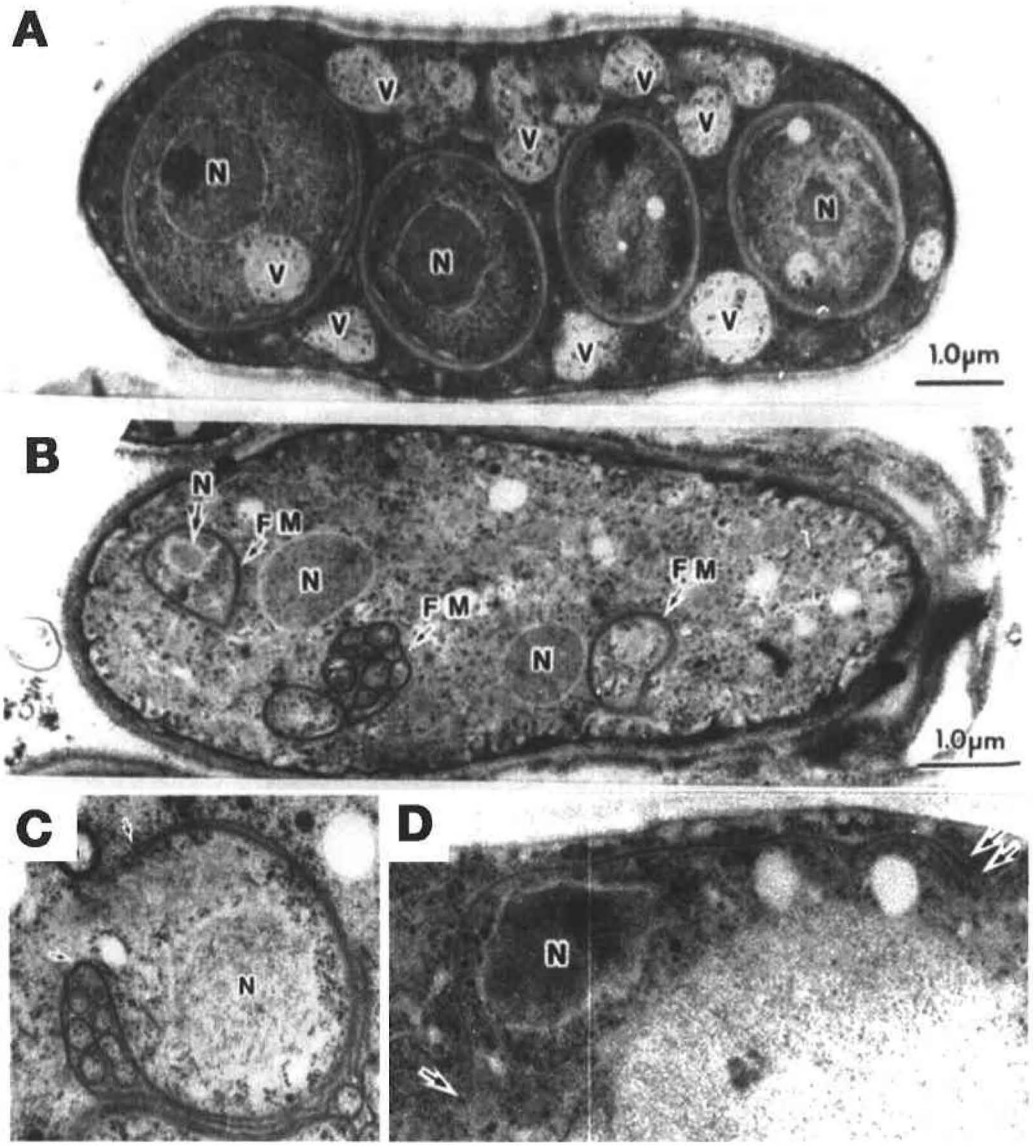

Figure 3 Electron microscopic analysis of *pik3Δ/Δpik3Δ* cells

Sporulation of wild-type or *pik3Δ/pik3Δ* diploid cells were induced on an SSA plate for 12 h., and were analyzed by electron microscopy. (A) a wild-type ascospore. Nuclei are correctly encompassed by the spore membranes. (B) a *pik3Δ/pik3Δ* ascospore. Three nuclei are found, but two of them are not encompassed by spore membranes. (C) bubble-like structure observed in *pik3Δ* cell. Vesicle like bodies are found between the lipid bilayer. (D) a FSM extended in a disorientated manner in *pik3*Δ cell. Leading edges are indicated by the arrow and the double arrows. N: nucleus, V: vacuole, FM: forespore membrane.

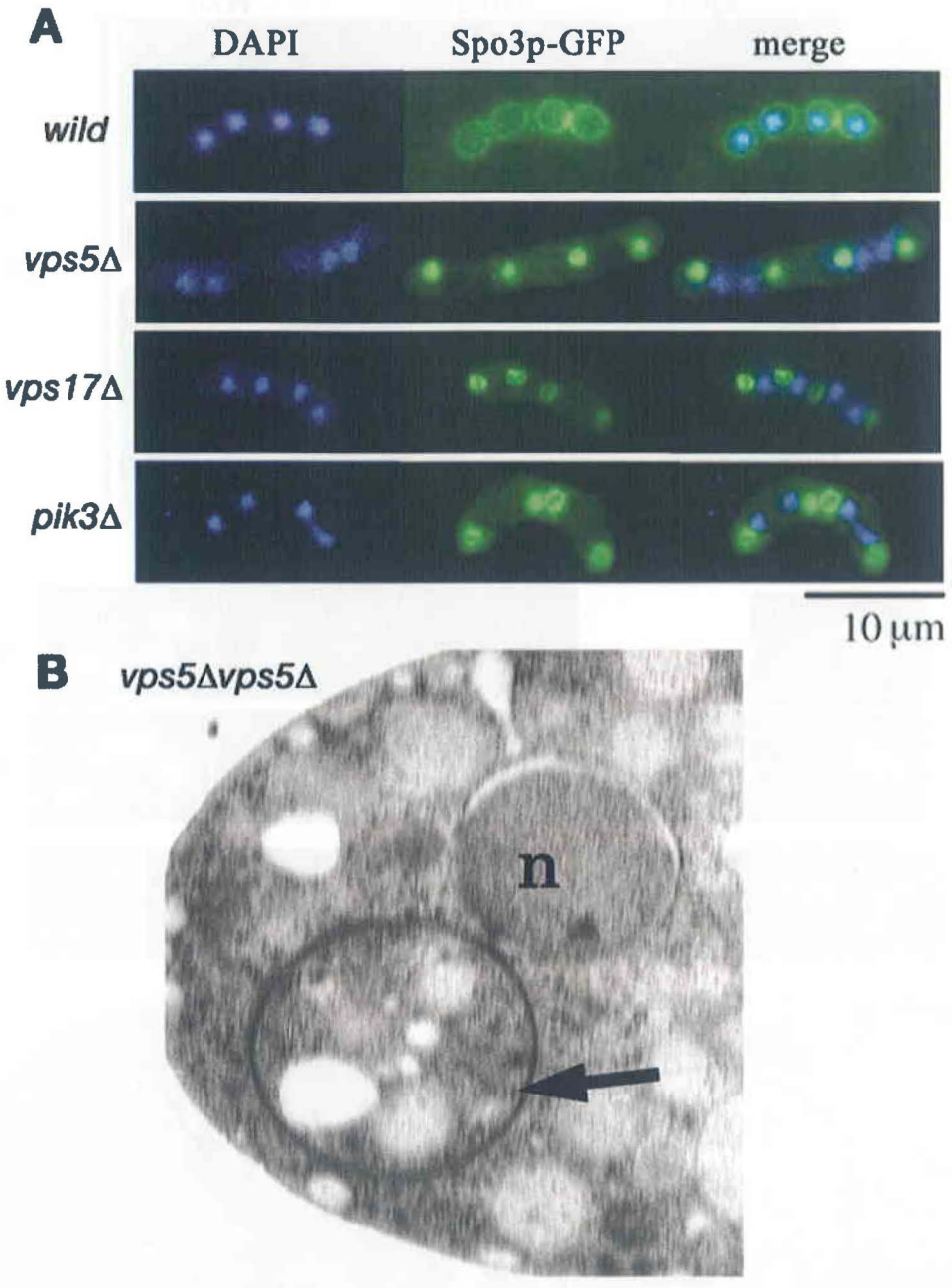

Figure 4 FSM morphology in *vps5*Δ and *vps17*Δ cells

*vps5*Δ and *vps17*Δ cells exhibited FSM morphology similar to the *pik3*Δ. (A) strains noted left expressing Spo3-GFP were induced sporulation. *vps5*Δ and *vps17*Δ cells formed small membrane structure nearby the nuclei, as was the case with *pik3*Δ. (B) an electron micrograph of FSM in a *vps5*Δ cell. FSM left the nucleus bare (arrow).

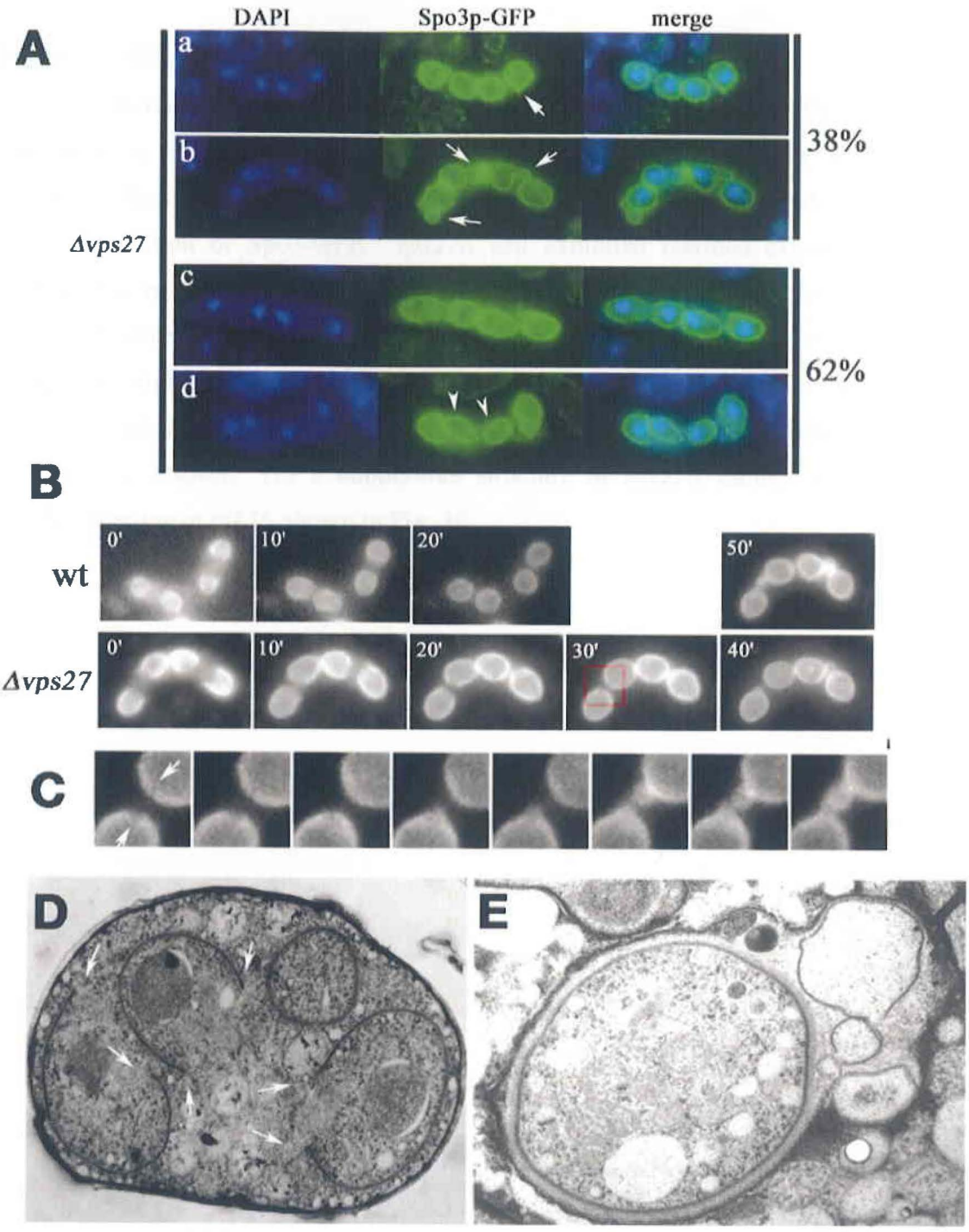
A
DAPI
Spo3p-GFP
merge
a
b
c
d
38%
62%
Δvps27
B
wt
Δvps27
0'
10'
20'
30'
40'
50'
C
D
E

Figure 5 FSM morphology in *vps27*Δ cells

*vps27*Δ cells failed to close FSM and formed bubble-like structure. (A) localization of spo3-GFP in *vps27*Δ cells. Bubble-like structures were frequently formed (a,b, arrows). These cells occasionally failed to close FSM (c,d, arrowheads). (B) time-lapse observation of Spo3-GFP. *vps27*Δ cell exhibited retarded extension of FSM compared to wild-type cell. (C) higher magnification of region indicated by red square in (B). Bubble-like structures were emerged from the unclosed leading edges (arrows). Images are aligned by 2 min. intervals. (D) an electron micrograph of a *vps27*Δ ascus. FSMs extended to enclose the nuclei but they failed to close. Leading edges are indicated by arrows. (F) a bubble-like structure in *vps27*Δ ascus. Compare with similar structure in *pik3*Δ shown in Fig. 3C.

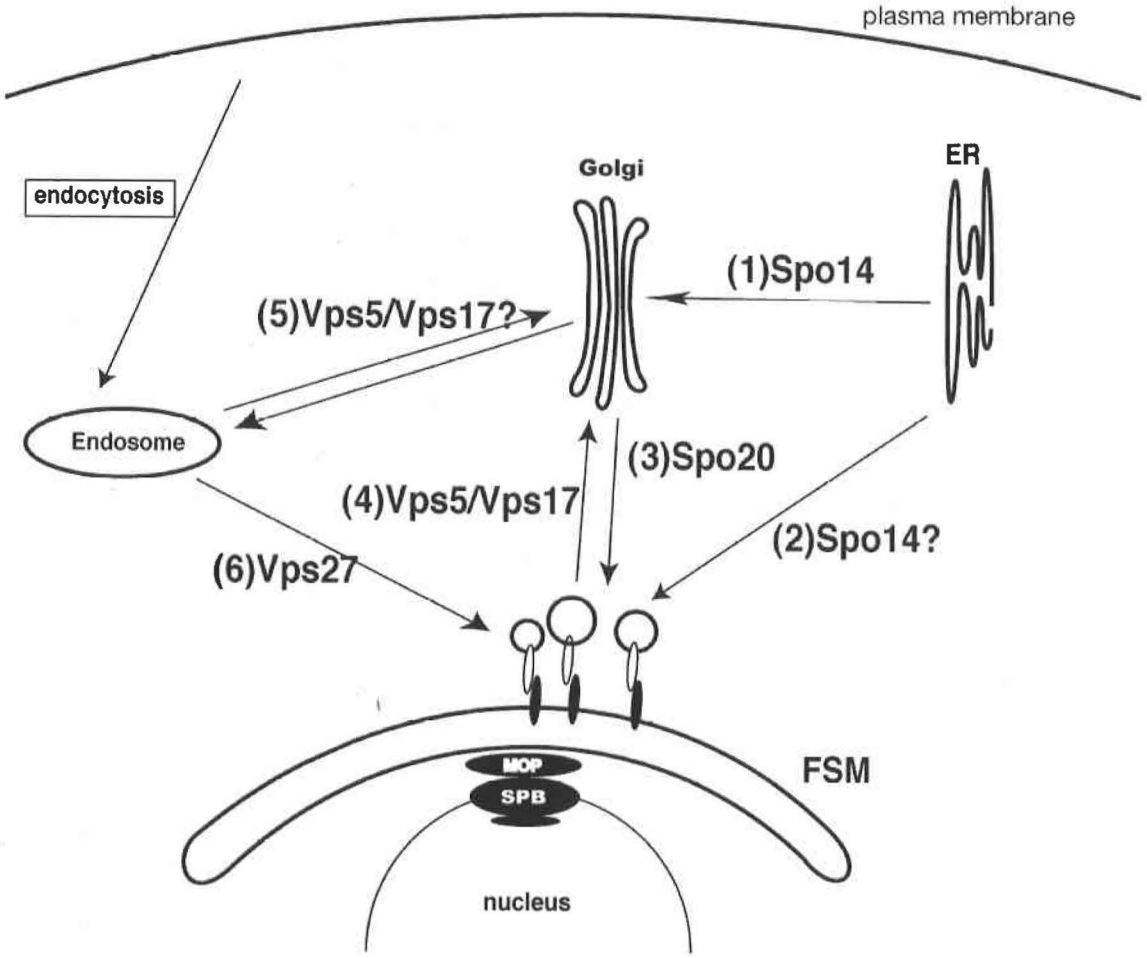

Figure 6 a model for vesicle traffic to FSM

See text for detail.

Orientated extension of forespore membranes

Studies of vesicle transport to FSMs may not be sufficient to explain the how FSMs extend properly around the nuclei, to form four sacs encapsulating daughter nuclei. There must be some mechanism that regulates the orientation of FSM extension. Observation that the FSM is attached to SPBs until the prespore formation completes suggests that SPB may regulate extension of FSMs as a landmark of starting point of extension [4]. On the other hand, the leading edge of the prospore membrane (*S. cerevisiae* counterpart of FSM) is coated with leading edge proteins (LEPs) in *S. cerevisiae* [26]. *S. pombe* Meu14 also localizes at the leading edges of FSMs, and deletion of the gene causes aberrant FSM formation in addition to failure in modification of SPBs [27]. However, SPB and LEPs may not be sufficient for FSM to form sac, leaving an important question, how FSM is regulated to curve to the proper direction. In this study, I focused on septins as a novel component along FSM that control the orientation of FSM extension.

Septins

Septins are conserved eukaryotic GTP binding proteins that associate with membranes and the actin microtubule cytoskeletons [28] [29] [30]. They polymerize to form filamentous structures associating with membrane domains and act as molecular scaffolds for membrane- and cytoskeleton-binding proteins. These features of septins reflect their functions in various cellular processes. Septins consist of a central GTP-binding domain containing P-loop, a septin-unique sequence, a diverged N-terminal extension, and, in many cases, a C-terminal coiled-coil domain.

Septins were originally identified in budding yeast *S. cerevisiae,* in a genetic screen for cytokinesis-defective mutants [28] [29]. Proteins encoded by *CDC3*, *CDC10*, *CDC11*, *CDC12* form a oligomeric complex with 2:2:1:2 stoichiometry, and localize at the bud neck to form a ring[31]. Another septin Shs1p is also known to localize at the ring but its interaction with other septins might be non-obligate[32]. This neck filament has been suggested to contribute to keep cell morphology by blocking cytoplasm and/or plasma membrane of mother and daughter cells [28,31,33]. Analysis of septin-interacting proteins suggest that septin filaments also contribute to the signal transduction as a scaffold for the signaling proteins at the bud neck[34,35].

Septins are also present in metazoan cells, implicating not only in cytokinesis but also in diverse cellular processes, such as exocytosis in nerve cell, actin stress fiber organization, destabilization of interphase microtubules, chromosome segregation, and diffusion barrier formation at sperm annulus [36-40]. Several lines of evidence also suggest septins involvement in cancer[41,42].

In *S. cerevisiae,* two additional septins, Spr3 and Spr28, are expressed specifically in sporulating cells, form double bars at the regions following leading edges together with Cdc3 and Cdc10[43,44]. The Gip1-Glc7 complex may control organization of these septins [45]. However, it has not been clear whether or not these septins are essential for sporulation and what is the role for them. An *spr3*Δ*spr28*Δ strain exhibits no apparent defect in sporulation efficiency probably due to the redundancy of the genes. Because *CDC3* and *CDC10* mutants are lethal at the restriction temperature, sporulation of these strains at restriction temperature could not be examined [43,46]. Thus, whether or not septins contribute to spore formation have been totally unknown.

Septins in *S. pombe* have not been well investigated until recently. There are seven septin genes in the genome database, named *spn1*$^+$ to *spn7*$^+$[47]. Recent reports show that hetero-oligomer complex of Spn1-4p form a ring at the septum, maintain its size constant during cytokinesis[48,49]. An anillin homolog Mid2p probably interacts with septins and stabilizes them to keep a ring[50,51]. Proper localization of two endo-glucanases, Eng1p and Agn1p, requires the septin ring, resulting in delayed cell separation in *spn1*Δ-*spn4*Δ cells[52].

Two genes, *spn5*$^+$ and *spn6*$^+$, are induced by the Mei4p transcription factor during meiosis and sporulation, but their biological roles have not been elucidated[53]. Considering the septins localization in sporulating budding yeast described above, *spn5*$^+$ and *spn6*$^+$ might play some role during FSM formation. These prompted me to investigate the biological function of septins in sporulation of *S. pombe*.

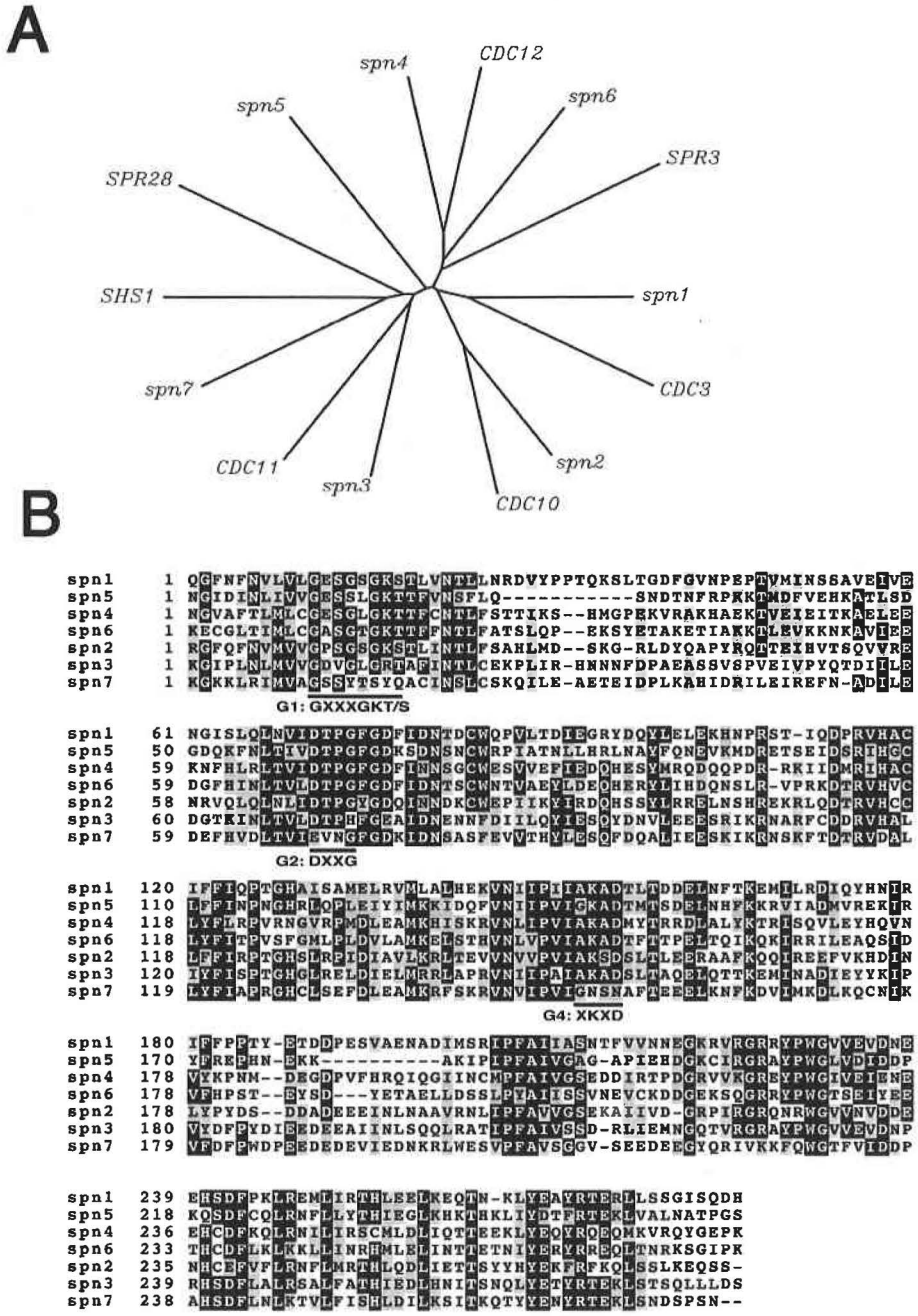

Figure 7 septins in *S. pombe*

(A) a phylogenic tree of septin proteins in *S. pombe* and *S. cerevisiae*. (B) an alignment comparison of amino acid sequences of the GTP-binding domains of septins in *S. pombe*. Residues in black indicate identity and residues in gray indicate similarity. Three sequences conserved in small GTPases (G1, G2, and G4) are indicated by the underlines. Note that Spn7p lacks all these sequences.

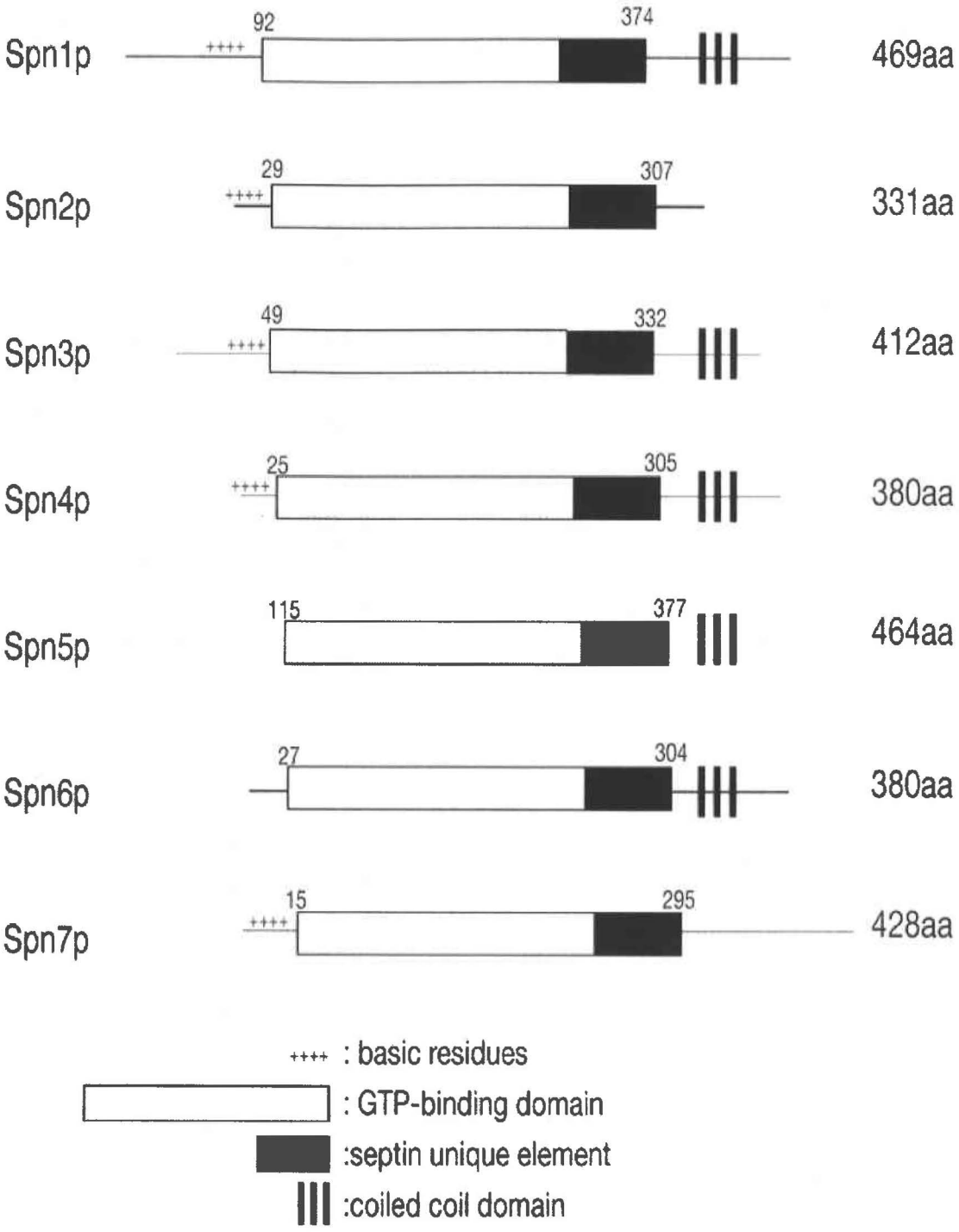

Figure 8 A schematic model of septins in *S. pombe*

CHAPTER II: CLASSIFICATION OF SEPTIN GENES IN *S. POMBE*

INTRODUCTION

In *S. pombe*, there are seven putative septin genes on its genome, as is the case with *S. cerevisiae*, and they were named as *spn1*$^+$ to *spn7*$^+$. Spn1p, Spn2p, Spn3p, and Spn4p are most homologous to Cdc3 (45%), Cdc10 (52%), Cdc11 (42%), and Cdc12 (51%), respectively, whereas Spn5p, Spn6p, and Spn7p show relatively low similarity to the septins in *S. cerevisiae* (26-39%) (Fig. 7A). Septins in *S. pombe* basically consist of three regions as is the case with most septins in other organisms: the central conserved GTPase domains, carboxyl-terminal coiled-coil domains, and the various extensions at their amino-terminus (Fig. 8). Spn2p lacks the coiled-coil domain, and Spn7p lacks both the coiled-coil domain and all three of the motifs of the conserved GTP-binding site (Fig. 7B and Fig. 8). Among seven septin genes in *S. pombe,* transcription of *spn5*$^+$ and *spn6*$^+$ has been reported to be upregulated by meiotic transcription factor Mei4p [53]. Recent microarray data suggests that *spn2*$^+$ and *spn7*$^+$ were highly upregulated under nitrogen starvation condition [54]. In general, septins are known to have nature to form a hetero-origomeric complex. *S. cerevisiae* may use two complexes possibly one for mitosis and another for sporulation. The mitotic complex consists of Cdc3, Cdc10, Cdc11, Cdc12, and Shs1 [35]. Although the sporulation complex has not been examined in full detail, it is considered to consist of Cdc3, Cdc10, Spr3, and Spr28 [44] [43] [45]. Although mammalian septin complexes are diverged among cell types and cellular properties, Sept2/6/7 may form a core subcomplex in most cases [55] [56]. At the beginning of this study, functions of septins in *S. pombe* was unknown. To investigate the role of septins in sporulation, it was necessary to identify which septin genes are involved in sporulation. For this aim, I planned to classify septin genes by their mutant phenotypes and localizations.

MATERIALS AND METHODS

Strains and media

The yeast strains used in this chapter are listed in Table 1. They are the derivatives of those originally described by Leupold [57]. YE (complete medium) and MM (synthetic medium) were used for growing *S. pombe* strains [58] [2]. SSA was used for induction of mating and sporulation [59]. 15 mg/ml agar was added to make solid media plates.

To create septin deletion mutant strains, gene ORFs were amplified by RT-PCR from RNA extracted from wild-type strain THP18, and cloned into pT7blue vector (Novagen). Total RNA extraction was done by the simplified hot-phenol method [54]: In brief, frozen cell pellet was thawed on ice and suspended with 500 ml TE, mixed with 500 ml phenol-chloroform by vortexing, and incubated at 65^{o}C for 1 h with periodic vortexing. After centrifugation at 14,000 rpm for 5 min at room temperature, the aqueous phase was taken and phenol-chloroform extraction was repeated. Finally, total RNA was precipitated with ethanol and dissolved in Diethylpyrocarbonate (DEPC)-treated water.

Primer sets for amplification of septin ORFs are:

spn1^{+} : 5'- cagatctc(*Bgl* II)atggcgtcaatggtactcg-3' and
5'- ctcgag(*Xho* I)taaggagactatttaaaaaacttcc-3'

spn2^{+} : 5'- cagatct(*Bgl* II)aatggaagttccttctgcagttacc-3' and
5'- ctcgag(*Xho* I)gaagaagactattgagcggtg-3'

spn3^{+} : 5'- cagatct(*Bgl* II)aatgtggtatacatataacgaagac-3' and
5'- ctcgag(*Xho* I)caccattaaattggttatgactgg-3'

spn4^{+} : 5'-aaacccggg(*Sma* I)atgaatgaagaagagacaaacttcg-3' and
5'-aaatctaga(*Xba* I)ctaacgtttgcgagagctggtagc-3'

spn5^{+} : 5'- cagatct(*Bgl* II)gatggatagctcaaatttgtcttcatc-3' and
5'- ctcgag(*Xho* I)tttatgctaagatgcctgc-3'

spn6^{+} : 5'- ttagatct(*Bgl* II)cacgatgtctttgactgaaaaccttcaattat -3' and
5'- ttcccggg(*Sma* I)tcatttttttatgaccgcggcccttgt -3'

spn7^{+} : 5'- cagatct(*Bgl* II)gatgaataaaggcccaagacatcg-3' and
5'- ctcgag(*Xho* I)cactctcaaatgtttaatttagc-3'

Plasmids for gene disruption were constructed as shown in Table 2. Wild-type strain THP18 was transformed with the resulting plasmids digested by appropriate restriction enzymes to yield *ura*$^+$ transformants. Proper integration at the target locus was confirmed by PCR with the appropriate primers.

Plasmid construction

To generate the plasmids for expression of GFP-fused septins, septin-coding sequences cloned as described above were subcloned between the *Bgl* II and the *Xho* I sites of pGFT41 vector in frame to GFP^{S65T} [8]. The resulting plasmids express septins with N-terminal GFP under the control of the thiamine repressible *nmt41* promoter. The genomic sequences including ORFs and promoters of *spn2*$^+$, *spn5*$^+$, *spn6*$^+$, and *spn7*$^+$ were amplified by PCR with appropriate primer sets, and inserted between the *Bam* HI and the *Not* I sites of pAL(GFP) to yield pAL(spn2-GFP), pAL(spn5-GFP), pAL(spn6-GFP), and pAL(spn7-GFP), respectively. Primers used for amplification were,

spn2$^+$: 5'- AAGGATCC(*BamH* I)AGCGCTAATTATTTGTGAATCTGG-3' and
5'- TTGCGGCCGC(*Not* I)TGAGCGGTGGCTGTATGGAG-3'

spn5$^+$: 5'- AAGGATCC(*BamH* I)TCCCGCCACTTCACTAAG-3' and
5'-TTGCGGCCGC(*Not* I)GCTAAGATGCCTGCTTTTTTC-3'

spn6$^+$: 5'-AAAGATCT(*Bgl* II)ATTCGATCCTTGACACTGTC-3' and
5'-TTGCGGCCGC(*Not* I)TTTTTATGACCGCGGCCCTTG-3'

spn7$^+$: 5'-AAAGATCT(*Bgl* II)TAAACCTGCAGCTCAACTC-3' and
5'-TTGCGGCCGC(*Not* I)CGATAGAAAGGGAGGTTTTCG-3.'

pAL(GFP) was generated by inserting *Not* I-*Sac* I fragment of pGFT41 containing GFP and *nmt1* terminator between the same sites of pAL-SK.

Table 1. Yeast strains used in Chapter II

Name	Description	Source of reference
THP18	*h^{90} ade6-M216 ura4-D18 leu1-32*	(Koga et al., 2004)
MO246	*h^{90} ade6-M216 ura4-D18 leu1-32 spn1Δ::ura4^{+}*	this study
MO250	*h^{90} ade6-M216 ura4-D18 leu1-32 spn2Δ::ura4^{+}*	this study
MO371	*h^{90} ade6-M216 ura4-D18 leu1-32 spn3Δ::ura4^{+}*	this study
MO372	*h^{90} ade6-M216 ura4-D18 leu1-32 spn4Δ::ura4^{+}*	this study
TK144	*h^{90} ade6-M216 ura4-D18 leu1-32 spn5Δ::ura4^{+}*	this study
MO277	*h^{90} ade6-M216 ura4-D18 leu1-32 spn6Δ::ura4^{+}*	this study
MO229	*h^{90} ade6-M216 ura4-D18 leu1-32 spn7Δ::ura4^{+}*	this study
MO660	*h^{90} ade6-M216 ura4-D18 leu1-32 spn2Δ::ura4^{+} spn7Δ::LEU2*	this study
MO662	*h^{90} ade6-M216 ura4-D18 leu1-32 spn5Δ::ura4^{+} spn7Δ::LEU2*	this study
MO664	*h^{90} ade6-M216 ura4-D18 leu1-32 spn6Δ::ura4^{+} spn7Δ::LEU2*	this study
TK278	*h^{90} ade6-M216 ura4-D18 leu1-32 spn5Δ::ura4^{+} spn6Δ::LEU2*	this study
MO684	*h^{90} ade6-M210 ura4-D18 leu1-32 spn2Δ::kanMX6*	this study
TW747	*h^{+}/h^{-} ade6-M210/ade6-M216 leu1-32/leu1-32 ura4-D18/ura4-D18*	(Onishi et al., 2003)
MO705	*h^{90}/h^{90} ade6-M210/ade6-M216 leu1-32/leu1-32 ura4-D18/ura4-D18 spn2Δ::ura4^{+}/spn2Δ::ura4^{+}*	this study
TK172	*h^{+}/h^{-} ade6-M210/ade6-M216 leu1-32/leu1-32 ura4-D18/ura4-D18 spn5Δ::ura4^{+}/spn5Δ::ura4^{+}*	this study
TK367	*h^{+}/h^{-} ade6-M210/ade6-M216 leu1-32/leu1-32 ura4-D18/ura4-D18 spn6Δ::ura4^{+}/spn6Δ::ura4^{+}*	this study
MO706	*h^{90}/h^{90} ade6-M210/ade6-M216 leu1-32/leu1-32 ura4-D18/ura4-D18 spn7Δ::ura4^{+}/spn7Δ::ura4^{+}*	this study

Table 2

gene locus	structures of disrupted gene
spn1$^+$ **SPCPJ732.01**	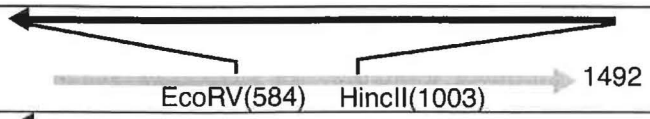
spn2$^+$ SPAPJ696.01c	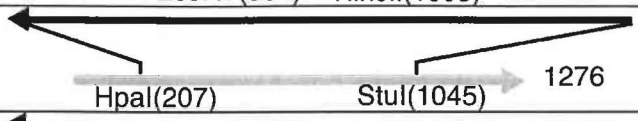
spn3$^+$ SPBC14F5.11c	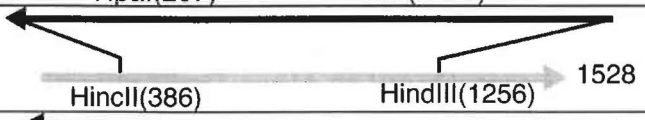
spn4$^+$ **SPBC887.06c**	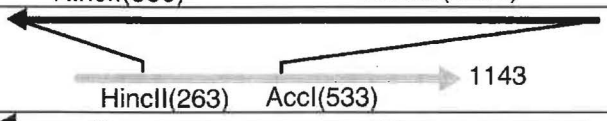
spn5$^+$ **SPCC16A11.04**	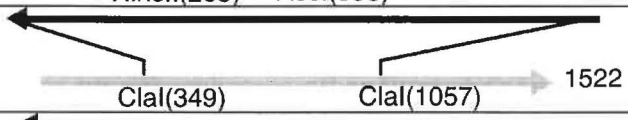
spn6$^+$ SPAC6F6.12	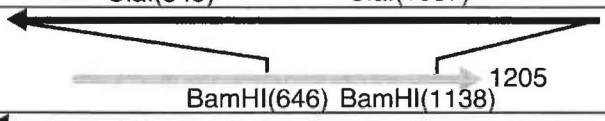
spn7$^+$ SPCC16A11.08	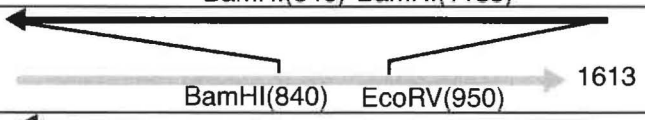
pik1$^+$ **SPBC1711.11**	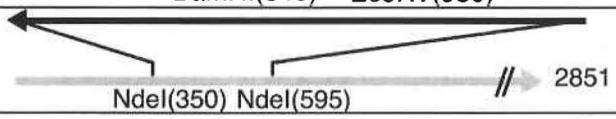

RESULTS

Spn1p, Spn2p, Spn3p, and Spn4p were involved in cell separation

To address which septins in *S. pombe* are involved in sporulation, septin deletion mutants were generated by replacing protions of the ORFs with the *ura4*$^{+}$ marker gene (Table 2, Materials and Methods). All the mutants were viable, unlike the case with *S. cerevisiae*. *spn1*Δ and *spn4*Δ showed defect in cell separation after cytokinesis at 30 °C, resulting in chained cell morphology as reported before (Fig. 9). When cells were shifted to 37 oC, *spn1*Δ and *spn4*Δ occasionally formed branches. *spn2*Δ and *spn3*Δ showed no defects at 30 °C, but exhibited chained cell morphology at 37 °C (Fig.9). *spn5*Δ, *spn6*Δ, and *spn7*Δ showed no defects in vegetative growth (data not shown). These results suggest that four septins, Spn1p, Spn2p, Spn3p, and Spn4p are involved in vegetative growth, whereas other three, Spn5p, Spn6p, and Spn7p are not. Consistently, GFP-Spn1p, GFP-Spn2p, GFP-Spn3p, and GFP-Spn4p localized at the middle of the cell as a ring, whereas other three septins did not show any specific localizations in vegetative cells (Fig. 12A, not shown).

Spn1p, Spn2p, Spn3p, and Spn4p were involved in conjugation

To examine the phenotypes under the nitrogen starvation condition, the mutants were spread on SSA plates and incubated for one day. Under this condition, homothallic wild-type cells form mating tubes that fuse to form zygote, followed by the expansion of the furrow to the cell diameter, to finally form four spores per ascus (Fig. 10A). *spn1*Δ and *spn4*Δ, formed spores which were indistinguishable from the wild type cells (Fig. 10B), but spores in these mutants were frequently formed inside the one of the parental cell body leaving the other empty, probably because segregated chromosomes were misplaced (Fig. 11AB). Δ*spn1*, Δ*spn2*, and Δ*spn4* zygotes exhibited relatively narrow furrows even after the maturation of the spores (Fig. 10A, arrows), suggesting that these septins are also involved in cell conjugation, especially in expansion of mating furrow. Behavior of F-actin in these septin mutants was monitored by staining the zygotes with rhodamine-phalloidin. As reported before, F-actin localized as cortical dots at the projection tip during the cell fusion, and becomes dispersed cytoplasmic dots during horsetail movement of nucleus in the wild type cells

[60] (Fig. 11C). Accumulation of dots around the mating furrow remained by the time of karyogamy. In contrast, F-actin dots in Δ*spn1*, Δ*spn2*, and Δ*spn4* became dispersed before the karyogamy occurred in Δ*spn1*, Δ*spn2*, and Δ*spn4* cells (Fig. 11C). A similar phenotype was found in Δ*spn3* but not in Δ*spn5*, Δ*spn6*, and Δspn7 cells (Fig. 11C, data not shown). When localization of septins were monitored by GFP-septins, Spn1p, Spn2p, Spn3p and Spn4p localized as rings at the furrows in the conjugated cells, suggesting that these septins indeed function at this site (Fig. 12B). Therefore, it is likely that the same set of septins functioning in mitotic division is involved in conjugation.

Spn2p, Spn5p, Spn6p, and Spn7p were involved in sporulation

*spn2*Δ, *spn5*Δ, *spn6*Δ, and *spn7*Δ showed defect in sporulation. 42-70 % of *spn2*Δ, *spn5*Δ, *spn6*Δ, and *spn7*Δ cells formed asci with spores less than four (Fig. 10A arrowheads, and B). *spn1*Δ, *spn3*Δ and *spn4*Δ did not show such a phenotype (Fig. 10AB). Because double knockout strains within *spn2*Δ, *spn5*Δ, *spn6*Δ, and *spn7*Δ did not show any additional defect (Fig. 10B), Spn2p, Spn5p, Spn6p, and Spn7p may functions in the same process during sporulation. *spn2*Δ/*spn2*Δ, *spn6*Δ/*spn6*Δ, *spn5*Δ/*spn5*Δ or *spn7*Δ/*spn7*Δ diploid strains also formed asci with aberrant numbers of spores (not shown), but had no obvious abnormality in meiotic nuclear division, suggesting that the defect was indeed within sporulation procedure (Fig. 10C). Spn2p-GFP, Spn5p-GFP, Spn6p-GFP, and Spn7p-GFP localized at the immature spores as rings (Fig 12C). Taken together, four septins, Spn2p, Spn5p, Spn6p, Spn7p were involved in sporulation, which were required for formation of proper number of spores per ascus. Precise investigation of septins function in sporulation are described in the next chapter.

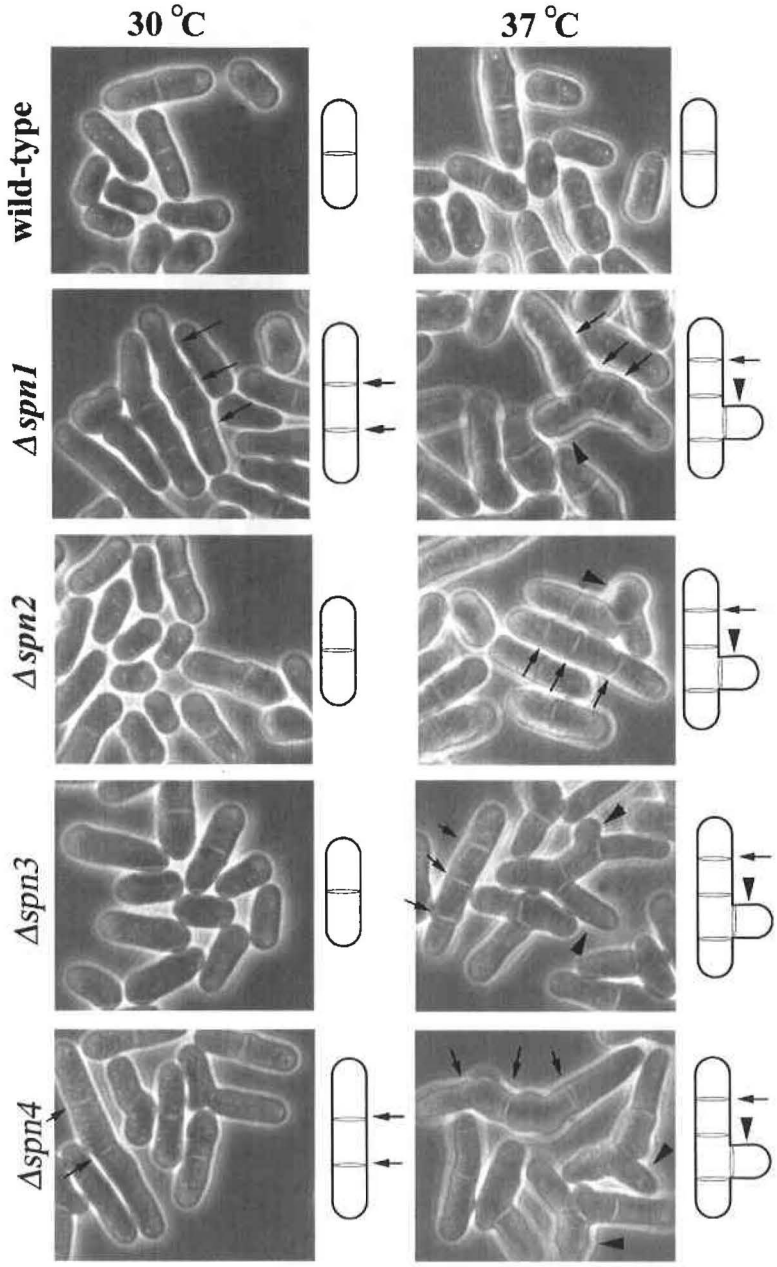

Figure 9 (next page) **Vegetative growth of septin mutants**

Strains THP18 (wild type), MO246 (Δ*spn1*), MO250 (Δ*spn2*), MO371 (Δ*spn3*), and MO372 (Δ*spn4*) were cultured overnight in YEA media 30 °C or 37 °C to mid-logarithm phase. *spn1*Δ and *spn4*Δ formed cells with multiple septa at 30 °C whereas *spn2*Δ and *spn3*Δ exhibited the same phenotype only at 37 °C. Some cells formed branches. Arrows indicate the multiple septa, and arrowheads indicate the branched cells. Schematic representations of each phenotype are shown in right.

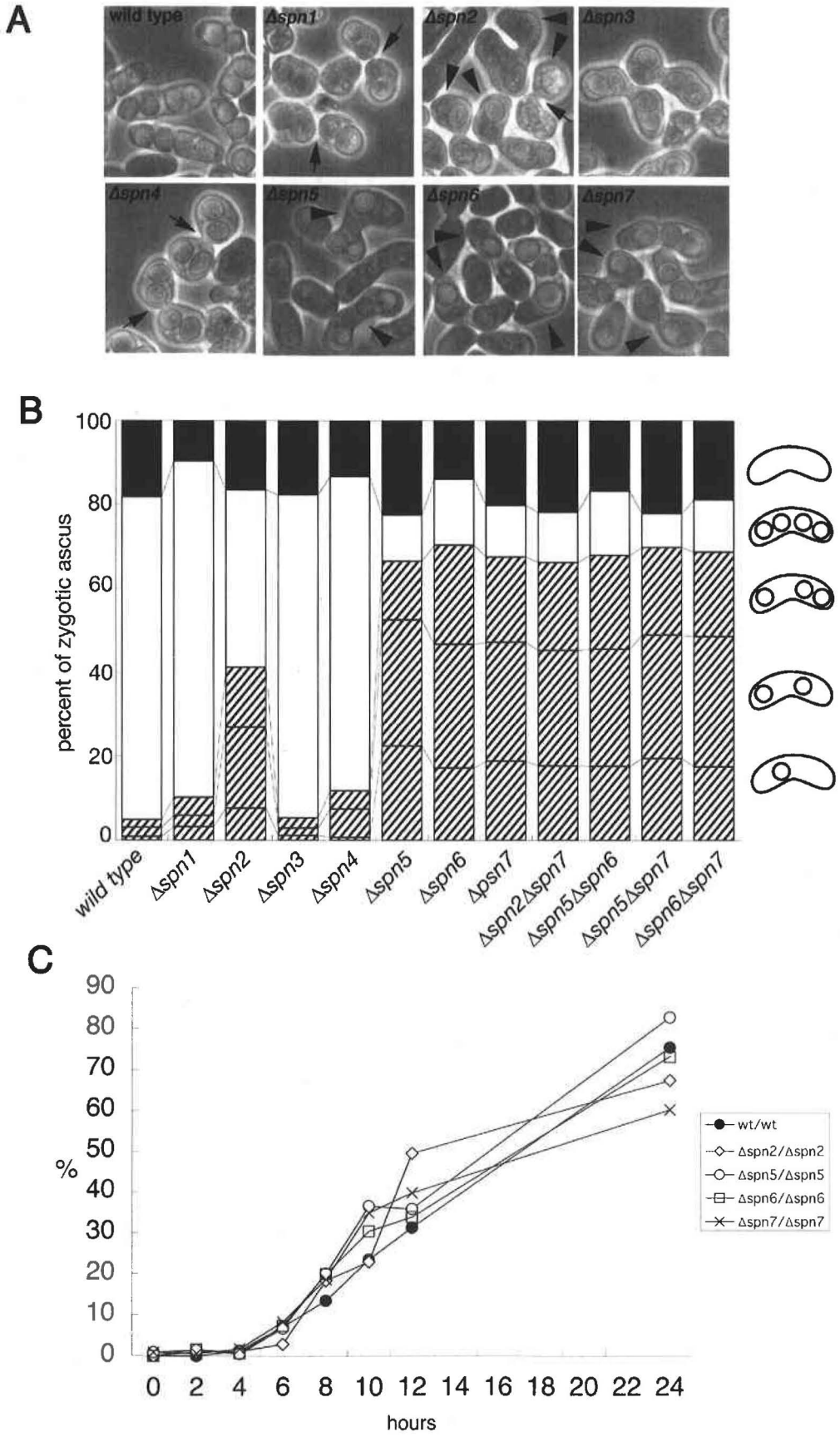
A
wild type
Δspn1
Δspn2
Δspn3
Δspn4
Δspn5
Δspn6
Δspn7
B
percent of zygotic ascus
100
80
60
40
20
0
wild type
Δspn1
Δspn2
Δspn3
Δspn4
Δspn5
Δspn6
Δpsn7
Δspn2Δspn7
Δspn5Δspn6
Δspn5Δspn7
Δspn6Δspn7
C
%
90
80
70
60
50
40
30
20
10
0
0 2 4 6 8 10 12 14 16 18 20 22 24
hours
wt/wt
Δspn2/Δspn2
Δspn5/Δspn5
Δspn6/Δspn6
Δspn7/Δspn7

Figure 10 Sporulation of septin mutants

Four septin genes are required for proper sporulation. (A) Phase-contrast images of sporulating septin-deleted strains. Strains THP18 (wild type), MO246 (Δ*spn1*), MO250 (Δ*spn2*), MO371 (Δ*spn3*), MO372 (Δ*spn4*), TK144 (Δ*spn5*), MO277 (Δ*spn6*), and MO 229 (Δ*spn7*) were incubated on SSA plates for 2 days. Δ*spn2*, Δ*spn5*, Δ*spn6*, and Δ*spn7* cells formed aberrant numbers of spores (arrowheads). Δ*spn1*, Δ*spn2*, and Δ*spn4* cells formed narrow mating furrows (arrows). (B) The percentages of ascus with various numbers of spores. >200 asci of cells were counted. Frequency of ascus with no spores, four spores, and aberrant number of spores (one, two, or three) were colored in black, white, and gray, respectively. Strains sane as (A) were used, except for MO660 (Δ*spn2*Δ*spn7*), MO662 (Δ*spn5*Δ*spn7*), MO664 (Δ*spn6*Δ*spn7*), and TK278 (Δ*spn5*Δ*spn6*). (C) Meiotic nuclear division occurred properly in septin-deleted strains. Strains TW747 (wt/wt), MO705 (Δ*spn2*/Δ*spn2*), TK172 (Δ*spn5*/Δ*spn5*), TK367 (Δ*spn6*/Δ*spn6*), and MO706 (Δ*spn7*/Δ*spn7*) were grown overnight in MM media to mid-log phase, washed with MM-N, and resuspended in MM-N. After incubation for the indicated periods, cells were collected, fixed with 30 % ethanol, stained with DAPI. >200 cells were counted at each time point. Percentages of tetranucleate cells were plotted in the graph.

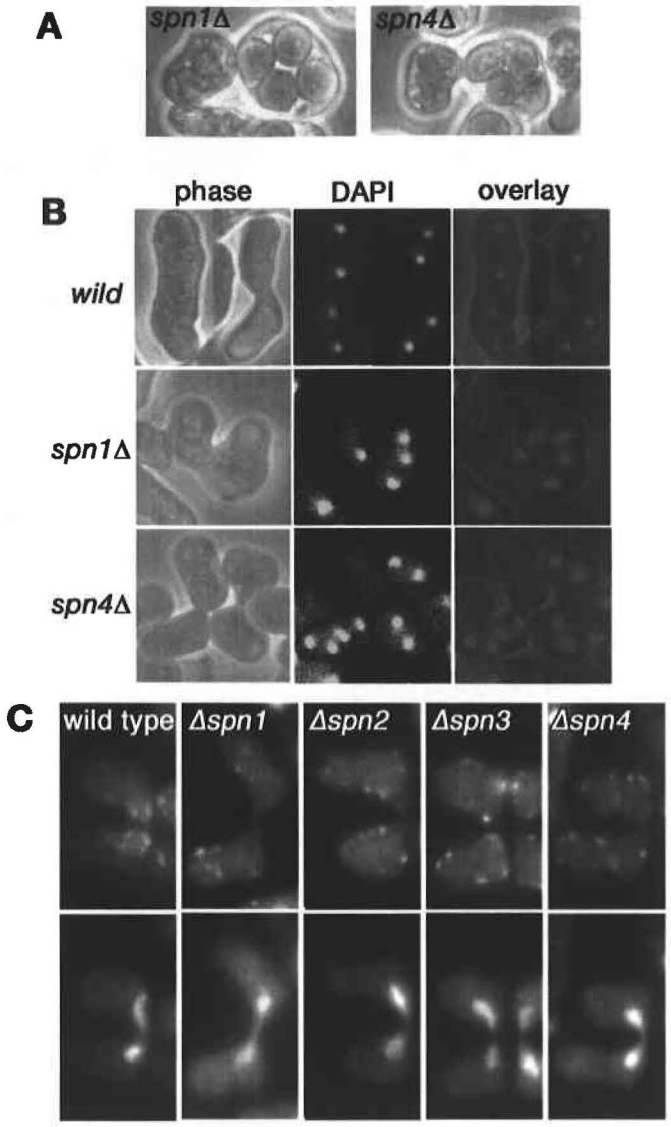

Figure 11 Other phenotypes of septin mutants

(A) aberrant spore positioning in *spn1*Δ and *spn4*Δ cells. Representative images from the same culture to Fig. 10A are shown. All four spores were formed within one of the parental cell body. (B) abnormal nuclear positioning in *spn1*Δ and *spn4*Δ cells. Cells were fixed by ethanol and stained with DAPI. (C) Cortical dots of F-actin at mating furrows were dispersed by the time of karyogamy in Δ*spn1*-Δ*spn4* cells. Conjugation were induced on an SSA plate for 6 h. Cells were fixed, stained with DAPI and Rhodamine-Phalloidine, observed under the fluorescent microscope. Wild type cells always harbored F-actin dots at mating furrows, which were not observed in Δ*spn1*-Δ*spn4* cells.

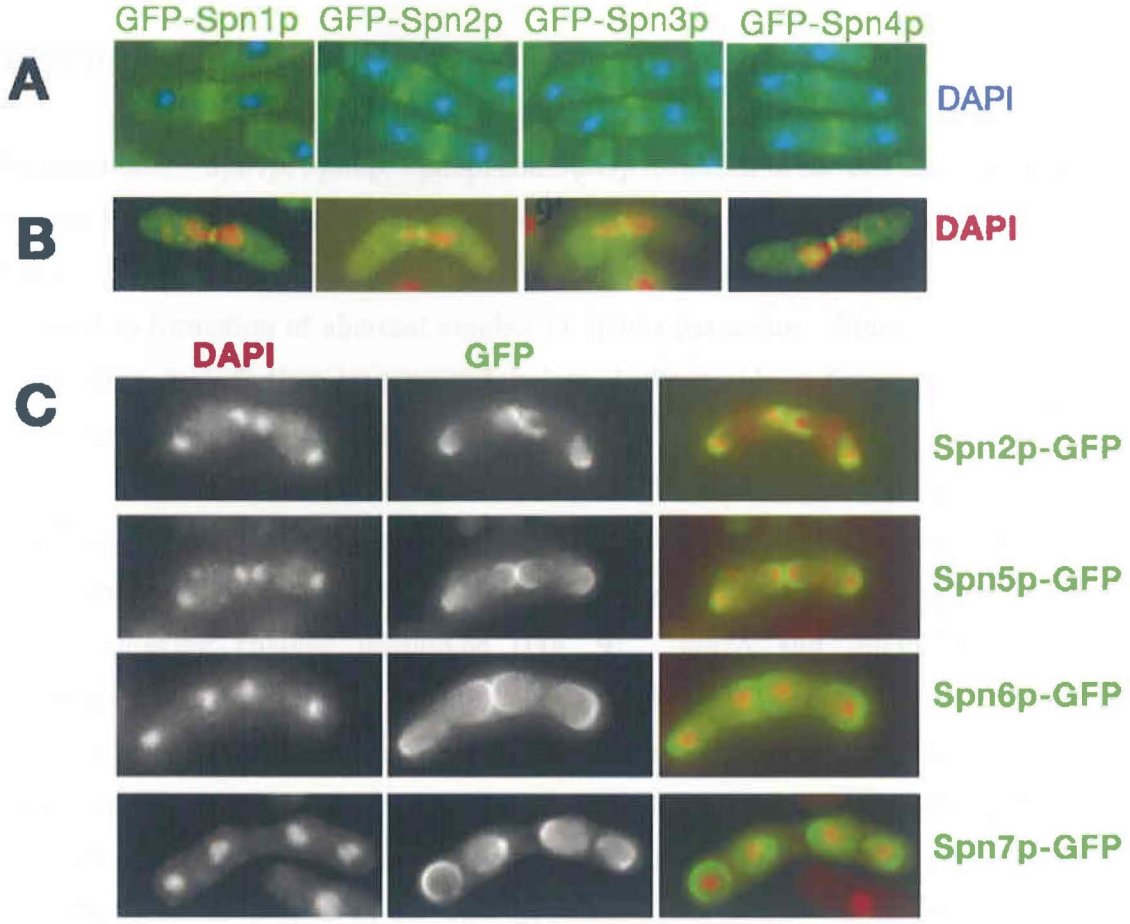

Figure 12 Localization of septins

(A) vegetative septins localize at division plane. Strains MO246 (Δ*spn1*), MO250 (Δ*spn2*), MO371 (Δ*spn3*), and MO372 (Δ*spn4*) harboring pREP41(GFP-Spn1p), pREP41(GFP-Spn2p), pREP41(GFP-Spn3p), and pREP41(GFP-Spn4p), respectively, were grown overnight in MM media, fixed, and stained with DAPI. (B) septins localize at mating furrow until the end of horsetail movement of the nucleus. Conjugation of cells were induced conjugation on an SSA plate for 6 h. Cells were fixed and stained with DAPI. (C) four septins localize at spores. Sporulation of strains MO250 (Δ*spn2*), TK144 (Δ*spn5*), MO277 (Δ*spn6*), and MO 229 (Δ*spn7*) harboring pAL(spn2-GFP), pAL(spn5-GFP), pAL(spn6-GFP), pAL(spn7-GFP), were induced an SSA plate for 12 h, fixed, and stained with DAPI.

DISCUSSION

In this study, I classified septin genes by their mutant phenotypes and localizations. Spn1p, Spn2p, Spn3p, and Spn4p localized to the cell division plane and mating furrow, and were required for cells separation and mating furrow expansion. Spn2p, Spn5p, Spn6p, and Spn7p localized at immature spores and lack of these genes resulted in formation of aberrant number of spores per ascus. Since role of septins in sporulation was further investigated below, I discuss here focusing on septins in vegetative growth and conjugation.

Recent biochemical report indicates that Spn1p and Spn4p form a core subcomplex even in the absence of Spn2p or Spn3p, playing central role in septin ring formations [48]. Vegetative growth of *S. pombe* was affected by deletion of *spn1*$^+$, *spn4*$^+$, showing chained phenotype (Fig. 9). *spn2*Δ and *spn3*Δ affected more moderately because these mutants showed chained phenotype only at a high temperature. These results suggest that Spn1p and Spn4p are more responsible than Spn2p and Spn3p for formation of chained cells, consistent with the biochemical property of the septin complex. Because general growth rates of these mutants were virtually identical to those of the wild-type strain, and because formation of contractile actin ring were not affected by deletion of septins, chained phenotype can be considered to be due to delayed cell separation rather than to defect of cell cycle or cytokinesis. Recently, it has been reported that two endo-glucanases are recruited to the site of cell separation in a septin ring dependent manner [52]. Because these enzymes are required for digestion of primary septum after the cytokinesis, cell separation defect of septin-deleted cells can be explained by the absence of these enzymes at the septum.

Under the nitrogen starvation condition, Spn1p-Spn4p localized at the furrow of the conjugated cells. Among these septins, lack of Spn1p and Spn4p caused abnormal positioning of the misplaced nuclei. Considering the temperature-dependent defects of *spn2*Δ and *spn3*Δ in vegetative cells, it might be possible that these mutants were also involved in positioning of the nuclei. However, I could not examine it because even the wild-type *S. pombe* did not enter into meiosis at the high temperature. Spn1p, Spn2p, and Spn4p were required for efficient expansion of mating furrow (Fig. 10A). To my knowledge, no such a mutation affecting mating furrow expansion have been reported so far, and little is known about the mechanism underlying this process.

Because both furrow expansion and actin patch condensation around the furrow required septins (Fig. 11C), the furrow expansion might be mediated by the accumulated actin cytoskeleton. One candidate protein that might be involved in this hypothesis is Fus1p, a FH-domain protein that acts as a scaffold for association of F-actin with fusion zone [61] [60] [62]. Physiological experiments to solve the interplay among septins, F-actin, and furrow expansion may be required to solve how septins work in conjugation.

CHAPTER III: ANALYSIS OF SEPTINS IN SPORULATION

INTRODUCTION

In Chapter II, I identified four septin genes involved in sporulation. *spn2*Δ, *spn5*Δ, *spn6*Δ, and *spn7*Δ cells frequently formed spores less than four per ascus although their meiosis was indistinguishable from that of the wild-type cells, suggesting that some defect in sporulation existed at the procedure later than the meiosis, such as FSM formation. Here, I describe analysis of FSM formation in septin mutants and the localization of septins during sporulation in more detail, which suggests that septin structures act as backbones for FSMs to extend in an orientated manner.

MATERIALS AND METHODS

Strains and media

Strains used in this chapter are listed in Table 3. Media used in this study were identical to those in Chapter II. C-terminal tagging with GFP or RFP at the endogenous loci or deletion of the gene with *kanMX6* module was done by PCR-based method using 80-mer oligonucleotides with 60-bp homologies to targeting gene [63]. Primer sets used for amplification were:

Dspn2Fw (for *spn2*$^+$ deletion):
5'- tacaatgttgacttggccaaaaccaacaaattccaaattcattcaattcgcaacttgcaacggatccccgggttaattaa-3'
Cspn2Fw (for *Spn2*$^+$ C-terminal tagging):
5'-atgggaagtcccgcacctgtgtacccttctgaaccacatctccatacagccaccgctcaacggatccccgggttaattaa-3'
Dcspn2Rv (for *spn2*$^+$ deletion and C-terminal tagging):
5'- gacagtcatacaaatggtttagtctttgttctaaacatactatatattaccttaggaagagaattcgagctcgtttaaac-3'
Proper integration at the locus was confirmed by PCR with appropriate primers.

Plasmids construction

Site-directed mutagenesis of *spn2*$^+$ was done by the methods described by

Sawano and Miyawaki [64] with a primer 5'- aaccaacagttaattcaacaaggt-3'. Plasmids pMAL(spn2N), pMAL(spn5N), pMAL(spn6N), and pMAL(spn7N) were constructed as follows: N-terminal half of gene ORFs were cut out from pT7(*spn2*$^{+}$) (*Bgl* II-*Acc* I, 1-408 bps), pT7(*spn5*$^{+}$) (Bgl II-Hind III, 1-561 bps), pT7(*spn6*$^{+}$) (*Bgl* II-*BamH* I, 1-585 bps), and pT7(*spn7*$^{+}$) (*Bgl* II-*BamH* I, 1-594 bps). The fragments were inserted into the *Bgl* II-*Hinc* II, *Bgl* II-*Hind* III, *Bgl* II, and *Bgl* II sites of the pMALBB vector, respectively. pMALBB vector was generated by inserting *Bgl* II linker into the *Bam* HI site of pMAL-cRI expression vector (NEB). A plasmid pAU(Spo3-HA) was generated by inserting a *Bam* HI-*Sac* I fragment containing *spo3*$^{+}$ promoter and ORF flanked by the C-terminal HA tag and the *nmt1* terminator from pAL(spo3-HA) [11] into pAU-SK. A plasmid pREP41(GFP-PH^{Osh2}-dimer) was constructed by swapping the DNA fragment containing two copies of Osh2 PH domains between two GFPs from pTL511 [65] (a kind gift from T. Levine) to pREP41. A plasmid pREP41(GFP-PH^{FAPP1}) was constructed as follows: a DNA fragment coding for the PH domain of FAPP1 was amplified by RT-PCR from total RNA extracted from a human epitherial cell line A431, using following primers

5'- cagatct(*Bgl* II)tatggaggggtgttgtacaag-3' and

5'- ctcgag(*Xho* I)ttaccttgtatcagtcaaacatgc-3'. Amplified fragment was cloned into pT7 blue vector, and subcloned into the *Bgl* II-*Xho* I sites of pGFT41. A plasmid pREP41(GFP-PH$_2^{Cla4}$) was constructed as follows: a DNA fragment containing the PH domain of Cla4 was amplified by PCR from *S. cerevisiae* genome, using primers

5'-cagatct(*Bgl* II)caaaaaaaaaagcgggtgggtgtcc-3' and

5'-tggatcc(*BamH* I)cttaataatggacatttagcaaaaatgg-3', and were cloned into pT7. Two copies of PH domain sequences were cut out from pT7 with combination of *Bgl* II-*BamH* I and *Bgl* II-*Sal* I, then ligated tandemly into the *Bgl* II-*Xho* I sites of pGFT41. A template plasmid for RFP tagging by PCR-based method was generated by inserting mRFP5 sequence from pFA6a-mRFP5-His5 (a kind gift from T. Yoko-o, unpublished) into the *Bam* HI-*Bgl* II sites of pFA6a-kanMX6. A plasmid pAL(Gms1-GFP) was kindly provided by K. Takegawa [66] (Kagawa University).

Fluorescence microscopy

Cells were fixed with 3.7 % formaldehyde at 30 °C for 1h, collected, and washed with PEM buffer (100 mM PIPES (pH 6.9), 1 mM EGTA, and 1 mM $MgSO_4$). Cells were

incubated with PEMS (PEM with 1.2 M Sorbitol) containing 1 mg/ml Zymolyase 20T at 37 °C for 10 min. and treated with PEMS containing 1% Triton X-100 for 1 min., followed by washing with PEM three times. Immunostaining of HA-tagged proteins were done by combination of a rat anti-HA high-affinity antibody (1:200, Roche) and Alexa595-conjugated goat anti-rat IgG (1:10000, Molecular Probes) in PEMBL (PEM containing 1 % BSA and 1 % Lysine-HCl). The nuclear chromatin region was stained with 4',6-diamidino phenylindole (DAPI) at 1 mg/ml. F-actin was stained with Tetra-Methyl-Rhodamine-Phalloidine (Sigma). Cells were observed by a fluorescence microscope, Zeiss Axiovert 100. For 3D deconvolution, raw images were captured at 2 μm intervals using IPLab 3.6 software. Time lapse imaging was done as follows. MM-N media containing 1.2 % agarose-S (Wako) was dropped on the glass surface of a glass-bottomed dish. The solidified media was removed from the dish, and cells were spotted on the flat surface of the media, put back on the dish to sandwich the cells between the glass and the media. 6-8 Z-sections at 5 μm intervals were captured by each 1 min. under the control of IPLab 3.6, and the obtained image sequence was stacked along the Z-axis by "Max intensities" method.

Electron microscopy

Cells were mounted on a copper grid to form a thin layer and immersed in liquid propane cooled with liquid nitrogen (Leica EM CPC, Leica Mikrosystems, Vienna, Austria). The frozen cells were transferred to 2% Os04 in dry acetone and kept at -80 °C for 3 days and warmed gradually from -80 °C to 0 °C over 5 h ,held for 1 h at 0 °C , warmed from 0°C to 23°C(room temperature) for 2 h.(Leica EM AFS, Leica Mikrosystems). After washing with dry acetone three times, the samples were infiltrated with increasing concetrations of Spurr's resin in dry acetone and finally with 100% Spurr's resin. After polymerization, ultrathin sections were cut on an ultramicrotome (Leica Ultracut UCT, Leica Mikrosystems), and stained with uranyl acetate and lead citrate. The sections were viewed on an electron microscope(H-7600, Hitachi Co., Tokyo, Japan) at 100kV.

Protein-lipid overlay assay

E. coli strain *BL21* harboring plasmids for MBP-fusion proteins was cultured at 15 °C for 2days. MBP-fusion proteins were purified by the standard method [67]. 2.5 μl of

lipid solution containing 100 pmol of phosphoinositides dissolved in chloroform/methanol (1:1) was spotted onto a Hybond-C extra membrane (Amersham) and dried at room temperature. All phosphoinositides were purchased from WAKO co. Ltd. (Tokyo, Japan). The membrane was incubated with 3 % fatty acid-free BSA in TBS-T (10mM Tris-HCl (pH 8.0), 150mM NaCl, and 0.1 % Tween-20) for 1 h, and then with the TBS-T containing 0.5 μg/ml of the MBP fusion proteins overnight at 4 °C. Proteins interacted with phosphoinositides were detected with an anti-MBP monoclonal antibody (Santa Cruz) and an HRP-conjugated anti-mouse antibody (Biosource International).

Table 3. Yeast strains used in Chapter III.

Name	Description	Source of reference
THP18	*h^{90} ade6-M216 ura4-D18 leu1-32*	(Koga et al., 2004)
MO246	*h^{90} ade6-M216 ura4-D18 leu1-32 spn1Δ::ura4^{+}*	this study
MO250	*h^{90} ade6-M216 ura4-D18 leu1-32 spn2Δ::ura4^{+}*	this study
MO371	*h^{90} ade6-M216 ura4-D18 leu1-32 spn3Δ::ura4^{+}*	this study
MO372	*h^{90} ade6-M216 ura4-D18 leu1-32 spn4Δ::ura4^{+}*	this study
TK144	*h^{90} ade6-M216 ura4-D18 leu1-32 spn5Δ::ura4^{+}*	this study
MO277	*h^{90} ade6-M216 ura4-D18 leu1-32 spn6Δ::ura4^{+}*	this study
MO229	*h^{90} ade6-M216 ura4-D18 leu1-32 spn7Δ::ura4^{+}*	this study
MO660	*h^{90} ade6-M216 ura4-D18 leu1-32 spn2Δ::ura4^{+} spn7Δ::LEU2*	this study
MO662	*h^{90} ade6-M216 ura4-D18 leu1-32 spn5Δ::ura4^{+} spn7Δ::LEU2*	this study
MO664	*h^{90} ade6-M216 ura4-D18 leu1-32 spn6Δ::ura4^{+} spn7Δ::LEU2*	this study
TK278	*h^{90} ade6-M216 ura4-D18 leu1-32 spn5Δ::ura4^{+} spn6Δ::LEU2*	this study
MO815	*h^{90} leu1-32 spn2^{+}-mRFP5::kanMX6*	this study
MO684	*h^{90} ade6-M210 ura4-D18 leu1-32 spn2Δ::kanMX6*	this study
MO599	*h^{90} ade6-M216 ura4-D18 leu1-32 pik1Δ::ura4^{+}*	this study
MO701	*h^{90} ade6-M216 ura4-D18 leu1-32 spn2^{+}-GFP::kanMX6*	this study
MO817	*h^{90} leu1^{+}::GFP-psy1^{+}*	this study
MO822	*h^{90} ura4-D18 pik1Δ::ura4^{+} leu1^{+}::GFP-psy1^{+}*	this study
MO832	*h^{90} ura4-D18 pik1Δ::ura4^{+} leu1^{+}::GFP-psy1^{+} spn2^{+}-mRFP5::kanMX6*	this study

RESULTS

Septin mutants extend forespore membranes in a disorientated manner

Examination of FSMs using Spo3-GFP as a marker protein in *spn5*Δ cells revealed that signals of Spo3p-GFP were not well-shaped, leaving bare nuclei, whereas the signals in wild-type cells exhibited cup shaped structures or spheres surrounding four meiotic nuclei (Fig. 13A) [11]. Spo3-GFP in *spn2*Δ, *spn6*Δ, *and spn7*Δ gave essentially the same result (data not shown). Time-lapse analysis of FSM extension in *spn5*Δ using GFP-Psy1, another FSM marker driven by the from *nmt41* promoter, which gave the bright signal [11], was performed (Fig. 13B). At the onset of FSM extension, some FSMs extended to the opposite side to the counterpart, and formed small spheres (Fig. 13B, arrows). Membranes then grew to the size of normal spore membranes but with aberrant shape (Fig. 13B, 20'-50'). Other FSMs which extended to the proper direction seemed to follow the normal procedure of spore membrane formation. Nine, three, and two images for *spn5*Δ, *spn6*Δ, and *spn5*Δ*spn6*Δ, respectively, gave essentially the same results (data not shown). DIC images in Figure 13C indicates that if FSMs enclosed the nuclei, they maturated with thick spore wall that appeared as double lined thick peripheral rim (Fig. 13C, arrowheads). In contrast, FSMs without nucleus did not maturate (Fig. 13C, arrows), suggesting that incorporation of nuclei is required for formation of mature spore. To analyze in more detail, electron-microscopic analysis was performed with *spn2*Δ, *spn5*Δ, or *spn6*Δ diploid cells. Compared to the wild-type cells whose nuclei were always engulfed by spore membranes, FSMs in septin-deleted cells frequently left bare nuclei behind (Fig. 14, arrows). Although FSMs appeared to start extension close to SPBs (Fig. 15, arrowheads), images of a curved FSM facing to the side opposite to nucleus or a small sphere locating next to he nucleus were obtained, confirming time lapse experiment of GFP-Psy1 (Fig. 15, arrows). Another finding to be noted is the uneven extension of FSMs from the position of SPBs in septin-deleted cells (Fig. 15, arrowheads). Correlation between uneven extension and disorientated extension is unknown. These results indicate that septins were important for proper extension of FSM in an orientated manner, and that formation of aberrant numbers of spores in septin mutants may be due directly to the reduced fidelity of FSM extension to right direction.

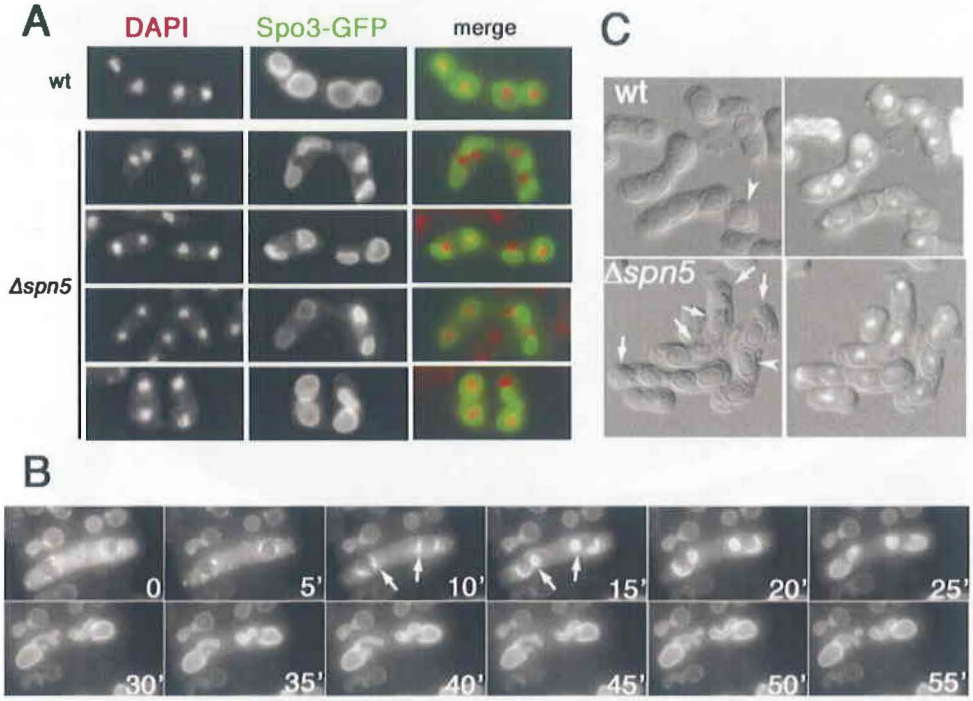

Figure 13 Sporulation of *spn5*Δ cells

(A) Disorientated FSM extension in Δ*spn5* cells. Strains THP18 (wild type) and TK144 (Δ*spn5*) harboring pAL(spo3-GFP) were precultured on an MM plate for 12 h, transferred onto an SSA plate, and incubated for 12 h. Images of Δ*spn5* show the cells leaving four, three, two, or one bare nuclei (from top to bottom). (B) Representative time-lapse images of aberrant FSM extension in Δ*spn5* cells. In my observation with nine independent zygotic asci (i.e., 36 spores), 15 FSMs extended in a disorientated manner. (C) DIC images of sporulating cells (left columns). Same images are overlaid with DAPI images on the right side. Wild type cells always form mature spores with double lined thick peripheral rim, whereas Δ*spn5* contains some immature spores without nuclei (arrows).

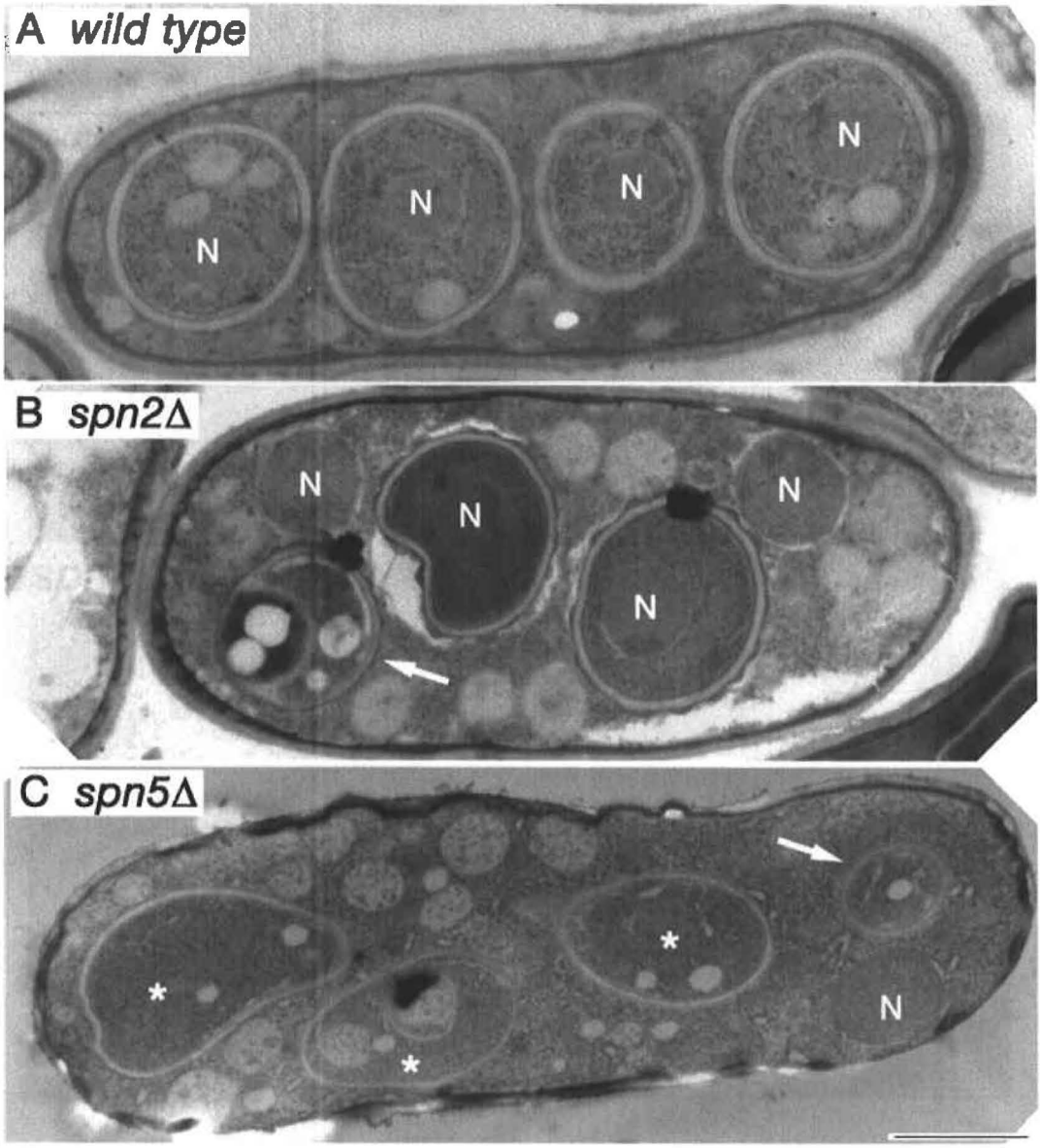

Figure 14 Electron microscopic analysis

Strains TW747 (wt/wt), MO705 (Δ*spn2*/Δ*spn2*), or TK172 (Δ*spn5*/Δ*spn5*) were pregrown on an MM+N plate for 12 h, transferred onto an MM-N plate, and incubated for 6 h. (A) a sporulating wild-type cell. All of the four nuclei were encompassed by FSM. (B) a representative image of sporulation of Δ*spn2*. Two out of four nuclei were not encapsulated by FSMs. The arrow indicates a FSM extended opposite to the nucleus. (C) a representative image of sporulation of Δ*spn5*. FSM failed to encompass the nucleus (arrow) Three nuclei are not seen in this section (asterisks). Bar, 2 μm.

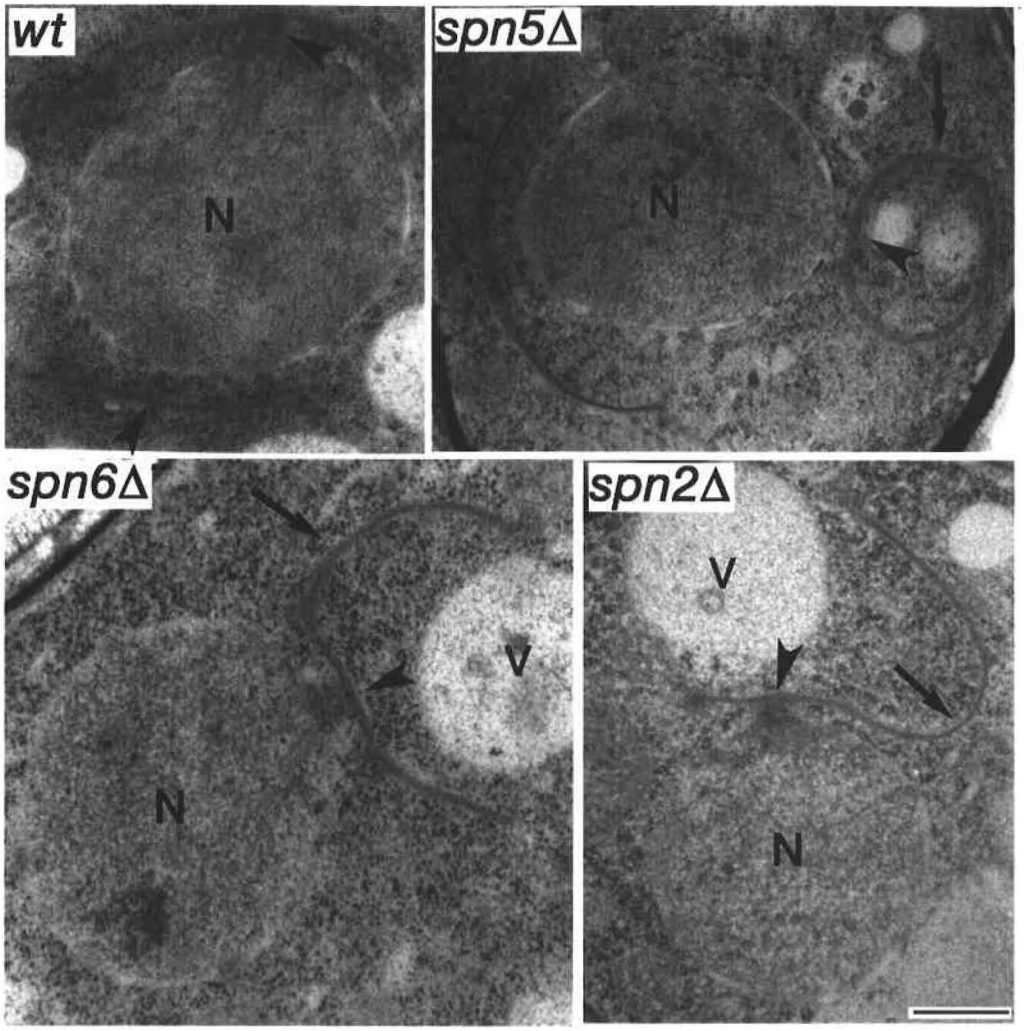

Figure 15 Enlarged images of extending FSMs.

FSM extended from nearby the SPB (arrowheads) but curved to the opposite side to the nuclei or already become a small sphere without nucleus (arrows) in septin-deleted cells. Strains, TW747 (wt/wt), MO705 (Δ*spn2*/Δ*spn2*), TK367 (Δ*spn6*/Δ*spn6*), and TK172 (Δ*spn5*/Δ*spn5*). Bar, 0.5 μm.

Septins form horseshoe like structure along the extending forespore membrane

To address how septins regulate growth direction of FSMs, localization of septins during sporulation was examined in detail. Spn2p-RFP and Spn5p-GFP, Spn6p-GFP, and Spn7p-GFP completely co-localized with each other, suggesting that these septins formed a complex as is the cases with vegetative septins [48] (Fig. 16A). Figure 16B shows time-lapse images of GFP-Spn2p in a sporulating cell. Four punctuate dots were formed as the diffuse signal of GFP-Spn2p disappeared, then the dots altered their shape to the 'horseshoe'-like filamentous structures. Finally, four even-sized rings were formed (Fig. 16C). To see the spatial and temporal relationship among nuclear division, elongation of the septin structure, and FSM; both HA-tagged Spo3p and GFP-Spn5p were expressed in a cell. Figure 17 shows the images of Spo3p-HA and GFP-Spn5p along the procedure of meiotic nuclear division. Preceding the second meiotic chromosome segregation, both Spo3p-HA and GFP-Spn5p appeared as four punctuate dots or arcs adjacent to the poles of the nuclei (Fig. 17 a). As the meiosis II proceeded, septin formed 'horseshoe', whereas FSMs grew to form cups surrounding the nuclei (Fig. 17b,c). Finally GFP-Spn5p formed rings at the equatorial plane of each spherical sac of prespores (Fig. 17d). Considering the fact that septin-deleted cells show aberrant extension of FSMs, it is likely that septin structure support FSM for proper growth orientation to form spheres.

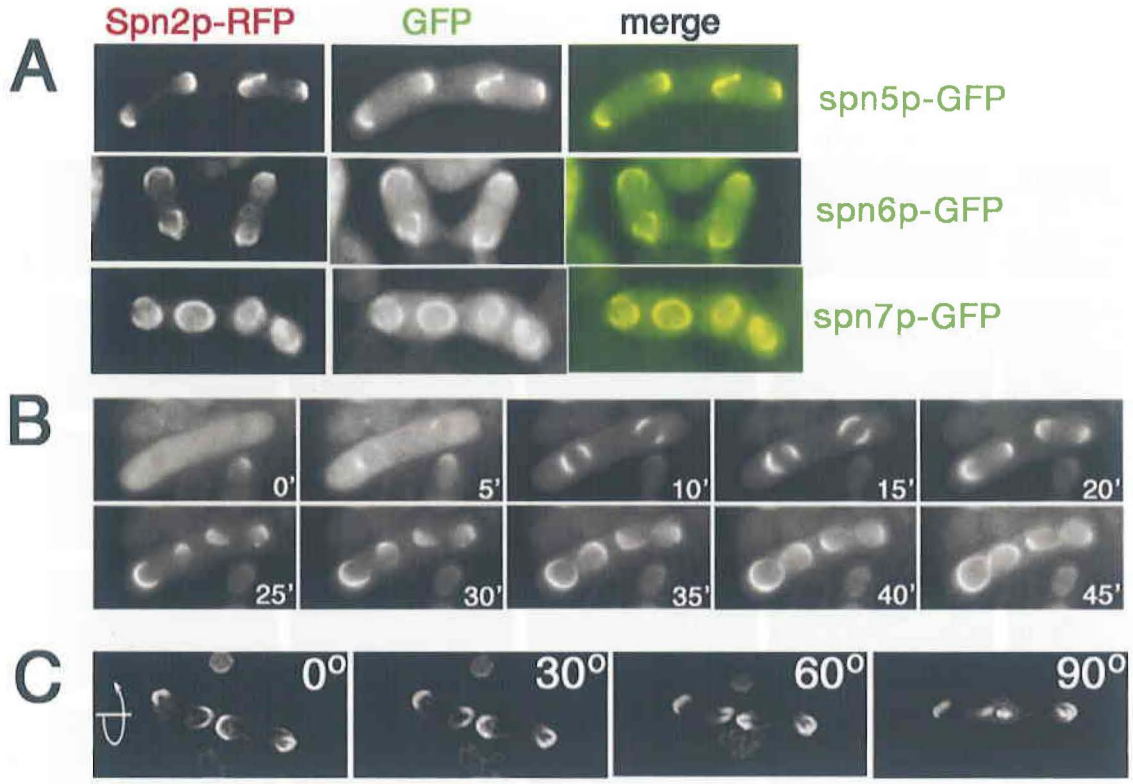

Figure 16 Septins form horseshoe-like structures

(A) colocalization of septins during sporulation. Sporulation of strain MO815 (*spn2*$^{+}$-*mRFP5::kanMX6*) harboring pAL(spn5-GFP), pAL(spn6-GFP), or pAL(spn7-GFP) were induced and localization of GFP and RFP were observed by fluorescence microscopy. (B) GFP-Spn2p formed horseshoe-like structures which maturated to four rings. Wild type strain THP18 harboring pREP41(GFP-spn2) was cultured under the sporulation condition, and was observed by the time lapse microscopy as described in EXPERIMENTAL PROCEDURES. GFP-Spn2p under the control of *nmt41* promoter was used to benefit bright signals for short exposure time. (C) Rotated view of three-dimensional deconvoluted images for Spn2p-GFP. Strain, MO701 (*spn2*$^{+}$-GFP).

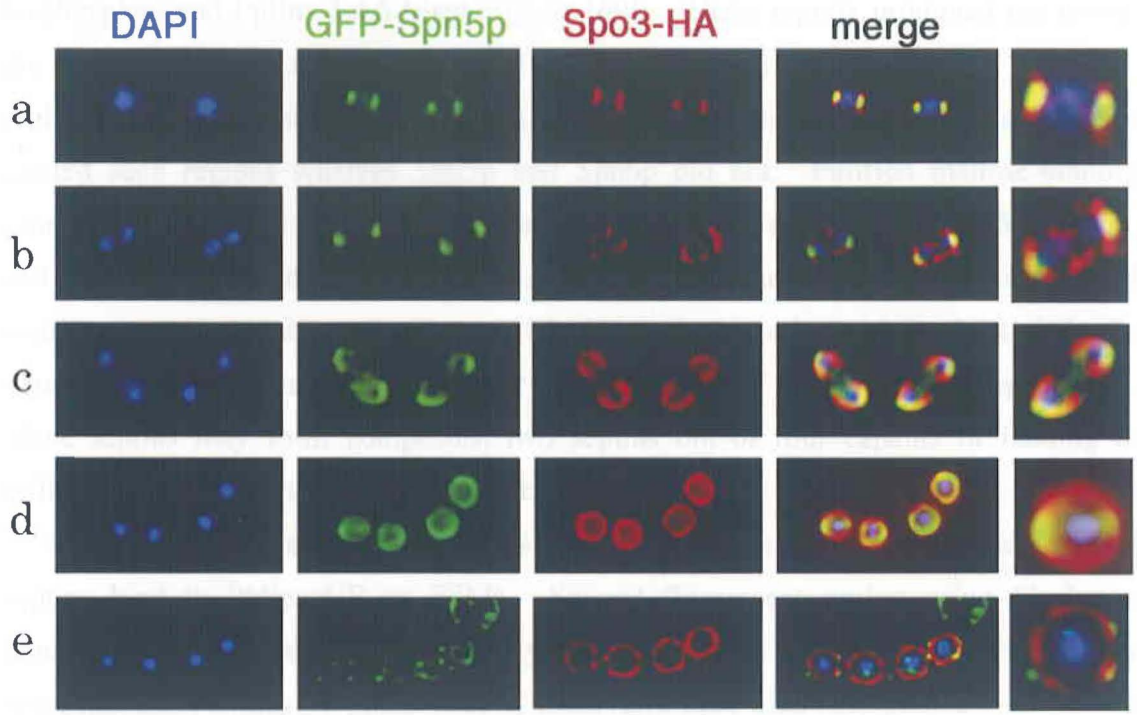

Figure 17 Horseshoe-like structure localize at the equatorial plane of the FSM

Wild type strain THP18 harboring pREP41(GFP-spn5) and pAU(spo3-HA) was immunostained with an anti-HA antibody. Two-dimensional projections of three-dimensional deconvoluted images captured by 2μm interval for z-axis were aligned along the procedure of meiosis II. a, metaphase ; b and c, anaphase ; d, telophase of meiosis II. e, septin rings in a mature ascus disappeared as the signals of Spo3-GFP declined. Magnified images are shown in right.

Septins bind PtdIns(4)P which is enriched on forespore membranes

To act as a cytoskeletal backbone for FSMs, septins should have an ability to interact with FSMs. Recently, Casamayor and Snyder reported that budding yeast mitotic sepitns directly bind to PtdIns(4)P and PtdIns(5)P *in vitro* via their amino-terminal polybasic regions [68]. Mammalian septin H5 are also known to bind PtdIns 4,5-bisphosphate and PtdIns 3,4,5-trisphosphate [69]. These reports prompted me to test the phosphoinositide binding ability of *S. pombe* septins. I searched for polybasic regions within the septins in sporulation. As shown in Figure 18A, Spn2p and Spn7p carried such regions whereas Spn5p and Spn6p did not. Purified maltose-binding protein (MBP) fusion proteins containing N-terminal halves of Spn2p, Spn5p, Spn6p, and Spn7p, were tested for their binding ability to phosphoinositides by the protein-lipid overlay assay. As shown in Figure 18B, N-terminal portions of Spn2p and Spn7p bound to PtdIns(4)P and to PtdIns(5)P whereas those of Spn5p and Spn6p did not. Since septins may form complexes, two septins out of four capable of binding to PtdIns(4)P can be sufficient for a whole complex to interact with membrane.

Since PtdIns(5)P has not been found in eukaryote, I postulated that septins bind to PtdIns(4)P on FSMs. Several fluorescent probes using Pleckstrin homology (PH) domain with affinity to PtdIns(4)P have been developed for visualization of PtdIns(4)P, , but none of them have been used in *S. pombe*. Indeed no information about PtdIns(4)P localization in *S. pombe* have been reported to date. First of all, therefore, I tested properties of three PH domains to be used as a PtdIns(4)P probe in *S. pombe*. As shown in Figure 19A, GFP-PH^{FAPP1} [70] localized as intracellular dots probably representing Golgi, whereas GFP-PH^{Cla4}[71] localized to the plasma membrane. Differential localization of these domains suggests that they cannot be used as probes for general PtdIns(4)P localization in *S. pombe*. Recently, PH domain of GFP-PH^{Osh2}-dimer was developed as a probe which can represent both Golgi-pool and plasma membrane-pool of PtdIns(4)P in *S. cerevieiae* [65]. In vegetative *S. pombe* cells, this probe localized strongly at the septa and weakly on the plasma membrane, and also localized as intracellular dots presumably representing Golgi-apparatus (Fig. 19B). These localizations are similar to those in *S. cerevisiae* suggesting that GFP-PH^{Osh2}-dimer successfully works as general PtdIns(4)P probe in *S. pombe*. Signals were not affected by the deletion of *pik3*$^{+}$/*vps34*$^{+}$, a PtdIns 3-kinase, suggesting that this localizations was independent of 3'-phosphorylated

phosphoinositides (PtdIns(3)P, PtdIns(3,4)P_2, PtdIns(3,5)P_2, PtdIns(3,4,5)P_3) (data not shown). During sporulation, GFP-PH^{Osh2}-dimer was enriched on FSMs, while the signals on the plasma membrane and the Golgi apparatus disappeared or declined (Fig. 19B). These results suggest that PtdIns(4)P is enriched on FSMs during sporulation and that septins may bind to the lipid.

In *S. cerevisiae*, there are two type III PtdIns 4-kinases genes, *PIK1* and *STT4*. Pik1p and Stt4p synthesize PtdIns(4)P on the plasma membrane and on the Golgi apparatus, respectively [72] [70] [73]. *S. pombe* genome contains putative counterparts of both genes. *S. pombe pik1*Δ strain is viable unlike its counterpart in *S. cerevisiae*. Under the nitrogen starvation condition, *pik1*Δ cells exhibited no defect in meiotic nuclear division (Fig. 20B), but formed asci without visible spores (Fig. 20A). GFP-Psy1p appeared adjacent to the poles of metaphase II nuclei in *pik1*Δ as well as in wild-type cells (Fig. 20B), but remained as small aberrant membranes that finally became four masses. These results suggest that Pik1p plays an important role in sporulation. However, GFP-PH^{Osh2}-dimer successfully localized even on these aberrant FSM-like structures although localization on Golgi apparatus during vegetative growth was totally abolished by *pik1* deletion (Fig. 19C), suggesting that Pik1p was not responsible for PtdIns(4)P production on FSM. Rather, it is likely that Pik1p is required for PtdIns(4)P production on Golgi membrane which is important for membrane trafficking between Golgi apparatus and FSM. An observation that Spo3p-GFP, an FSM protein newly synthesized after nitrogen starvation condition, did not localize at FSM in *pik1*Δ cells but accumulated as intracellular dots may support this idea (Fig. 20C). Localization of these dots were similar to that of Golgi membrane protein Gms1p, suggesting that Spo3p was not transported out of the Golgi apparatus [66](Fig. 20C). In contrast, Spn2p-GFP in Δ*pik1* were always accompanied by FSM-like membranes (Fig. 20D). A notable observation was that some short bandles of septin structure extended opposite to nuclei (17-36%) and most rings were apart from the nuclei (76-89%), suggesting that intact FSM is required for proper extension of septins. Taken together, $pik1^+$ plays important role during FSM formation, but is related neither to the production of PtdIns(4)P on FSM nor to the septins. I was not able to set up a condition in which no PtdIns(4)P present on FSM because another putative PtdIns 4-kinase gene, $stt4^+$, was an essential gene (K. Takegawa, personal communitcation).

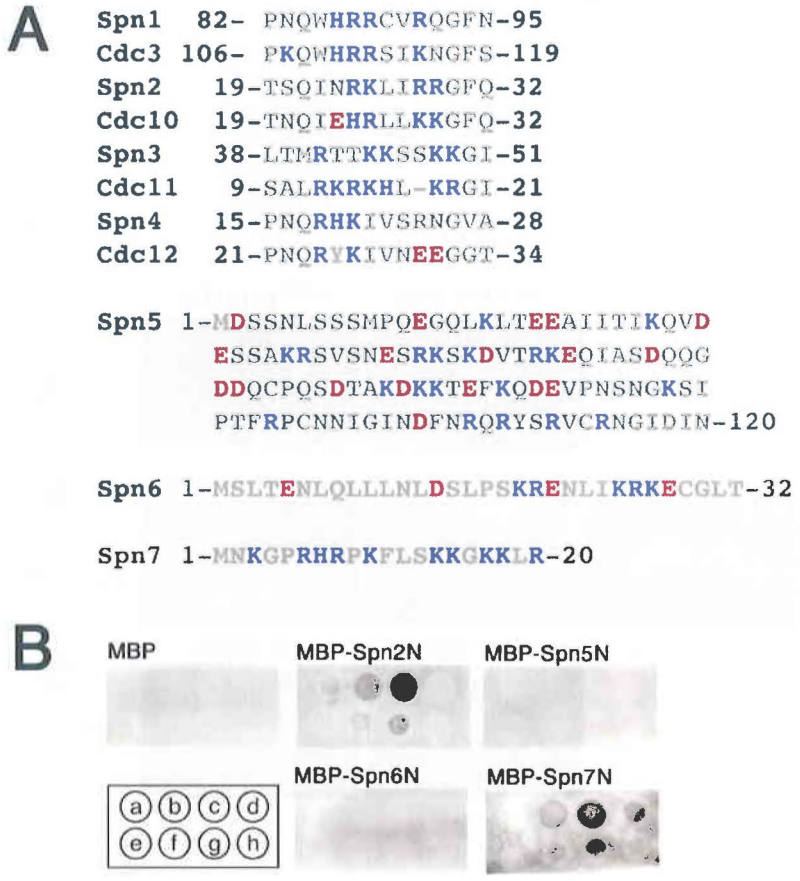

Figure 18 Two septins interacted with phosphoinositides *in vitro*

(A) Spn2p and Spn7p contained clusters of basic residues. Basic residues of Spn1p-Spn4p were aligned with their *S. cerevisiae* counterparts. Asterisks indicate conserved basic amino acids. For Spn5p-Spn7p, whole sequences of N-terminal extension were shown. Numbers indicate amino acid positions; asterisks indicate conserved basic amino acids; basic and acidic amino acids are colored in blue and red, respectively. (B) Spn2p and Spn7p bound to PtdIns(4)P and PtdIns(5)P in protein-lipid overlay assay. 100 pmol of each phosphoinositides were spotted at the positions shown in the left hand bottom; a, PtdIns; b, PtdIns(4)P; c, PtdIns(5)P; d, PtdIns(4,5)P_2; e, PtdIns(3)P; f, PtdIns(3,4)P_2; g, PtdIns(3,5)P_2; h, PtdIns(3,4,5)P_3. This experiment was performed with the truncated septin proteins: Spn2p, 1-135 aa.; Spn5p, 1-248 aa.; Spn6p, 1-194 aa.; Spn7p, 1-198 aa. Small, uneven signals (such as seen in MBP-Spn2N, position g) are non-specific backgrounds because they were not dose-dependent.

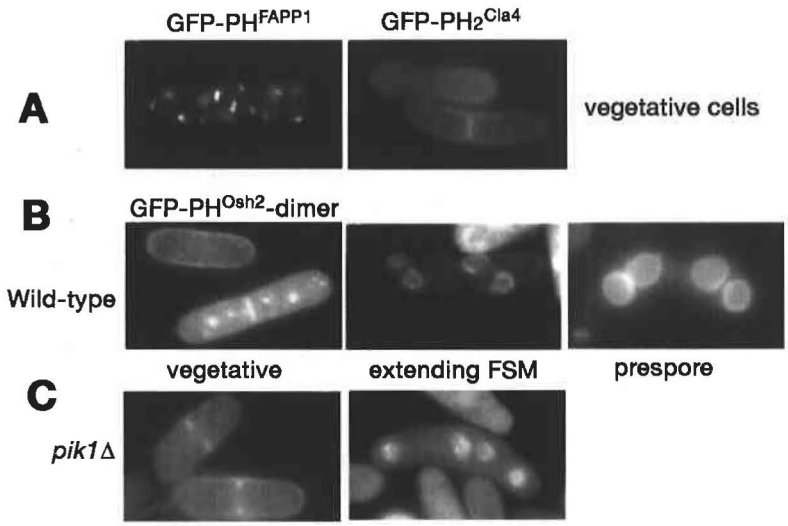

Figure 19 PtdIns(4)P is enriched on the FSM

(A) localization of PtdIns(4)P probes in *S. pombe*. Wild-type strain THP18 harboring pREP41(GFP-PH^{FAPP1}) or pREP41(GFP-PH_2^{Cla4}) were cultured overnight in MM media at 27 °C. Localization of these probes was suggested to represent the restricted pool of PtdIns(4)P. (B) localization of GFP-PH^{Osh2}-dimer. THP18 harboring pREP41(GFP-PH^{Osh2}-dimer) were cultured overnight in MM media (left). Sporulation of the same strain was induced sporulation in MM-N media for 8 h (middle and right) at 27 °C. (C) localization of GFP-PH^{Osh2}-dimer in *pik1*Δ cells. Strain MO599 (*pik1*Δ*::ura4*$^+$) harboring pREP41(GFP-PH^{Osh2}-dimer) was cultured as in (B). Localization of GFP-PH^{Osh2}-dimer at Golgi was totally abolished in this mutant but its localization at FSM was not affected.

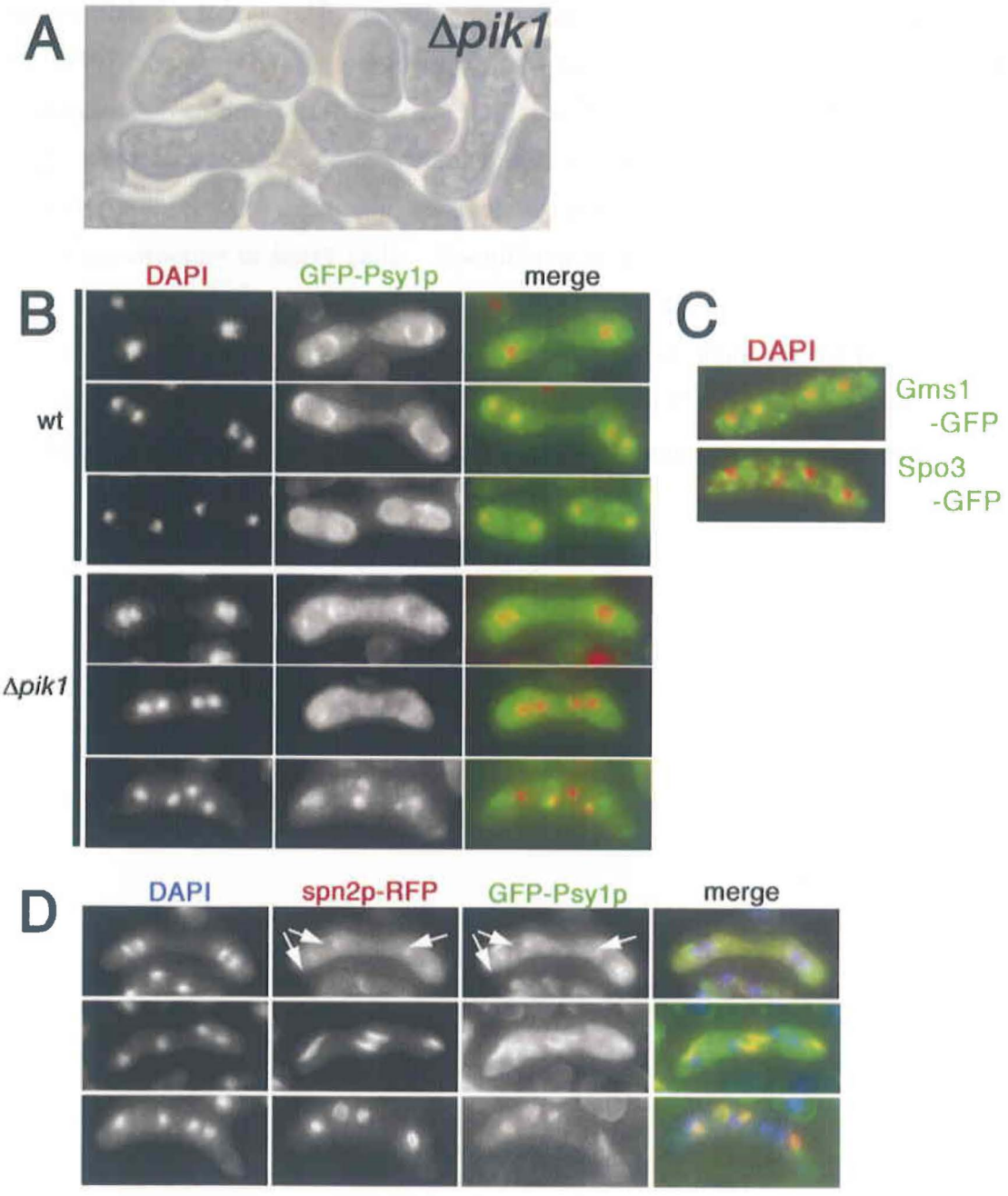
A
Δpik1
B
DAPI
GFP-Psy1p
merge
wt
Δpik1
C
DAPI
Gms1
-GFP
Spo3
-GFP
D
DAPI
spn2p-RFP
GFP-Psy1p
merge

Figure 20 Pik1p plays important role in sporulation

(A) Δ*pik1* cells completely failed to sporulate. Strain MO599 (Δ*pik1*) was cultured on an SSA plate for 2days. No spores were visible under the phase-contrast microscope. (B) GFP-Psy1p revealed the presence of FSM-like membrane structure in Δ*pik1* cells. Sporulation of strains MO817 (*leu1*$^{+}$::GFP-*psy1*$^{+}$) and MO822 (Δ*pik1*, *leu1*$^{+}$::GFP-*psy1*$^{+}$) were induced. Cells in metaphase II, anaphase II, and telophase II of each strain (top to bottom, respectively) are shown. (C) Spn2p is associated with FSM-like membrane structure in Δ*pik1* cells. Sporulation of strain MO832 (Δ*pik1*, *leu1*$^{+}$::GFP-*psy1*$^{+}$, *spn2*$^{+}$-mRFP5::*kanMX6*) were induced. (D) Sporulation of strain MO599 (Δ*pik1*) harboring pAL(spo3-GFP) was induced on SSA plate for 12 h. No signal representing FSMs was observed. Instead, Spo3-GFP distributed as dots (lower panels), which was similar to Gms1-GFP, a Golgi membrane protein (upper panels).

PtdIns(4)P binding activity of Spn2p is important for septin filament to bind to forespore membranes in vivo.

The conserved basic residues in Spn2p were substituted by uncharged glutamine residues (24-RKLIRR-29 to 24-QQLIQQ-29). The resulting protein, Spn2p^{QQLIQQ}, showed only faint signal at the spot of 500 pmole PtdIns(4)P in the protein-lipid overlay assay (Fig. 21A). Spn2p^{QQLIQQ}-GFP successfully formed filaments or rings in Δ*spn2* cells (Fig. 21B), suggesting that the mutant protein could act as a subunit of the septin complex, and that binding of Spn2p to PtdIns(4)P was dispensable for polymerization of septins. However, the mutation *spn2*^{QQLIQQ} abolished the activity to complement the defect in sporulation of Δ*spn2* cells (Fig. 21C). It is likely that the mutation weakened the interaction between septin filament and FSM, resulting in the failure to encapsulate nuclei. To address this, spatial relationship between Spn2p^{QQLIQQ}-GFP and HA tagged Spo3p in Δ*spn2* was examined. In these cells, FSMs extended separately from septin filament, making it impossible for FSM to determine the orientation of its extension. This result supports the idea that septins bind to PtdIns(4)P on FSMs allowing extension in a orientated manner (Fig. 21D, E). Septins apart from FSMs frequently drifted away from the nuclei (Fig. 21D, E), suggesting that FSMs may be required partly for proper positioning of septins. Taken together, it is likely that septin filaments are the backbone of FSM giving them regulated extension to engulf the nuclei.

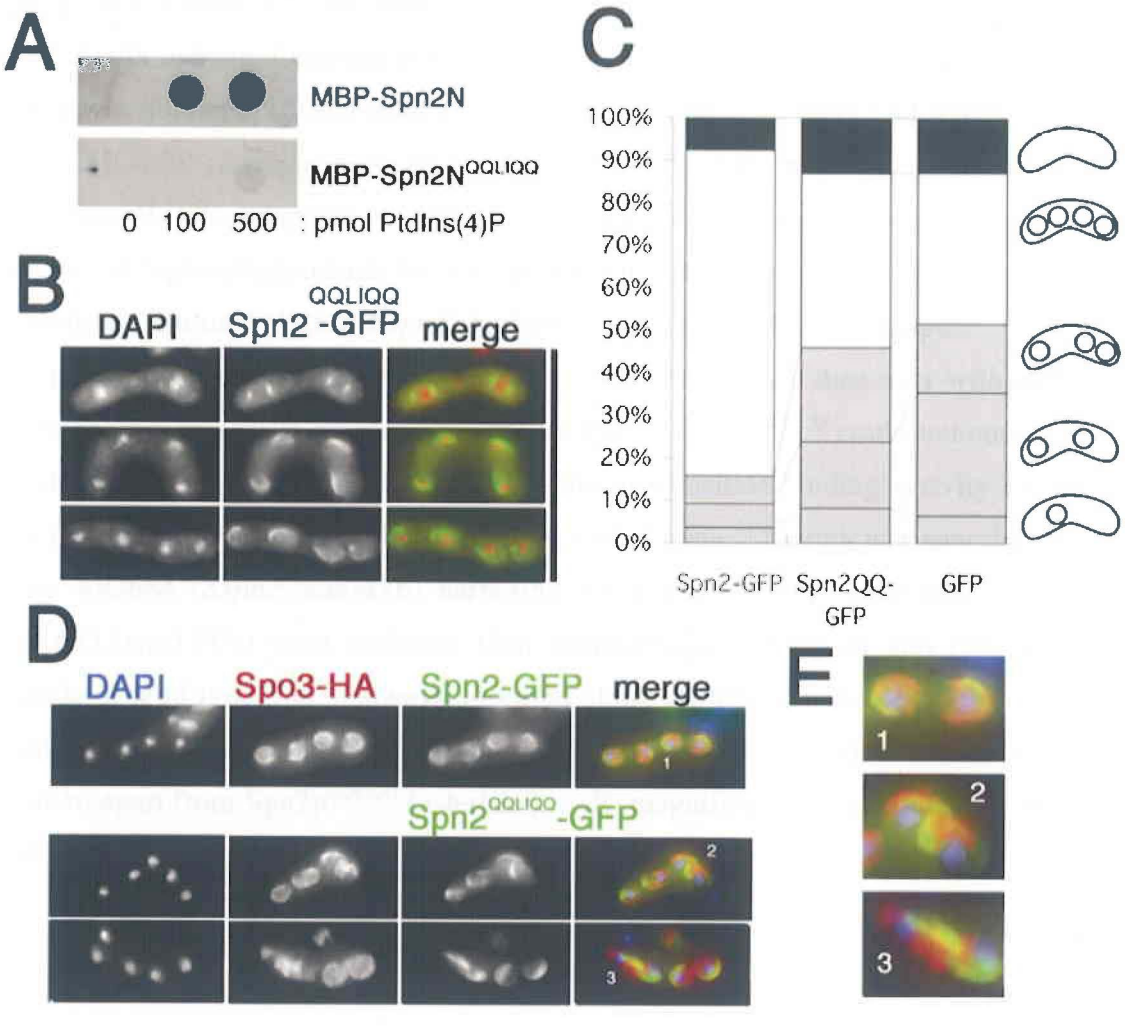
A
MBP-Spn2N
MBP-Spn2N^QQLIQQ
0 100 500 : pmol PtdIns(4)P
B
DAPI
Spn2^QQLIQQ -GFP
merge
C
100%
90%
80%
70%
60%
50%
40%
30%
20%
10%
0%
Spn2-GFP
Spn2QQ-GFP
GFP
D
DAPI
Spo3-HA
Spn2-GFP
merge
Spn2^QQLIQQ-GFP
E
1
2
3

Figure 21 Phosphoinositide-binding activity of Spn2p is required for proper FSM extension

(A) mutations in basic residues of Spn2p abolished its binding activity to PtdIns(4)P in vitro. Interaction of a wild type or a mutant (24-RKLIRR-29 to 24-QQLIQQ-29) Spn2p with PtdIns(4)P was tested by protein-lipid overlay assay, using membranes spotted with indicated amount of PtdIns(4)P. (B) phosphoinositide-binding activity of Spn2p was not required for formation of septin structures. Mating and sporulation of a strain MO250 (Δ*spn2*) harboring pAL(spn2^{QQLIQQ}-GFP) was induced. Cells in metaphase II (top), anaphase II (middle), and after completion of meiosis II (bottom) are shown. (C) phosphoinositide-binding activity of Spn2p was required for proper spore formation. Strain MO250 (Δ*spn2*) harboring pAL(spn2-GFP), pAL(spn2^{QQLIQQ}-GFP), and pAL(GFP) were incubated on an SSA plate for 2 days, then asci with different numbers of spores were counted as in Figure 10B. Spn2p^{QQLIQQ} could not complement the defect of Δ*spn2* in sporulation. (D) phosphoinositide-binding activity of Spn2p was required for FSMs to extend in contact with septins. Mating and sporulation of a strain MO684 (Δ*spn2::kanMX6*) harboring pAL(spn2-GFP) or pAL(spn2^{QQLIQQ}-GFP) and pAU(spo3-HA) were induced, then immunostained with an anti-HA antibody. Signals of wild type Spn2p always appeared along the FSMs which extended properly (top). In cells expressing mutant Spn2p, FSMs frequently extended in a disorientated manner, apart from Spn2p^{QQLIQQ} (asterisks). (E) magnified images around the numbers in (D).

DISCUSSION

In this chapter, I analyzed the function of septin genes in sporulation of fission yeast. Deletion of one of the four septin genes, *spn2*$^{+}$, *spn5*$^{+}$, *spn6*$^{+}$, and *spn7*$^{+}$, caused disorientated extension of the FSM, resulting in formation of aberrant number of spores per ascus (Fig. 10, 13-15). Appearance of healthy spores is about 40-60%, implicating that the sporulation efficiency depends on the probability whether FSMs extend toward right or wrong direction. Fluorescence and electron micrographic analysis revealed that FSM extension occurred normally, but the probability of extension toward the right direction at the early stage is lower in septin-deleted cells than in wild-type cells. Septins form the structure that dramatically alters its shape from 'horseshoe' to a ring at the equatorial plane of spherical spore membrane, suggesting that there may be regulated elongation of septins on the FSM (Fig. 16).

Septins in various organisms forms ring structures. For example, septins in budding yeast form a ring at the bud neck [28]; purified Sept2/6/7 from mammalian cells form a ring *in vitro*, and the same complex becomes spiral structure when actin stress fiber are destabilized by cytochalasin D treatment *in vivo* [37]; septins form a ring at the annulus of the mouse spermatozoon [40]. These observations suggest that septins have a nature to polymerize in a constant curvature to form a ring or a spiral. Therefore, it is likely that a septin structure polymerized in a constant curvature acts as a backbone of an FSM so that the FSM can extend to the proper direction.

As described above, there are two machineries that have been proposed to contribute to formation of the spore membrane, SPB and LEPs. However, these two machineries may not be sufficient for the proper extension of FSMs. This is because FSMs are likely to be fragile and flexible, requiring assistance of some solid frame between SPBs and LEPs. I propose septins as a third member of machinery that contributes to the extension of the FSM. This will solve the question how the growing membrane curves to form a sac. Further analysis of sporulation focusing on these components should be a great hint to understand common mechanism how biological membranes assemble to form their shapes.

I also showed that Spn2p and Spn7p bound to PtdIns(4)P and PtdIns(5)P *in vitro*, through the clusters of basic residues in their N-terminal regions (Fig. 18). Spn5p and Spn6p did not bind to phosphoinositides, having no obvious basic regions in

the N-termini. N-terminal extensions of Spn5p and Spn6p may have roles other than binding to phosphoinositides, although I could not exclude the possibility that failure of these proteins to bind phosphoinositides was due to low quality of the purified proteins.

Because PtdIns(5)P has not been identified in yeasts whereas PtdIns(4)P is routinely identified by several methods [19] [20] [74], I hypothesized that Spn2p and Spn7p interact with the latter phosphoinositide on the FSM. To date, no information about the localization of PtdIns(4)P has been given in *S. pombe*. Two commonly used fluorescent probes for PtdIns(4)P, GFP-PH^{FAPP1} and GFP-PH_2^{Cla4}, localized differently, suggesting that these probes could not be used as a general probe for PtdIns(4)P in *S. pombe* (Fig. 19A). Recently, it has been reported that the PH domain of FAPP1, a protein that mediates vesicle traffic at the trans Golgi, exhibits the affinity to ARF on the Golgi membrane in addition to PtdIns(4)P [75]. Indeed GFP-PH^{FAPP1} localized at the Golgi apparatus in *S. pombe*. In contrast Cla4 is a *S. cerevisiae* kinase that function on the plasma membrane [71], and GFP-PH_2^{Cla4} localized at the plasma membrane in *S. pombe*. It is likely that this localization may be due to the additional affinity of this PH domain to the unknown target as is the case with GFP-PH^{FAPP1}. Therefore, these probes may not really reflect the localization of PtdIns(4)P in *S. pombe*. Another PtdIns(4)P probe, GFP-PH^{Osh2}-dimer, localized both at Golgi apparatus and plasma membrane, suggesting that this may be a good probe for PtdIns(4)P (Fig. 19B). Signals of this probe at Golgi apparatus were abolished by the deletion of *pik1*$^+$, a putative Golgi-associated PtdIns 4-kinase, supporting this idea (Fig. 19C). GFP-PH^{Osh2}-dimer revealed that PtdIns(4)P is present on the FSM (Fig. 19B).

Mutations in Spn2p PI-binding regions caused dissociation of septins from FSMs, and the mutant protein could not complement the sporulation defect of *spn2*Δ (Fig. 21). These results suggested that septins interact with FSMs through PtdIns(4)P and the interaction was important for function of septins *in vivo*. However, this binding activity to phosphoinositides was not required for septins to elongate because mutant Spn2p could elongate apart from FSMs. Moreover, septins formed rings in *pik1*Δ although it harbored aberrant membrane structure instead of intact FSM. Taken together, septin elongation requires neither interaction with membrane nor intact FSM. In agreement with this, it has been shown that septins have a nature to polymerize and form a ring or a spiral structure *in vitro*, independent of membranes [37]. On the other hand, some data suggested that direction of elongation and positioning of septin

structure was somewhat dependent on FSMs. The septin structure in the cells carrying Spn2p^{QQLIQQ} or in *pik1*Δ cells often failed to extend toward right direction, and drifted away from nuclei (Fig. 21D and Fig. 20B). As septins function to enhance the fidelity of orientated extension of FSMs, FSMs may help septin structure to elongate in an orientated manner. Thus, septins and FSMs may cooperate to develop in a proper orientation.

There are two putative type-III PtdIns 4-kinase genes in *S. pombe*. Between them, contribution of *pik1*$^{+}$ to PtdIns(4)P production on FSMs is denied in this study (Fig. 20). Δ*pik1* forms aberrant FSM-like structures, resulting in complete failure to form spores. However, aberrant FSM-like structure in *pik1*Δ contained PtdIns(4)P, indicating that Pik1p was not responsible for PtdIns(4)P production on FSM. Consistent with this, septin is associated even with the aberrant FSM-like structure. It is possible that another putative PtdIns 4-kinase gene, *stt4*$^{+}$, contributes to the production of PtdIns(4)P on FSM, although I could not investigate this possibility.

CHAPTER IV: IDENTIFICATION AND ANALYSIS OF SEPTIN INTERACTING PROTEINS

INTRODUCTION

Septin interacting proteins

Septins have been shown to be involved in various cellular processes as discussed in **GENERAL INTRODUCTION.** Analysis of molecules physically or genetically interacting with septins revealed many aspects of septin functions. Budding yeast Gin4, Kcc4p, and Hsl1p are such examples. These Nim1-related kinases localize to the bud neck septin ring, influence the septin ring organization, and are required for proper control of G2/M transition of the cell cycle [76]. Identification of Gin4-family kinases as septin-interacting molecules therefore shed light on a novel aspect of septin function to control cell cycle as a regulator of Nim1-Wee1-Cdk1 mediated mitotic checkpoint cascade [76]. In mammalian cells, septin interacting proteins, Syntaxin-1A, MAP4, and Anillin, are involved in exocytosis, microtubule organization, and actin stabilization, respectively, suggesting contribution of septins in these cellular processes [36] [38] [37]. Thus, identification and analysis of sepitn-interacting proteins may be useful to understand the function of septins in sporulation [77] [51] [78] [79]. In this chapter, I searched for proteins physically associate with sporulation septins in *S. pombe* by yeast two-hybrid screen and identified Moe1p, Plb1p, and Meu4p, as Spn2p binding proteins. Among them, *moe1*Δ was defective in sporulation. I therefore further analyzed *moe1*$^{+}$ for its physical and genetic interaction with *spn2*$^{+}$.

Moe1p

Moe1p is a protein playing diverse roles in yeast cells (Fig. 22), which is evolutionally conserved among mammals, fly, and fission yeast [80]. Moe1p was first identified in fission yeast as a binding protein of Scd1p, a guanine-nucleotide exchanging factor for spCdc42p, by yeast two-hybrid screen [80]. Subsequently, Int6p has been found to form a stable complex with Moe1p, and this complex was suggested

to regulate cell division and chromosome segregation via the ubiquitin-mediated proteasome [81] [82]. The Moe1p/Int6p complex directly interacts with Rpn5p in the 19S lid regulatory subcomplex of 26S proteasome in this process, and was required for degradation of polyubiquitinated proteins including securin/Cut2p and cyclin/Cdc13p [82]. Accumulation of these proteins and unidentified other targets in the cells may cause various defects in cell cycle progression. Consistently, human Int-6 localized at the mitotic spindle and silencing of it inhibited Cdk1 by activation of Wee1, resulting in abnormal mitosis completion [83] [84]. On the other hand, Moe1p and Int6p are required for formation of stable translation initiation complex, sharing amino-acid sequences highly homologous to the eukaryotic translation initiation factor subunits, p66 (eIF3d) and p48 (eIF3d), respectively [85,86] [87]. Although Moe1p/Int6p complex are not required for global translation since polysome profile are not affected by deletion of these genes [88], recent works showed that a restricted set of mRNAs associated with affinity-purified Int6p complex [89]. Because both of the eIF3 complex and the proteasome lid complex are evolutionally related to the COP9 signalosome (CSN) complex sharing some components, it is prospected that Moe1p/Int6p also regulate CSN to trigger Skp1/Cullin-1/F-box (SCF) E3-ligase mediated ubiquitinylation of proteins [90]. These results suggest that the Moe1p/Int6p complex may play a role in regulation of protein levels by degradation via the proteasome as well as by translation of mRNA. Besides these functions, each of Moe1p and Int6p may play some role independently: Fission yeast Mal3p was identified as a Moe1p interacting protein, with which Moe1p cosedimented with microtubules *in vitro*, probably independent of Int6p [91]. Overexpression of truncated Int6p upregulated Pap1-mediated transcription independent of Moe1p [92]. Taken together, proteins such as Moe1p and Int6p are multifunctional protein which can form complexes with various cellular components. Therefore, it was possible that Moe1p contributed to the formation of FSM in cooperation with septins.

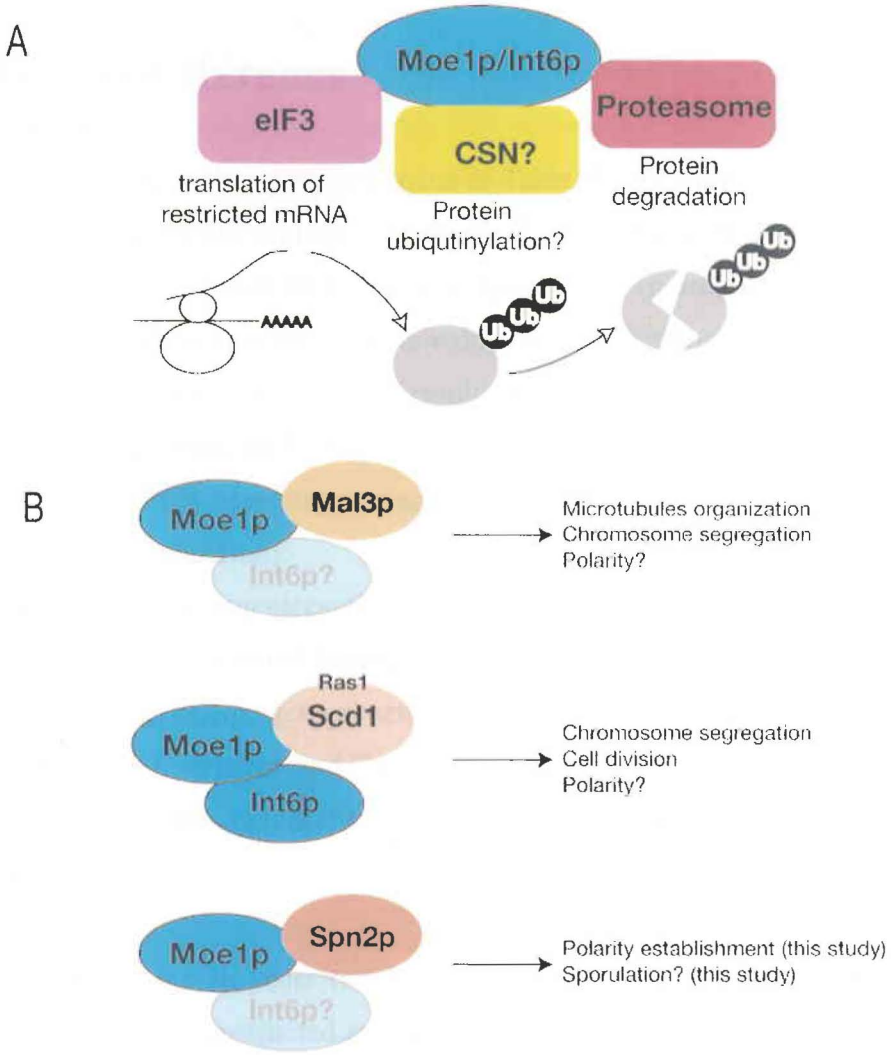

Figure 22 Moe1p

(A) Molecular function of Moe1p. The known functions of the Moe1p/Int6p complex that are illustrated. Moe1p/Int6p interact with eIF3 complex to regulate translation (left), and with 19S lid regulatory subcomplex of 26S proteasome to regulate proteolysis (right). Interaction of Moe1p/Int6p with CSN to trigger SCF E3-ligase mediated ubiquitinylation is predicted but has not been elucidated (middle). The Moe1p/Int6p complex may control protein levels through these interactions.

(B) Biological function of the Moe1p. Proteins interact with Moe1p are listed in left hand. Biological significance of each interaction are described in the right hand.

MATERIALS AND METHODS

Strain construction

Strains used in this study are listed in Table 4. Because *moe1*Δ cells did not grow in the synthetic media such as MM or SD, I was not able to transform this strain with plasmid for expression of GFP-Psy1p or Spo3p-GFP, in order to observe the FSM. Therefore, *moe1*Δ cells were crossed with wild-type cells harboring genomic integrated plasmid pBR(*leu1*$^+$::*GFP-psy1*$^+$). The resulting strain, MO820 (*moe1*Δ *leu1*$^+$::*GFP-psy1*$^+$), was viable allowing me to observe GFP-Psy1p in the rich media.

Primer sets used for PCR-based tagging and deletion were:

Dmoe1Fw (for *moe1*$^+$ deletion):

5'-cccagttcgtttgcacactatactggcgtccacttcgaagaaaacttcaccactcccaaacggatccccgggttaattaa-3'

Cmoe1Fw (for *moe1*$^+$ C-terminal tagging):

5'-gttccacccaacacttttgaagaagctgctggaccctcccttgaagcttcttctactgctcggatccccgggttaattaa-3'

DCmoe1Rv (for *moe1*$^+$ deletion and C-terminal tagging):

5'-ttgcacatgtaattgagtattatacatgtaacctttttaatgaactttctacatccgtccgaattcgagctcgtttaaac-3'

Plasmid construction

Plasmids used in yeast two-hybrid screen are listed below in this section. pART4(Flag-spn2) was constructed as follows: *Bam* HI linker was inserted into the *Nco* I site of pFLAG-CMV (lab stock), and resulting plasmid was digested with *Bam* HI and *Hind* III to yield a fragment containing FLAG sequence. This fragment and *Hind* III-*BamH* I fragment of pT7(*spn2*$^+$) containing the *spn2*$^+$ ORF, were ligated into the *BamH* I site of pART4 expression vector[18]. pREP41(HAmoe1ΔXhoI) was constructed by inserting *Not* I-*Xho* I fragment of pMH08 into the *Not* I-*Xho* I site of pGFT41[8]. pMH08 was isolated by yeast two-hybrid screen, which contained a *moe1*$^+$ sequence corresponding to 8-385 aa. of Moe1p. The *Bam* HI- *Xho* I fragment of pREP41(HA-moe1) was substituted with the fragment obtained by digestion of pBluescript SKII with *Bam* HI and *Xho* I, which contained the multiple-cloning site, to yield pREP41(HA). Full-length *moe1*$^+$ ORF was amplified by genomic PCR using primers

5'-cagatct(*Bgl* II)ccactcccaaatggcaactgg-3' and

5'- gtcgac(*Sal* I)ttaagcagtagaagaagcttcaagg-3', and was cloned into pT7 to yield pT7(*moe1*$^+$). The *moe1*$^+$ ORF was subcloned into the *Bam* HI-*Xho* I site of

pREP41(HA) to yield pREP41(HA-Moe1p) A plasmid for bacterial expression of GST-Moe1p was constructed by inserting the *moe1*$^+$ ORF cut out from pT7(*moe1*$^+$) with *Bgl* II and *Sal* I into the relevant site of pGEXBB. A plasmid for bacterial expression of GST-Spn2p was constructed by inserting the *spn2*$^+$ ORF cut out from pT7(*spn2*$^+$) with *Bgl* II and *Xho* I into the relevant site of pGEXBB. pGEXBB was generated by inserting a *Bgl* II linker (cgcagatctgag) into the *Bam* HI site of pGEX4T3 (Amersham Biosciences Corp). An integration plasmid pBR(*leu1*$^+$::*GFP-psy1*$^+$) for expression of GFP-Psy1p from *psy1*$^+$ promoter was kindly gifted by T. Nakamura (Osaka City University). This plasmid was digested with *SnaB* I before the transformation to allow the integration at the *leu1*$^+$ locus.

Yeast two-hybrid screening

This was done by Matchmaker system, following a distributor's manual (Clontech). In brief, a *S. cerevisiae* strain *AH109* was sequentially transformed with the bait and the prey libraries, and Ade$^+$ His$^+$ colonies were subsequently tested for galactosidase activity on an SD plate containing X-alpha-Gal. The prey plasmids were recovered from Gal$^+$ cells and the DNA sequences of the inserts were determined using a primer, 5'- taccactacaatggatgatg-3'. Full length *spn2*$^+$, *spn5*$^+$, *spn6*$^+$, and *spn7*$^+$ were inserted into *BamH* I-*Sal* I sites of pGBKT7 to yield the bait plasmids. As prey libraries, I used commercially distributed *S. pombe* library (Clontech) based on pGADGH and newly constructed "sporulation library".

"Sporulation library" was constructed as follows: sporulation of a diploid strain TW747 was induced on an SSA plate for 9 h. The cells were collected, and whole RNA was isolated as described in Chapter II. Poly-A RNA was purified using an Oligotex$(dT)_{30}$ column and reverse transcriptase reaction was done using 5'-(*Xho* I)-$(dT)_{15}$-(G/C/A)-3' as a primer. After the second strand synthesis, *EcoR* I adaptor (5'-aattcgcggccgcgtcgac-3' and 5'- gtcgacgcggccgcg-3' were hybridized) was ligated to the ends. The resulting dsDNA fragments were digested with *Xho* I. The fragments were loaded onto a 1.5 % agarose gel, and >400 bps dsDNA was excised out. The fragments were eluted from the gel and ligated into the *EcoR* I- *Xho* I site of pGADT7. Average insert length and the number of independent clones were 1.8 kb and $2x10^6$, respectively.

Fluorescence microscopy

This was done as describe in chapter III unless otherwise described. Immunostaining of Moe1p was done with an rabbit anti-Moe1 (1:20) (see below) and alexa-488 conjugated goat anti-rabbit IgG. Tubulin staining was done with a mouse TAT-1 antibody (1:10) [93] (a gift from Dr. Keith Gull) and alexa-488 conjugated goat anti-mouse IgG. Calcofluor was dissolvevd in citrate-phosphate buffer (50 mM potassium phosphate, 50 mM sodium citrate, pH6.0, at the concentration of 50 μg/ml) and used for the staining of the cells.

Production and purification of the anti-Moe1p antibody

E. coli strain *BL21[DE3]* transformed with pGEX(moe1) was incubated at 15 °C for 2 days to allow expression of full-length Moe1p tagged with GST. The protein was purified from the culture with Glutathione sepharose 4B column, following the distributor's manual. For immunization, 500 μg of GST-Moe1 premixed with an equal volume of Freund's complete adjuvant were injected subcutaneously into rabbits. Injection of 250 μg of GST-Moe1 mixed with an equal volume of Freund's incomplete adjuvant was given every two weeks, starting from three weeks after from the first immunization. After three times of booster injections, anti-Moe1p serum was obtained. The serum could be used at a 1:500 dilution to recognize a single band of 62 kDa in the wild-type *S. pombe* lysate in western blotting. No such a band was detected in the lysate from *moe1*Δ (Fig. 25A).

Purification of anti-Moe1p antibody was carried out as follows: 250 μg of GST-Moe1p was separated by SDS-PAGE and transferred onto a PSMF membrane. The membrane piece containing GST-Moe1p was cut out and blocked with 3 % skim milk for 1 h. 500 μl of anti-Moe1p antiserum was incubated with the membrane piece at 4 oC for overnight in 7 ml TBS-Tween. Membrane was washed three times with TBS-Tween, and the bound antibody was eluted with 0.1M Glycin-HCl [pH2.0] followed by immediate neutralization with 1M Tris-HCl [pH 9.0]. 1% BSA and 0.1% sodium azide were added to the eluate to the antibody preparation.

Pull-down assay and Immunoprecipitation

Pull down assay of HA-Moe1p with GST-Spn2p was done as follows: *E. coli*

strain *BL21[DE3]* transformed with pGEX(spn2) was cultured at 15 °C for 2 days to express full-length Spn2p tagged with GST. *E. coli* cells were lysed in a lysis buffer (20 mM Tris-Cl [pH7.5], 150 mM NaCl, 5 mM EDTA, 10 % Glycerol, 1 mM DTT, and 1 % Triton-X100) by sonication. After removal of the cell debris by centrifugation, the lysate was incubated with Glutathione sepharose 4B beads. For each sample, approximately 5 μg of GST-Spn2p was bound to 3 μl beads. Wild-type *S. pombe* cells harboring pREP41(HA-moe1) was cultured in 10 ml MM media for 18 h to $1.0x10^7$ cells/ml density, diluted by four volumes of media, and then further cultured for 6 h to the cell deisity of $1.0x10^7$. Pelleted cells were lyzed in an equal volume of TNE buffer (20 mM Tris-Cl [pH7.5], 150 mM NaCl, 5 mM EDTA) containing 10 μg/ml leupeptin, 10 μg/ml pepstatin, and 2 mM PMSF by vortexing four times for 1 min. with glass beads (Sigma). Four volumes of TNE buffer containing protease inhibitors and 1.25% Triton-X100 was added and incubated at 4 °C for 20 min. to extract proteins. The extract containing 10-15 mg protein was constantly obtained from 100 μl cell pellet. 5 mg of the lysate was incubated with GST-Spn2p beads for 1 h and washed 3 times with the lysis buffer. After elution with SDS loading buffer (50 mM Tris-HCl [pH 6.8], 100 mM DTT, 2 % SDS, 0.1 % Bromophenol blue, and 10 % glucerol), samples were resolved by SDS-PAGE.

Co-immunoprecipitation of Flag-Spn2p and HA-Moe1p was done as follows: Strain MO684 (*spn2Δ::kanMX6)* harboring pART4(Flag-spn2) and pREP41(HA-moe1) was incubated and cell extract was prepared as described above. 5 mg of cell lysate was incubated with protein-A agarose conjugated with a mouse anti-FLAG mAB (Santa Cruz) at 4 °C for 1 h. Beads were washed four times with TNE containing 1% Triton-X100, then the bound proteins were eluted with SDS loading buffer and resolved by SDS-PAGE. For detection of HA-Moe1p and FLAG-Spn2p, a mouse anti-HA mAB(12CA5) and the anti-Flag mAB, respectively, were used in combination with an HRP-conjugated goat anti-mouse antibody (Biosource International). The bands were visualized by ECL detection system (Amersham).

Table 4. Yeast strains used in Chapter IV.

Name	Description	Source of reference
TW747	*h⁺/h⁻ ade6-M210/ade6-M216 leu1-32/leu1-32 ura4-D18/ura4-D18*	(Onishi et al., 2003)
THP18	*h⁹⁰ ade6-M216 ura4-D18 leu1-32*	(Koga et al., 2004)
MO725	*h⁹⁰ ade6-M210 ura4-D18 leu1-32 spn2-13myc::kanMX6*	this study
JY7 (SG14)	*h⁹⁰ leu1-32*	(Gutz et al., 1974)
MO731	*h⁹⁰ leu1-32 moe1Δ::kanMX6*	this study
MO820	*h⁹⁰ moe1Δ::kanMX6 leu1⁺::GFP-psy1⁺*	this study
MO835	*h⁹⁰ ade6-M216 ura4-D18 leu1-32 moe1Δ::kanMX6 spn2⁺-GFP::kanMX6*	this study
MO665	*h⁹⁰ ura4-D18 leu1-32 spn2Δ::ura4⁺*	this study
MO730	*h⁹⁰ ura4-D18 leu1-32 spn2Δ::ura4⁺ moe1Δ::kanMX6*	this study
MO701	*h⁹⁰ ade6-M216 ura4-D18 leu1-32 spn2⁺-GFP::kanMX6*	this study
MO246	*h⁹⁰ ade6-M216 ura4-D18 leu1-32 spn1Δ::ura4⁺*	this study
MO371	*h⁹⁰ ade6-M216 ura4-D18 leu1-32 spn3Δ::ura4⁺*	this study
MO372	*h⁹⁰ ade6-M216 ura4-D18 leu1-32 spn4Δ::ura4⁺*	this study

RESULTS

Identification of Spn2p binding proteins

To identify *S. pombe* proteins physically associate with septins expressed during sporulation, yeast two-hybrid screen was carried out using Spn2p, Spn5p, Spn6p, and Spn7p as baits. Among them, Spn7p could not be used because expression of DNA-binding domain (BD)-Spn7p in budding yeast harmed the cells, exhibiting septin mutant phenotype. Two prey libraries were used: a commercially distributed *S. pombe* library of vegetative cDNA (Clontech), and a "sporulation library" newly synthesized by my own (see **MATERIALS AND METHODS**). For the remaining three baits, BD-Spn2p, BD-Spn5p, BD-Spn6p, more than $2x10^6$ colonies were tested in combination with each bait/library. As a result, 17 clones were obtained from BD-Spn2p/vegetative library (named pCH01-pCH17) and 27 clones form BD-Spn2p/sporulation library (named pMH01-pMH27). BD-Spn5p and BD-Spn6p gave no Ade^+ His^+ colonies for unknown reason. After plasmid recovery and re-transformation to exclude the non-specific colonies, 6 and 12 clones out of pCH and pMH were found to be dependent on BD-Spn2p (Table 5), respectively. DNA sequencing of these 18 clones resulted in identification of 8 clones of *moe1*$^+$ (two from pCH and six from pMH), 2 clones of *meu4*$^+$ (from pMH), and 2 clones of *plb1*$^+$ (one each from pCH and pMH) (Fig. 23, Table 5). Other 6 clones contained genes coding for proteins involved in metabolism, mitochondrial proteins, or ribosomal proteins, those are often identified in yeast two-hybrid system by non-specific interactions.

Table 5 genes identified by yeast two-hybrid screening

Bait: Spn2p Library: vegetative

plasmid	gene name	systematic gene name	included aa/total	product	comment
pCH05	rps1801	SPBC16D10.11c	7-152/152	40S ribosomal protein S18	ribosomal
pCH08	plb1	SPAC1A6.04c	275-613/613	phospholipase B homolog	
pCH12	rps102	SPAC22H12.04c	11-229/252	40S ribosomal protein S3a	ribosomal
pCH19	gpd1	SPBC215.05	71-385/385	glycerol-3-phosphate dehydrogenase	metabolism
pCH44	moe1	SPAC637.07	5-385/567	translation initiation factor eIF3d	
pCH67	moe1	SPAC637.07	6-385/567	translation initiation factor eIF3d	

Bait: Spn2p Library: sporulation

plasmid	gene name	systematic gene name	included aa/total	product	comment
pMH01	moe1	SPAC637.07	8-385/567	translation initiation factor eIF3d	
pMH02	sdh1	SPAC1556.02c	359-641/641	succinate dehydrogenase	metabolism
pMH08	moe1	SPAC637.07	8-385/567	translation initiation factor eIF3d	
pMH10	meu4	SPAC1F8.05	153-182/182	meiotic expression upregulated	
pMH11	sdh1	SPAC1556.02c	359-641/641	succinate dehydrogenase	metabolism
pMH14	moe1	SPAC637.07	8-385/567	translation initiation factor eIF3d	
pMH16	gpm1	SPAC26F1.06	18-221/211	phosphoglycerate mutase	metabolism
pMH21	moe1	SPAC637.07	8-385/567	translation initiation factor eIF3d	
pMH23	meu4	SPAC1F8.05	153-182/182	meiotic expression upregulated	
pMH24	moe1	SPAC637.07	8-385/567	translation initiation factor eIF3d	
pMH26	moe1	SPAC637.07	8-385/567	translation initiation factor eIF3d	
pMH27	plb1	SPAC1A6.04c	482-613/613	phospholipase B homolog	

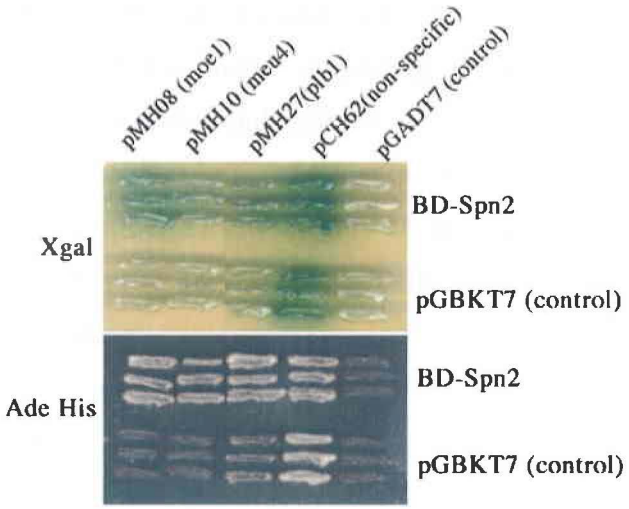

Figure 23 Yeast two-hybrid interactions of Moe1p, Meu4p, and Plb1p with Spn2p

S. cerevisiae strain *AH109* was co-transformed with the combination of plasmids listed top and right hand. Three colonies were picked up for each transformants, and streaked on a SD+Xgal plate (top panel) and a SD-Ade-His plate (bottom panel). Plates were incubated at 30 °C for two days.

Physical interaction of Spn2p and Moe1p

Given above results, I concluded that three of them might be the Spn2p interacting proteins. Among them, *meu4*$^+$ had already been identified a gene whose mRNA was upregulated upon nitrogen starvation although its function is still unknown [94,95]. It has been suspected whether or not *meu4*$^+$ mRNA is really translated because it contains strange amino acid composition[47]. Plb1p is a phospholipase B homolog that may catalyze release of fatty acid from lysophospholipids[96]. Recent reports suggest that Plb1p is required for nutrient-mediated repression of sexual differentiation upstream of the cAMP pathway[96]. Fungal Plb1 is not conserved in higher eukaryotes. In this study, I focused on Moe1p, because it was a highly conserved protein and was most repeatedly identified in my yeast two-hybrid screen.

First of all, physical interaction of Moe1p with Spn2p was analyzed. HA-tagged Moe1p expressed in *S. pombe* was successfully pulled-down by glutathione S-transferase (GST) tagged Spn2p purified from *E. coli* but not by GST alone (Fig. 24A). Co-immunoprecipitation of HA-Moe1p and FLAG-Spn2p was observed using an anti-HA antibody or an anti-FLAG antibody, suggesting the interaction of these proteins *in vivo* (Fig. 24BC). However, endogenous Moe1p was not detected in the immunoprecipitate of endogenously tagged Spn2p-13myc (Fig. 24D). The reason for this result can be due to either 1) low affinity of the binding of these proteins or 2) problem in experimental procedure such as inefficient immunoprecipitation or low sensitivity of immunoblotting.

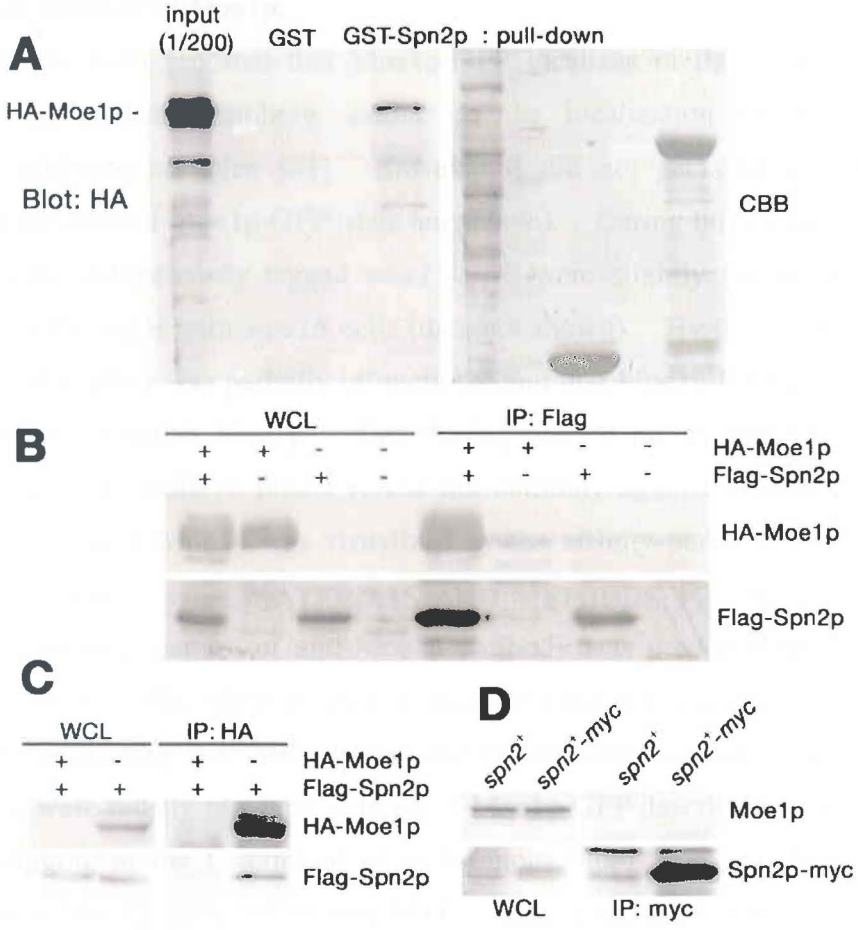

Figure 24 Physical interaction of Spn2p and Moe1p

(A) Pull-down analysis of interaction between Spn2p and Moe1p. GST control and GST-Spn2p bound to the glutathione beads were incubated with lysate from strain THP18 expressing HA-Moe1p. The HA-tagged proteins bound to the beads were analyzed by western blots using an anti-HA antibody (left). The presence of GST proteins on the glutathione beads was determined by Coomassie blue staining (right). (B)(C) co-immunoprecipitation of overproduced Spn2p and Moe1p. 5 mg of whole-cell lysates (WCL) from strain MO684 (*spn2Δ::kanMX6*) expressing indicated proteins were immunoprecipitated with 2 μg of anti-Flag antibody (B) or 50 μl of anti-HA antiserum conjugated to protein-A sepharose beads. The precipitates were analyzed by western blotting with an anti-HA or an anti-Flag antibody. 50 μg lysates were loaded onto each WCL lane. (D) endogenous Moe1p and Spn2p-HA did not co-precipitate. 40 mg ysates from strain THP18 (*spn2*$^{+}$) and MO725 (*spn2-myc*) were incubated with 5 μg anti-myc antibody conjugated protein A sepharose beads.

Localization analysis of Moe1p.

It has been reported that Moe1p-GFP localizes in the cytosol with slight enrichment at nuclear periphery, similar to the localization of proteasome and translation initiation complex [81]. However, I did not get such a result, having uniform distribution of Moe1p-GFP (data not shown). During this experiment, I found that cells with endogenously tagged *moe1*$^{+}$*-GFP* were slightly wider than wild-type cells, as were the cases with *moe1*Δ cells (data not shown). By this result, I suspected that *moe1*$^{+}$*-GFP* allele was partially infunctional and that Moe1p-GFP did not represent the localization of native Moe1p. This finding pushed me to detect localization of native Moe1p. To achieve this, I raised the antibody against Moe1p. Subcellular localization of native Moe1p was visualized by the affinity-purified rabbit polyclonal antibody against Moe1p (see **MATERIALS AND METHODS**, Fig. 25A). As shown in Figure 25B, staining pattern of anti-Moe1p antibody was predominantly cytosolic in growing wild-type cells, whereas only a faint background staining was observed in *moe1*Δ cells, suggesting that this antibody successfully detected native Moe1p. These localizations were mostly identical to those of Moe1p-GFP described above, suggesting that GFP tagging at the C-terminal of endogenous *moe1*$^{+}$ did not affect the global localization of Moe1p (data not shown, [81]). Moe1p did not localize to any specific structure including septins during sporulation (Fig. 25B). I have tried various conditions for staining of Moe1p, however, I did not detect any obvious changes in localization under any condition. This was true when Moe1p-GFP were used (data not shown). Staining of Moe1p in *spn2*Δ showed a pattern similar to that of wild-type cells (data not shown). These results suggest that localization of Moe1p does not depend on Spn2p although I cannot exclude the possibility that restricted pool of Moe1p interacting with Spn2p was not detectable in fluorescence microscopy, because Moe1p was much more abundant than Spn2p when both proteins were tagged with 3xHA and examined by western blots (data not shown). When HA-Moe1p and Flag-Spn2p were co-overexpressed, in contrast, these proteins colocalized at the region adjacent to the nucleus (Fig. 25C). This localization might be artificial, being induced by the overexpression of HA-Moe1p, because expression of HA-Moe1p alone was sufficient for its localization at this region (data not shown). Nonetheless, this result suggests that Spn2p and Moe1p can interact *in vivo,* although this localization may be artifitial.

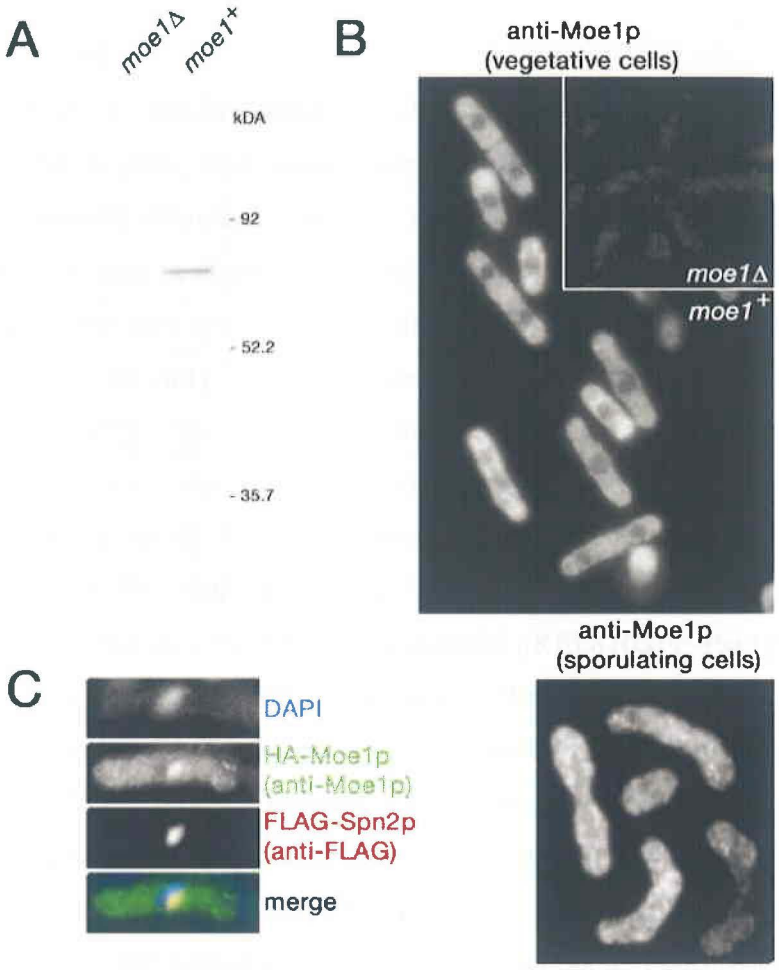

Figure 25 Localization of Moe1p

(A) Detection of endogenous Moe1p by an anti-Moe1p antibody. 50 μg lysates from strains JY7 (*moe1*$^{+}$) and MO731 (*moe1*Δ*::kanMX6*) were analyzed by Western blotting with anti-Moe1p antiserum at 1:500 dilution. (B) localization of Moe1p. Strains used in (A) were cultured overnight in YES media (left panel). Sporulation of the same strain were induced on an SSA plate for 12 h (right panel). Cells were fixed and immunostained with purified anti-Moe1p antibody at 1:20 dilution. (C) co-localization of overproduced HA-Moe1p and Flag-Spn2p. Strain THP18 harboring pREP41(HA-Moe1p) and pART4(FLAG-Spn2p) was incubated in MM media for 18 h at 30 °C. Cells were fixed and immunostained with purified anti-Moe1p antibody and an anti-FLAG antibody.

Sporulation of moe1Δ

Phenotype of *moe1*Δ during sporulation was examined. When cells were spread onto an MEA plate, they formed asci with aberrant number of spores whose shape were occasionally abnormal (Fig. 26A, arrows). It has been reported that *moe1*Δ exhibited several defects in chromosome segregation in mitosis, including monopolar spindle attachment and missegregation resulting in formation of a daughter cell without nucleus[80,81]. Consistently, *moe1*Δ had defect in meiotic chromosomal segregation. DAPI staining of *moe1*Δ cells revealed that they harbored chromosomes with abnormal shape (Fig. 26B). These cells frequently showed some defects in meiosis II, harboring uncorrectly segregated nuclei (Fig. 26B, arrows). To examine if Moe1p play any role during FSM formaion, morphology of FSMs in *moe1*Δ cells were observed. It was not possible to transform the *moe1*Δ cells with a plasmid pREP81(GFP-Psy1p) because this strain did not form colony in synthetic media. Therefore, I adopted expression of single copy GFP-Psy1p integrated at *leu1*$^+$ locus to visualize FSMs in *moe1*Δ cells. As shown in Figure 26C, FSMs extension did occur in *moe1*Δ but they frequently encompassed a nucleus which failed to undergo meiosis II or two nuclei within a sac. These results implicate that orientated FSM extension was not inhibited by the absence of Moe1p, unlike the case with *spn2*Δ cells. It is also notable that FSM extension was not orchestrated with meiosis II in *moe1*Δ cells. Consistently, assembly of septin structures successfully started at metaphase II in *moe1*Δ but most of them failed to form rings (Fig. 26D). This result may not be interpreted as direct effect of absence of Moe1p directly affected the septin ring formation. Rather, it was likely that predominant defects in meiosis of *moe1*Δ affected the structures of septin rings and FSMs as side effects. In conclusion, I could not find any functional relationship between Moe1p and Spn2p in the sporulation procedure. Further investigation such as the functional dissection of Moe1p into meiosis and the FSM formation would be required.

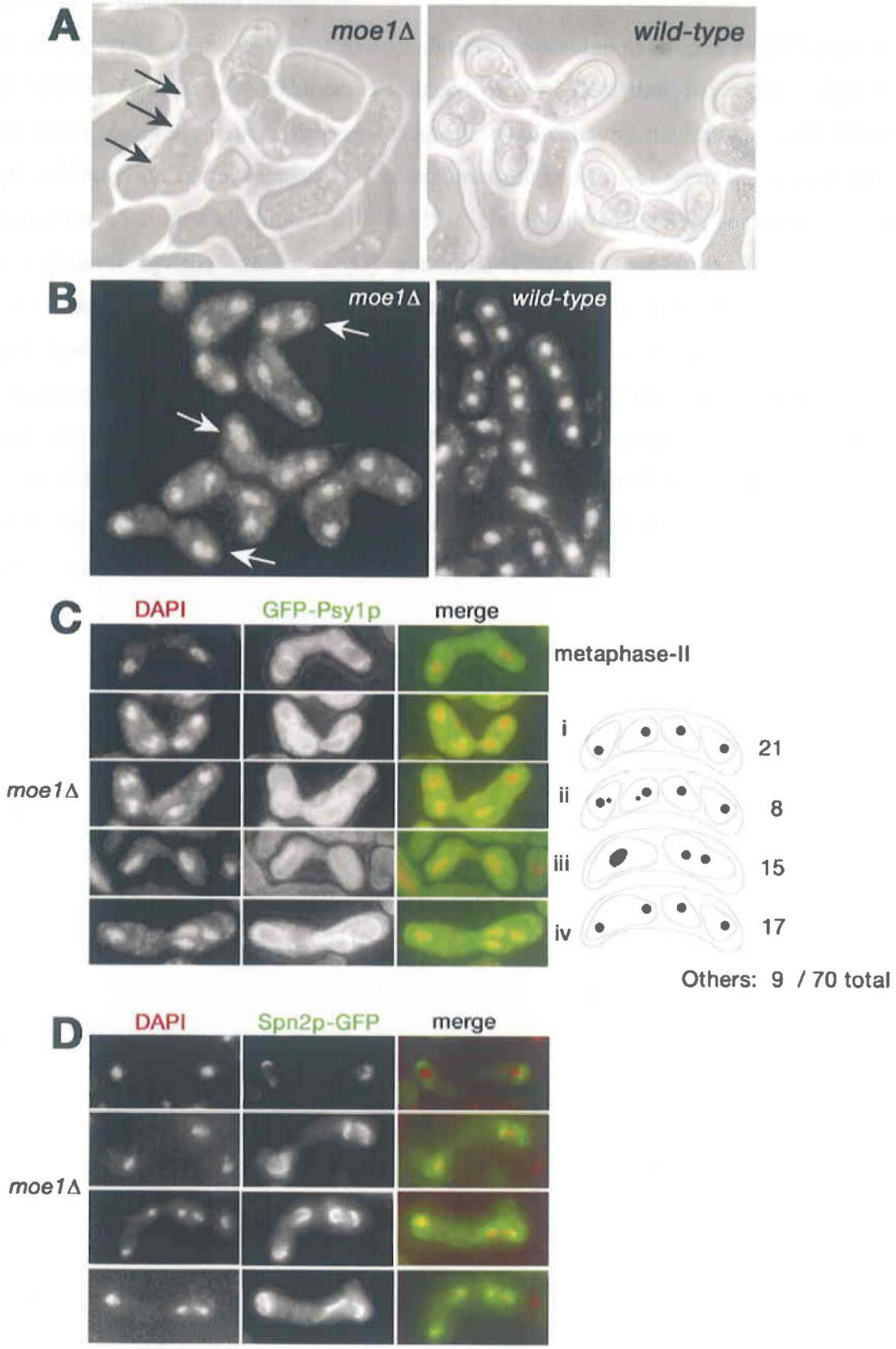
A
moe1Δ
wild-type
B
moe1Δ
wild-type
C
DAPI
GFP-Psy1p
merge
moe1Δ
metaphase-II
i
21
ii
8
iii
15
iv
17
Others: 9 / 70 total
D
DAPI
Spn2p-GFP
merge
moe1Δ

Figure 26 Sporulation of *moe1Δ*

(A) *moe1Δ* cells were devective in sporulation. Sporulation of strains JY7 (*moe1*$^{+}$) and MO731 (*moe1Δ::kanMX6*) were induced on an MEA plate for a day. Zygotes with incomplete tetrads with abnormal shapes are indicated by the arrows. (B) *moe1Δ* cells exhibited defect in meiosis. The cultures used in to (A) were fixed with 50 % ethanol for 15 min. and stained with DAPI. Unsegregated or over-segregated nuclei are indicated by the arrows. (C) abnormal FSMs in *moe1Δ*. Strain MO820 (*moe1Δ::kanMX6 leu1*$^{+}$*::GFP-psy1*$^{+}$) were precultured on a YEA plate for 18h, transferred onto an MEA plate, and incubated for 12 h. Cells were fixed with formaldehyde and stained with DAPI. Top panel indicates the FSMs extended from poles of metaphase-II nuclei. Panels below show the representative images of abnormal FSMs in *moe1Δ*. Schemes and counts for each panels are listed in right hand. (D) septin structure in *moe1Δ*. Sporulation of strain MO835 (*moe1Δ::kanMX6 spn2*$^{+}$*-GFP::kanMX6*) was induced as in (C).

Genetic interaction of spn2⁺ and moe1⁺

Genetic interaction of *moe1*$^+$ with *spn2*$^+$ was examined. It was reported that *moe1*Δ cells exhibited sensitivity to low temperature, hypersensitivity to a proteasome inhibitor tosylsulfonyl phenylalanyl chloromethyl ketone (TPCK), and resistance to microtubules depolymerizing drug Thiabendazole (TBZ) [80,82]. To analyze if these phenotypes are related to septins, wild-type, *spn2*Δ, *moe1*Δ, and *spn2*Δ*moe1*Δ cells were tested for responses to drugs or low temperature. As shown in Figure 27, all the *moe1*Δ phenotypes reported were reproduced in my hand. In contrast, *spn2*Δ showed no significant differences from wild-type cells in growth at 20 °C, and sensitivity to TPCK or TBZ. Interestingly, *spn2*Δ*moe1*Δ was not resistant to TBZ, indicating that TBZ resistance of *moe1*Δ required *spn2*$^+$. This result suggests that a genetic interaction between *spn2*$^+$ and *moe1*$^+$ lies in the context of TBZ sensitivity.

Because TBZ is a microtubules depolymerizing drug, Moe1p might function together with Spn2p to regulate microtubules organization, or might be a linking molecule between two cytoskeleton, septins and microtubules. *S. pombe* microtubules form several distinct cytoskeletal filaments[97]: In the interphase cells, 2-4 antiparallel microtubule bundles extend from interphase microtubules organizing center (MTOC) near the nucleus, along the long axis of the cell[98]. Upon entry into mitosis, intranuclear microtubules appear to control the axis of the chromosome segregation, and then spindle microtubules segregate the chromosomes[99]. Once the nuclei moves toward the cell ends at anaphase B, the spindle breaks down and microtubules appear at the middle of cell as a ring, which is termed as post-anaphase array (PAA) [100]. TBZ resistance of *moe1*Δ has been suggested to be due to the long interphase microtubules in this mutant cell although the precise mechanisms underlying this phenotype has not been known (Fig. 27B, arrowheads, [80]). Immunostaining of tubulin with TAT-1 antibody showed that length of microtubules in *spn2*Δ and *spn2*Δ*moe1*Δ was indistinguishable from those in wild-type and *moe1*Δ, respectively, suggesting that Spn2p is not required for formation of long interphase microtubules (Fig. 27B). This result also suggests that long microtubules in *moe1*Δ might not be related to its resistance to TBZ because *spn2*Δ*moe1*Δ was sensitive to TBZ despite its long interphase microtubules.

Next, I tested if Spn2p and Moe1p have any relationship with PAA. Tubulin

staining in *spn2*Δ and *moe1*Δ showed no significant defect in PAA formation, suggesting that Spn2p and Moe1p were not the upstream factors of PAA_(Fig. 27C). To address if PAA act downstream of Spn2p and Moe1p, Carbendazim (MBC) on septin ring formation were analyzed. MBC is another microtubules depolymerizing drug that is commonly used to destruct PAA[101]. As shown in Fig. 27D, septin rings were formed even in the cells with nucleus failed to enter anaphase B because of MBC treatment, suggesting that PAA was not required for septin ring formation. Taken together, PAA formation and septin ring formation were independent of each other.

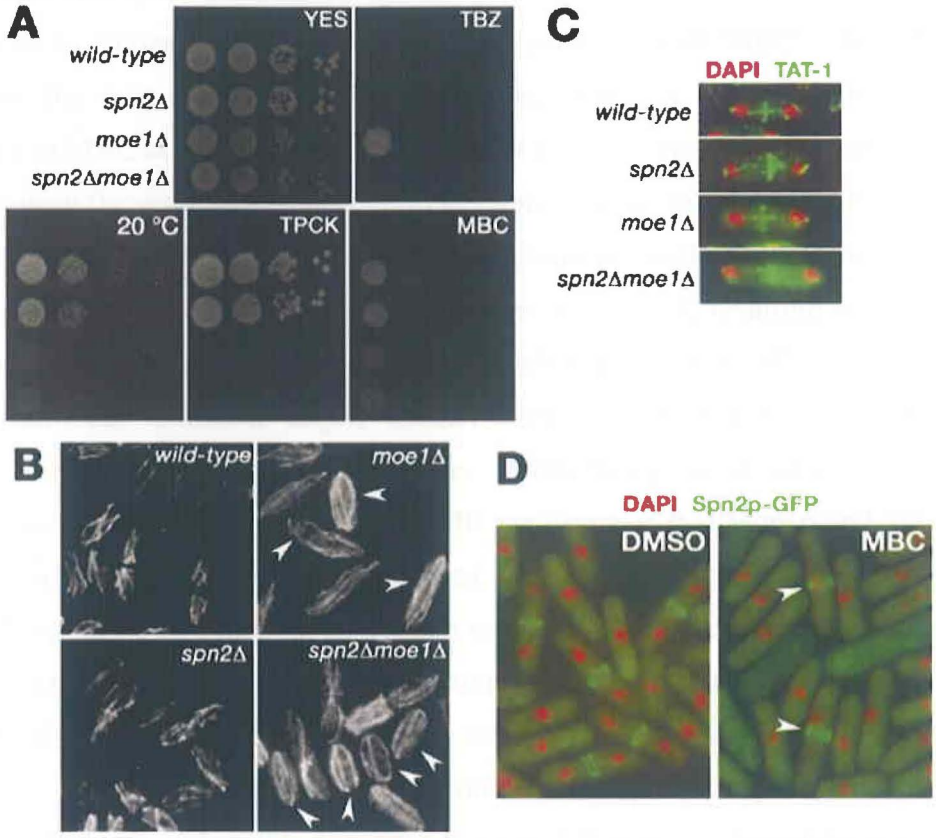

Figure 27 Genetic interaction between *moe1*$^+$ *and spn2*$^+$

(A) *moe1*Δ exhibited to TBZ in an *spn2*$^+$ dependent manner. Cells with indicated genotypes were spotted with ten-fold serial dilutions (10^4-10^1) onto YES plates and cultured for 5 days. Concentrations of drugs added were: TBZ (20 μg/ml), TPCK (120 μM), MBC (15 μg/ml). (B,C) cells with indicated genotypes were incubated overnight in YES media at 25 °C, and immunostained with TAT-1 antibody. (B) *spn2*$^+$ was not related to the long interphase microtubules in *moe1*Δ. Long and bent microtubules in *moe1*Δ or *spn2*Δ*moe1*Δ cells are indicated by the arrowheads. (C) Spn2p and Moe1p were not required for PAA formation. Strains in (A-C): JY7 (wild-type), MO665 (*spn2*Δ), MO731 (*moe1*Δ), MO730 (*spn2*Δ*moe1*Δ). (D) PAA was not required for septin ring formation. Strain MO701 (*spn2*$^+$*-GFP*) was precultured overnight in YES media, and 25 μg/ml or control DMSO were added. After incubation for 120 min., cells were fixed and stained with DAPI.

Septins and Moe1p are require for efficient polarity establishment

There was an intriguing observation in the experiment with MBC. Both TBZ and MBC are the microtubules destabilizing drugs, although, *moe1*Δ cells showed no resistance to MBC at all (Fig. 27A). This result suggests that TBZ resistance of *moe1*Δ may not mean the resistance to the depolymerization of microtubules. Recently, Sawin and Snaith reported that TBZ but not MBC caused transient depolarization of the cortical actin cytoskeleton and a cell-end marker Ral3p-GFP, resulting in high-level of branching in *cdc10-129* mutant[102]. This result suggests that TBZ is likely to effect on an additional unknown target, distinct from tubulin, which is responsible for establishment of cell polarity in *S. pombe*. From this point of view, my result that *moe1*Δ was resistant to TBZ but not to MBC may suggest that Moe1p and Spn2p were involved in polarity establishment. During G1 phase after cell separation, *S. pombe* cells usually grows in a monopolar manner to the end of the parental cell. After entry into G2 phase, these cells exhibit a transition in cell polarization known as New End Take-Off (NETO), in which monopolar cells initiate bipolar growth (reviewed in [103,104]). Dynamic microtubules contribute to this process by depositing cell end proteins, which are responsible for accumulation of F-actin patches at the growth zone. To address if *moe1*Δ and *spn2*Δ affected polarized growth, Rhodamine-Phalloidine staining and Calcofluor staining were carried out to visualize F-actin polarity and growing end, respectively. As shown in Figure 28A, *moe1*Δ and *spn2*Δ cells exhibited higher percentages of cells with monopolar F-actin distribution compared to the wild-type cells, suggesting the inefficient NETO or elongated G1 phase. Calcofluor staining of these cells confimed that they did grow in a monopolar manner even in the septated cells (i.e. cells underwent mitosis) (Fig. 29), suggesting that monopolar F-actin distribution was indeed due to NETO defect but not to long G1 phase. These phenotypes were also observed in other vegetative septin mutants (Fig. 29). When these cells were treated with TBZ, wild-type and *spn2*Δ cells exhibited higher percentages of cells with monopolar F-actin distribution (Fig. 28B). In contrast, *moe1*Δ did not exhibit elevated monopolar F-actin distribution in response to TBZ, which was consistent with the result that *moe1*Δ cells grew on the TBZ plate (Fig. 28B). Taken together, both *moe1*Δ and *spn2*Δ exhibited monopolar growth, and *moe1*Δ was resistant to the TBZ mediated polarity destruction, for which Spn2p was required.

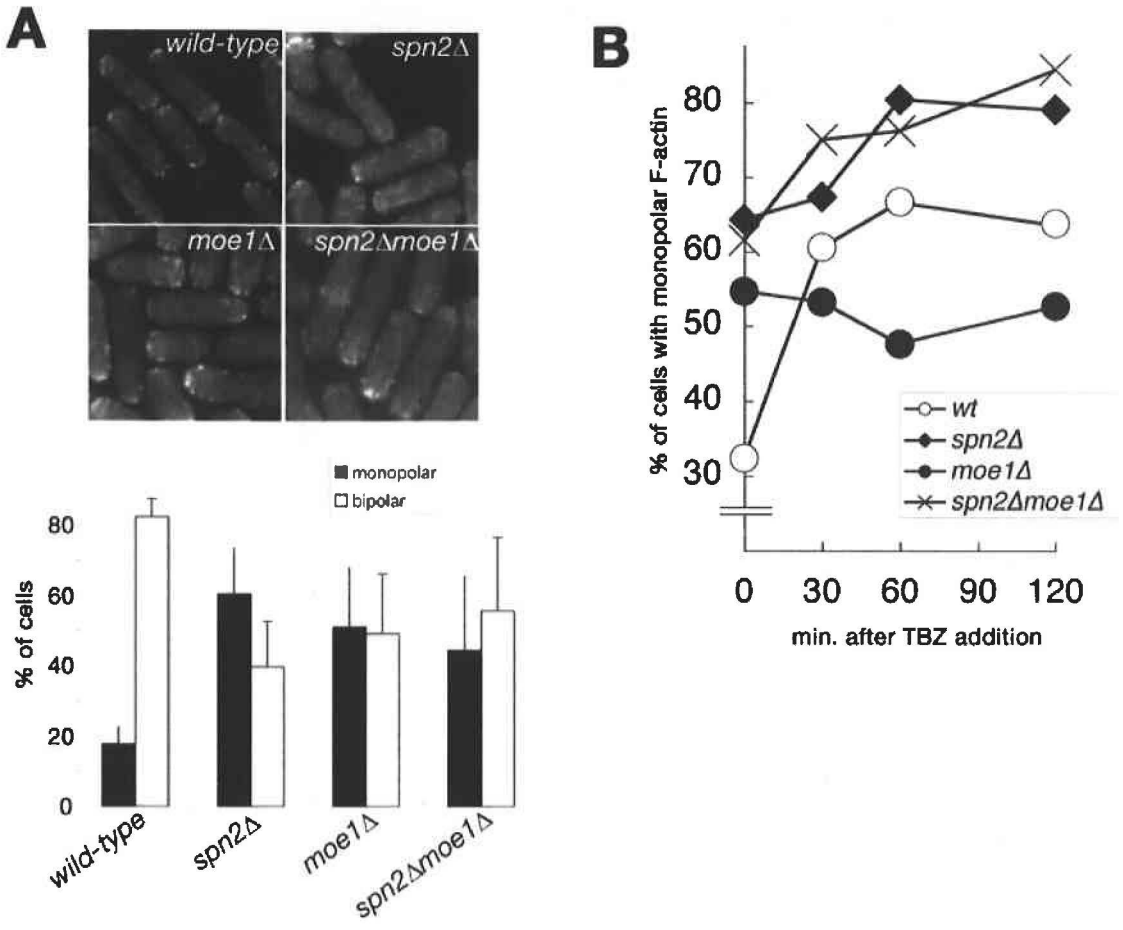

Figure 28 Spn2p and Moe1p were required for establishment of F-actin polarity

(A) monopolar F-acting distribution in *spn2*Δ and *moe1*Δ. Mid-log phase cultures ($0.2\text{-}0.5\text{x}10^7$) of cells with indicated genotypes were stained with Rhodamine-Phalloidine. Percentages of cells with monopolar and bipolar F-actin distributions are shown at the bottom. >200 cells were counted for each strains. (B) *moe1*Δ exhibited resistance to TBZ triggered depolarization of F-actin in an *spn2*$^+$ dependent manner. Cells with indicated genotypes were precultured overnight in YES media at 30 °C to mid-log phase ($0.2\text{-}0.5\text{x}10^7$), and 15 μg/ml were added. After further incubation for indicated times, cells were fixed and stained with Rhodamine-Phalloidine. Percentages of cells with monopolar F-actin distribution are indicated. >150 cells were counted at each time point. Strains used in (AB) were identical to those in Fig. 27A-C

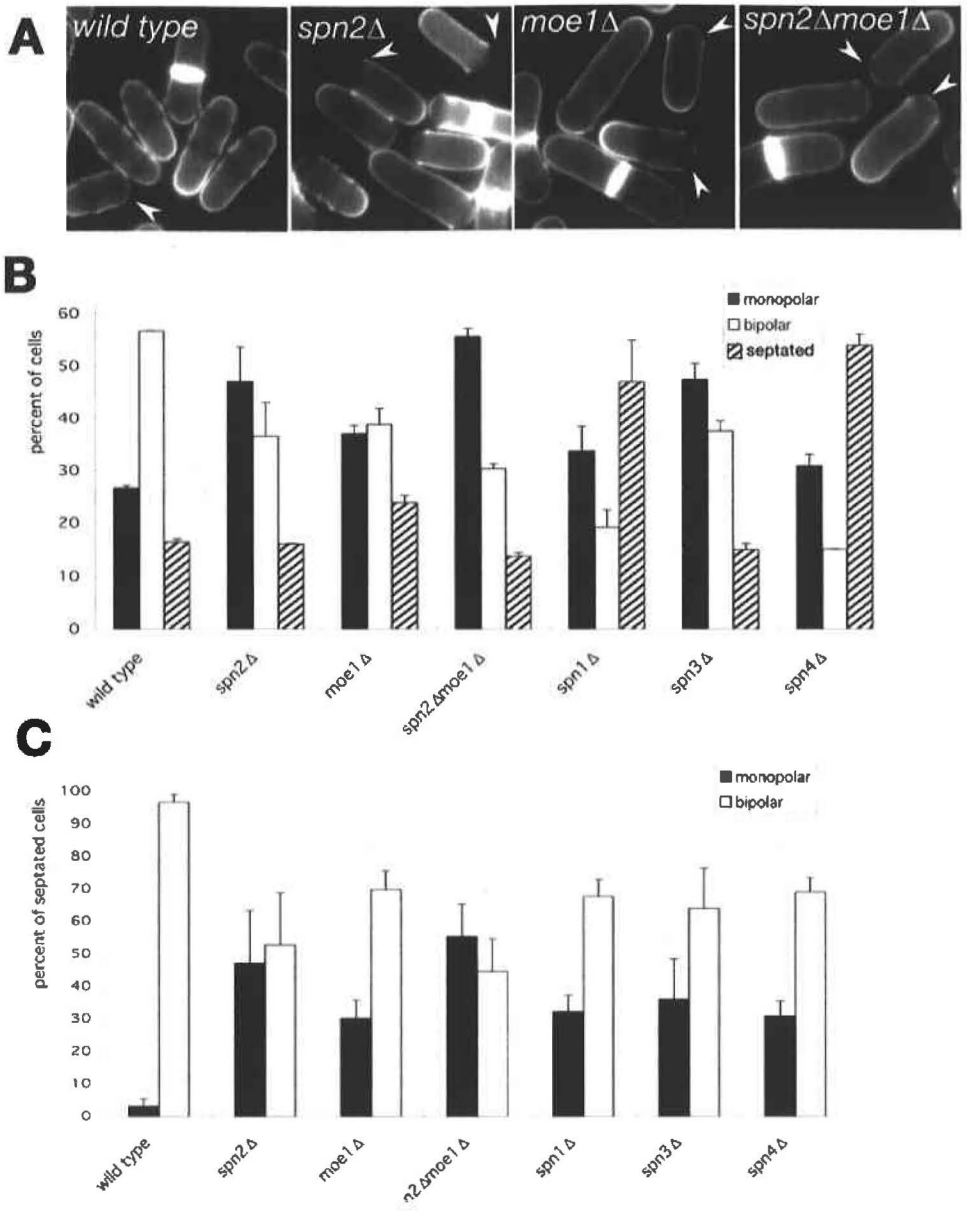

Figure 29 Spn2p and Moe1p were required for bipolar growth

(A) Calcofluor staining of indicated strains. Cells were cultured overnight in YES media at 30 °C to mid-log phase and stained with calcofluor. Examples of cells with non-growing end are indicated by arrowheads. (B) cells in (A) were classified into monopolar cells, bipolar cells, and septated cells. Note that *spn1*Δ and *spn4*Δ form multiple septa per cell in this culture condition. >200 cells were counted. (C) septated cells were further classified into monopolar and bipolar. *spn1*Δ and *spn4*Δ were counted only for cells with single septum. Strains used were identical to those in Fig. 27A-C except for MO246 (*spn1*Δ), MO371 (*spn3*Δ), and MO372 (*spn4*Δ).

DISCUSSION

In this chapter, I identified three Spn2p binding proteins and characterized one of them, Moe1p. Moe1p was detected in the cytosol throughout the vegetative growth and sporulation. No specific colocalization with septin structures was detected (Fig. 25B). Because physical interaction colocalization of Moe1p and Spn2p was detected only when both proteins were overproduced in yeast, interaction of these proteins might be temporal and highly regulated *in vivo* (Fig. 24, 25). Two previously identified Moe1p binding proteins, Scd1p and Mal3p, do not colocalize with Moe1p, and their interaction with Moe1p have not been elucidated *in vivo*[80,91]. Thus, Spn2p could be similar to these proteins.

Deletion of *moe1*$^{+}$ resulted in defective sporulation suggesting that it functions during gametogenesis (Fig. 26). The major defect of *moe1*Δ during this process lied in the meiosis. Although precise examination of this defect with diploid strain could not be carried out because *moe1*Δ cells were not able to grow in the synthetic media, major problem in these cells was likely to be due to some defect in meiosis II, a non-reductional chromosomal division equivalent to mitosis.

FSM extension occurred normally at the poles of the metaphase II nuclei in *moe1*Δ, but FSM frequently encompassed an unseparated nuclei failed to enter into anaphase II or two sister-chromatids (Fig. 26C). This result suggests that FSM extension and meiosis are not well orchestrated in *moe1*Δ cells. This phenotype does not agree with that of septin-deleted cells in which disorientated extension of FSM leaving some nuclei bare was observed, suggesting that the function of Moe1p in sporulation may be independent of septins.

To see if there is any relationship between Spn2p and Moe1p, contributions of Moe1p-associated proteins in sporulation in cooperation with septins was examined. I observed the FSM morphology of *scd1*Δ, *mal3*Δ, and *int6*Δ. Scd1p (also known as Ral1p) is a guanine-nucleotide exchanging factor (GEF) for Cdc42p, and its activity is regulated by Ras1p[105]. *scd1*$^{+}$/*ral1*$^{+}$ was originally identified by the search for mutant showing the phenotype similar to *ras1*Δ cells exhibiting round cell shape and defective conjugation (*ras*-like) [106]. *scd1*Δ as well as other *ral* deletants (*ral2*Δ, *ral3*Δ) formed healthy spores with wild-type morphology when defects in conjugation

were bypassed by the spheroplast fusion, indicating that these genes were dispensable for sporualtion (data not shown). Deletion of *mal3*$^{+}$, a gene that linked between Moe1p and microtubules (see **INTORDUCTIONS**) did not show drastic phenotype in sporulation, although a very limited member of the cells showed abnormal meiosis (data not shown). In contrast, *int6*Δ cells exhibited the defects essentially same to *moe1*Δ in sporulation, suggesting that major function of Moe1p during sporulation lies in the context analogous to the function of Moe1p/Int6p complex during vegetative growth (datat not shown). It is possible that Moe1p/Int6p controls degradation of cell cycle molecules required for proper meiosis. In any cases, relationship between sepntins and Moe1p or Int6p in FSM formation could not be determined in this study because of the predominant defect in meiosis. Dissection of Moe1p into septin-related function and others are required for further investigation.

To substantiate the relationship between Moe1p and Spn2p, I tried to narrow the binding region of Moe1p and Spn2p to each other by biochemical assay, and found that 210-343 aa of Moe1p was sufficient and 183-225 aa of Spn2p was required for interaction (data not shown). Based on the results, I am now trying to abolish the interaction by inducing several point mutations. However, I have not ontained such a mutation so far.

Taken together, I have not reached the conclusion that Moe1p is involved in the FSM formation. The result appears to be rather negative. The relationship between Moe1p and Spn2p was suggested in vegetative cells (discussed below). It is possible that the association of Moe1p and Spn2p is important only in the vegetative cells. For the yeast two-hybrid screen performed in this study, I produced a prey library using the cells cultured under the nitrogen starvation condition, but this might not have eliminated the mRNA functioning in the vegetative cells. Another problem of the screen might have been the use of Spn2p as a bait because it is involved in both vegetative and sporulation procedures. It might have been necessary to try hard to utilize other sporulation septins as baits, although it was not successful in this study. I am now thinking of other method to elucidate the role of septins in sporulation as well as to study the interaction of Moe1p and Spn2p in more detail.

There was an unexpected finding suggesting that Moe1p and Spn2p function together in vegetative cells, during the search for genetic interaction of them.

Although the relationship between this finding and sporulation has not been elucidated, I spare this paragraph for the discussion. During vegetative growth, both *moe1*Δ and *spn2*Δ strains exhibited in growth polarity establishment (Fig. 28, 29). Consistently, *moe1*Δ cells were resistant to TBZ mediated depolarization of F-actin, whereas *moe1*Δ*spn2*Δ cells were hypersensitive to TBZ. This result suggests that Spn2p and Moe1p function in series or in parallel to regulate the cell polarity. Establishment of growth polarity in *S. pombe* is known as transition of monoplar to bipolar growth, named new end take-off (NETO) [103,104]. In brief, microtubules plus end proteins (+TIPs) were transported and deposited to the ends, which subsequently recruits cell end proteins (end markers) to trigger the formation of F-actin patches and cables. Although relationship between septins or Moe1p and NETO have not been investigated to date, it have been reported that many of end markers, Mod5p, Tea3p, For3p, and Pom1p, localize to septum[107-110]. Therefore, it is likely that septins are involved in NETO processes. Moe1p might contribute this process by proteolysis or mRNA translation. An interesting report to be noted is that a deletion mutant of a gene encoding Ras1 GEF, *efc25*Δ, exhibited synthetic growth phenotype with *moe1*Δ, as well as with *tea1*Δ [111]. Tea1p is one of the +TIPs playing key role in NETO. Thus, Moe1p may be functionally related to Tea1p-mediated F-actin polarization. Downstream pathway of Efc25p consists of Ras1p, Scd1p, and Cdc42p (and its effectors), and lack of each of them results in loss of cell polarity with round morphology. As described above, Scd1p is a Moe1p binding protein [80]. In addition, Scd1p and Cdc42p localize at the septum[112]. It is interesting to speculate that Moe1p and septins are related to this pathway to coordinate the signals from environment and the cell morphology.

CHAPTER V: TOTAL DISCUSSION

The goal of my work was to elucidate the mechanism how biological membranes properly obtain their shapes. To approach this aim, I used the FSM formation of the fission yeast *S. pombe* as a model for de novo synthesis of the organelle membrane within a cell. The FSM formation is an intriguing biological process that membrane structures newly assembled in the cell develop to form the even-sized spherical membranes. There may be many steps to be strictly regulated to accomplish the FSM formation,: assembly of the FSM precursor, extension to the proper direction, and the closure of the leading edges. Each of these steps must be orchestrated with the meiosis in order to form gametes appropriately harboring the haploid nuclei. At the early stages of the study, I investigated the role of a PtdIns 3-kinase Pik3p, since this protein played multiple roles during FSM formation. Analysis of Pik3p provided me with several significant information about the mechanisms how FSMs were assembled. However, there was an important problem: How FSMs extend to form a sac? My following studies revealed contribution of septins to FSM extension, which shed light on this problem.

Septins are the eukaryotic proteins forming the heteroorigomeric complex that polymerize to form a filament, thus they are considered to form a novel class of cytoskeletal protein. Virtually, septin filaments have the nature to function in a membrane-associated manner, implying that they might play some role in the FSM formation of *S. pombe*.

In this study, I found that four out of seven septins were involved in sporulation. These septins localized at the equatorial planes of the extending FSMs that finally became rings with even sizes. Lack of even the one of the four septin genes caused the formation of the incomplete tetrad, suggesting that they did play important roles during sporulation. This result was different from the case with *S. cerevisiae,* whose sporulation was not affected by the deletion of the septins . Precise examination of the FSM morphology revealed that FSMs frequently extended to the wrong direction at the early stage in septin-deleted cells. Because I did not detect any defect in the later stage of the FSM extension and maturation of the spores, I concluded that role of septins in FSM formation was largely limited to enhance the- fidelity of extension in an orientated manner at the early stage of the extension. However, it is

also possible that septins play some additional roles in the FSM formation (discussed below), those I could not detect in this study.

I also demonstrated that two septins bound to phosphoinositides *in vitro*, and that mutations in phosphoinositide-binding region of Spn2p reduced its ability to associate with the FSM. Because PtdIns(4)P was enriched on the FSM, I proposed that this lipid glued the septin structure and the FSM to extend in a cooperated manner. Between two class III PtdIns 4-kinses in *S. pombe*, contribution of Pik1p to production of PtdIns(4)P on the FSM was denied in this study. The other kinase, Stt4p, has been left to be investigated.

As discussed above, I concluded that the major role of septins in sporulation was to facilitate the orientated extension of the FSM at the early stage. However, there are many questions: (i) How septins form their unique structure? What regulates it? Why septins form rings after they have accomplish their role to give growth orientation of the FMS in horseshoe state? (ii) Is there any relationship between septins and other FSM components? (iii) Do septins play a role as a signaling molecule or as a scaffold for other proteins as is the cases in other organisms? Search for the septin-binding proteins was done to answer any of the questions, as described in Chapter IV. Although the studies are not fully successful, I discuss about these questions and make some proposal for the future study:

Question i)

Regulation of septin assembly could be considered based on the information of septin ring formation in the vegetative cells. During this study, I found that Spn2p-GFP did not localize at septum in the cells treated with latrunculin A (Lat A), an F-actin depolymerizing reagent, even when the cells completed the miotosis (data not shown). In agreement with this, deletion of *myp2*$^{+}$, a gene coding for the myosin II heavy chain that localize at septum in a CAR dependent manner[113], totally abolishes the localization of all the vegetative septins (J. Pringle, personal communication). These results clearly indicate that septin ring formation is dependent on F-actin in vegetative cells. During the sporulation, F-actin patches accumulate at the poles of the metaphase II or prometaphase II nuclei, and subsequently translocate around the leading edges of FSMs ([60], T. Nakamura, personal communication). These F-actin (and possibly, Myb2p) might act as a template for septins to polymerize to form filament. A

physiological experiment to monitor the septin structure in the Lat A-treated ascus would be the first step to test this possibility.

One possible reason why septins form rings after growth orientation of FSM is determined is that it is required when the stress is given, to maintain the FSM morphology. The ring-shaped septins may not be required in the usual conditions, considering that septin-deleted cells forms healthy spore once FSMs extended to proper direction. In this case, the ring is just for safety and the phenotype should be seen only when some problem happens. Lack of septins might exhibit synthetic phenotype with some mutant that has defect in the FSM formation. A screen for such a mutant with "synthetic *spo*" phenotype might be useful.

To give the definitive answer to these questions, *in vitro* system for septin assembly and polymerization is required. Ultimately, *in vitro* reconstitution of FSM formation system is a goal to know how it is regulated by septins, as well as to answer many other questions including (ii) and (iii). Although there are many difficulties, combination of *in vitro* system and *in vivo* genetic and biochemical experiments will provide a great advantage to understand the FSM formation.

Question ii)

As described before, there are two known FSM components which might affect the FSM morphology: SPBs and LEPs. Vesicles accumulate at the cytoplasmic surface of the outer plaque of the SPB assemble to form a FSM precursor. This raises the question whether or not assembly of septin complex into the filament is dependent on SPBs. A leading edge protein Meu14p is required for proper FSM morphology. Interdependence of septins and Meu14p might be a key to know how FSMs take their shape. Investigation about interplay among septins, SPBs, and a LEP is now on its way by our group.

Question iii)

In Chapter IV, I identified three candidate proteins that bind to Spn2p by the yeast two-hybrid screen and characterized one of them, Moe1p. Investigation of other two candidates, Meu4p and Plb1p, has not been done yet. Genetic and physiological experiments suggested that Moe1p and Spn2p were involved in establishment of the growth polarity in vegetative cells termed NETO (discussed in Chapter IV). *moe1*Δ exhibited severe defect in sporulation to form incomplete tetrad with aberrant morphology, which was likely to be due to the defect in meiosis II. It is interesting

that *moe1*Δ extended FSMs even when it failed to undergo meiosis II, because this result suggest that the chromosome segregation and the FSM formation were not well orchestrated in this mutant cell. Although I could not detect any functional relationship between spn2p and Moe1p during sporulation in this study, it is interesting to speculate that septins are required for the orchestrated FSM extension with meiosis. Several lines of evidence imply that the existence of the regulation mechanism that prevent cell from starting the FSM formation until the completion of meiosis II. Blanco et. al. reported that Mfr1p, an activator of anaphase promoting complex/cyclosome (APC), was not required for meiosis but for sporulation[114]. Destruction of cyclin/Cdc13p by Mfr1p-mediated ubiquitinylation might be a trigger for the spore formation. Similarly, another APC activator Fzr1p was required not for meiosis but for the FSM formation to form spores with proper morphology[115]. Interestingly, phenotypes of both *mfr1*Δ and *fsr1*Δ are similar to those of septin-deleted cells (i. e. proper meiosis and aberrant number of spores). It is interesting to speculate that the APC-triggered proteolysis pathway involves septins, which orchestrates the meiosis and the FSM formation as a "checkpoint". Moe1p might contribute to this machinery by recruiting proteasome to FSMs via interaction with septins. Based on this model, septin-deleted cells might exhibit the defect in orchestration of FSM formation and meiosis only when meiosis was inhibited by some means, i. e., only when the "checkpoint" was required.

Sporulation is an important and intriguing procedures that provides us with many hints to understand how biological membranes take their shape. However, this field of research field is still at dawn. My findings in this study propose septins as a novel component of the FSM in *S. pombe* that contribute to the FSM to take proper shape. I hope that continuation of this study will shed light on the understanding of sporulation in the future.

REFERENCES

1. Shimoda C: **Forespore membrane assembly in yeast: coordinating SPBs and membrane trafficking**. *J Cell Sci* 2004, **117**:389-396.
2. Moreno S, Klar A, Nurse P: **Molecular genetic analysis of fission yeast *Schizosaccharomyces pombe***. *Methods Enzymol* 1990, **194**:795-823.
3. Chikashige Y, Ding DQ, Funabiki H, Haraguchi T, Mashiko S, Yanagida M, Hiraoka Y: **Telomere-led premeiotic chromosome movement in fission yeast**. *Science* 1994, **264**:270-273.
4. Hirata A, Shimoda C: **Structural modification of spindle pole bodies during meiosis II is essential for the normal formation of ascospores in Schizosaccharomyces pombe: ultrastructural analysis of spo mutants**. *Yeast* 1994, **10**:173-183.
5. Hagan I, Yanagida M: **The product of the spindle formation gene sad1+ associates with the fission yeast spindle pole body and is essential for viability**. *J Cell Biol* 1995, **129**:1033-1047.
6. Schweingruber AM, Hilti N, Edenharter E, Schweingruber ME: **Methionine induces sexual development in the fission yeast Schizosaccharomyces pombe via an ste11-dependent signalling pathway**. *J Bacteriol* 1998, **180**:6338-6341.
7. Yamashita A, Yamamoto M: **[Molecular mechanisms for the regulation of meiosis in fission yeast]**. *Tanpakushitsu Kakusan Koso* 1998, **43**:314-321.
8. Watanabe Y, Shinozaki-Yabana S, Chikashige Y, Hiraoka Y, Yamamoto M: **Phosphorylation of RNA-binding protein controls cell cycle switch from mitotic to meiotic in fission yeast**. *Nature* 1997, **386**:187-190.
9. Tanaka K, Hirata A: **Ascospore development in the fission yeasts Schizosaccharomyces pombe and S. japonicus**. *J Cell Sci* 1982, **56**:263-279.
10. Ikemoto S, Nakamura T, Kubo M, Shimoda C: **S. pombe sporulation-specific coiled-coil protein Spo15p is localized to the spindle pole body and essential for its modification**. *J Cell Sci* 2000, **113 (Pt 3)**:545-554.
11. Nakamura T, Nakamura-Kubo M, Hirata A, Shimoda C: **The Schizosaccharomyces pombe spo3+ gene is required for assembly of the forespore membrane and genetically interacts with psy1(+)-encoding syntaxin-like protein**. *Mol Biol*

Cell 2001, **12**:3955-3972.

12. Nakamura T, Kashiwazaki J, Shimoda C: **A fission yeast SNAP-25 homologue, SpSec9, is essential for cytokinesis and sporulation**. *Cell Struct Funct* 2005, **30**:15-24.
13. Nakase Y, Nakamura T, Hirata A, Routt SM, Skinner HB, Bankaitis VA, Shimoda C: **The Schizosaccharomyces pombe spo20(+) gene encoding a homologue of Saccharomyces cerevisiae Sec14 plays an important role in forespore membrane formation**. *Mol Biol Cell* 2001, **12**:901-917.
14. Nakamura-Kubo M, Nakamura T, Hirata A, Shimoda C: **The fission yeast spo14+ gene encoding a functional homologue of budding yeast Sec12 is required for the development of forespore membranes**. *Mol Biol Cell* 2003, **14**:1109-1124.
15. Nakano A, Muramatsu M: **A novel GTP-binding protein, Sar1p, is involved in transport from the endoplasmic reticulum to the Golgi apparatus**. *J Cell Biol* 1989, **109**:2677-2691.
16. Barlowe C, Schekman R: **SEC12 encodes a guanine-nucleotide-exchange factor essential for transport vesicle budding from the ER**. *Nature* 1993, **365**:347-349.
17. Stock SD, Hama H, DeWald DB, Takemoto JY: **SEC14-dependent secretion in Saccharomyces cerevisiae. Nondependence on sphingolipid synthesis-coupled diacylglycerol production**. *J Biol Chem* 1999, **274**:12979-12983.
18. Onishi M, Koga T, Morita R, Nakamura Y, Nakamura T, Shimoda C, Takegawa K, Hirata A, Fukui Y: **Role of phosphatidylinositol 3-phosphate in formation of forespore membrane in Schizosaccharomyces pombe**. *Yeast* 2003, **20**:193-206.
19. Takegawa K, DeWald DB, Emr SD: **Schizosaccharomyces pombe Vps34p, a phosphatidylinositol-specific PI 3-kinase essential for normal cell growth and vacuole morphology**. *J Cell Sci* 1995, **108 (Pt 12)**:3745-3756.
20. Kimura K, Miyake S, Makuuchi M, Morita R, Usui T, Yoshida M, Horinouchi S, Fukui Y: **Phosphatidylinositol-3 kinase in fission yeast: a possible role in stress responses**. *Biosci Biotechnol Biochem* 1995, **59**:678-682.
21. Koga T, Onishi M, Nakamura Y, Hirata A, Nakamura T, Shimoda C, Iwaki T, Takegawa K, Fukui Y: **Sorting nexin homologues are targets of**

phosphatidylinositol 3-phosphate in sporulation of Schizosaccharomyces pombe. *Genes Cells* 2004, **9**:561-574.

22. Pfeffer SR: **Membrane transport: retromer to the rescue**. *Curr Biol* 2001, **11**:R109-111.
23. Katzmann DJ, Stefan CJ, Babst M, Emr SD: **Vps27 recruits ESCRT machinery to endosomes during MVB sorting**. *J Cell Biol* 2003, **162**:413-423.
24. Bilodeau PS, Winistorfer SC, Kearney WR, Robertson AD, Piper RC: **Vps27-Hse1 and ESCRT-I complexes cooperate to increase efficiency of sorting ubiquitinated proteins at the endosome**. *J Cell Biol* 2003, **163**:237-243.
25. Takegawa K, Iwaki T, Fujita Y, Morita T, Hosomi A, Tanaka N: **Vesicle-mediated protein transport pathways to the vacuole in Schizosaccharomyces pombe**. *Cell Struct Funct* 2003, **28**:399-417.
26. Moreno-Borchart AC, Strasser K, Finkbeiner MG, Shevchenko A, Knop M: **Prospore membrane formation linked to the leading edge protein (LEP) coat assembly**. *Embo J* 2001, **20**:6946-6957.
27. Okuzaki D, Satake W, Hirata A, Nojima H: **Fission yeast meu14+ is required for proper nuclear division and accurate forespore membrane formation during meiosis II**. *J Cell Sci* 2003, **116**:2721-2735.
28. Longtine MS, DeMarini DJ, Valencik ML, Al-Awar OS, Fares H, De Virgilio C, Pringle JR: **The septins: roles in cytokinesis and other processes**. *Curr Opin Cell Biol* 1996, **8**:106-119.
29. Field CM, Kellogg D: **Septins: cytoskeletal polymers or signalling GTPases?** *Trends Cell Biol* 1999, **9**:387-394.
30. Finger FP: **One ring to bind them. Septins and actin assembly**. *Dev Cell* 2002, **3**:761-763.
31. Frazier JA, Wong ML, Longtine MS, Pringle JR, Mann M, Mitchison TJ, Field C: **Polymerization of purified yeast septins: evidence that organized filament arrays may not be required for septin function**. *J Cell Biol* 1998, **143**:737-749.
32. Mino A, Tanaka K, Kamei T, Umikawa M, Fujiwara T, Takai Y: **Shs1p: a novel member of septin that interacts with spa2p, involved in polarized growth in saccharomyces cerevisiae**. *Biochem Biophys Res Commun* 1998, **251**:732-736.
33. Byers B, Goetsch L: **A highly ordered ring of membrane-associated filaments in**

budding yeast. *J Cell Biol* 1976, **69**:717-721.

34. Chant J: **Septin scaffolds and cleavage planes in Saccharomyces**. *Cell* 1996, **84**:187-190.
35. Gladfelter AS, Pringle JR, Lew DJ: **The septin cortex at the yeast mother-bud neck**. *Curr Opin Microbiol* 2001, **4**:681-689.
36. Beites CL, Xie H, Bowser R, Trimble WS: **The septin CDCrel-1 binds syntaxin and inhibits exocytosis**. *Nat Neurosci* 1999, **2**:434-439.
37. Kinoshita M, Field CM, Coughlin ML, Straight AF, Mitchison TJ: **Self- and actin-templated assembly of Mammalian septins**. *Dev Cell* 2002, **3**:791-802.
38. Kremer BE, Haystead T, Macara IG: **Mammalian septins regulate microtubule stability through interaction with the microtubule-binding protein MAP4**. *Mol Biol Cell* 2005, **16**:4648-4659.
39. Spiliotis ET, Kinoshita M, Nelson WJ: **A mitotic septin scaffold required for Mammalian chromosome congression and segregation**. *Science* 2005, **307**:1781-1785.
40. Ihara M, Kinoshita A, Yamada S, Tanaka H, Tanigaki A, Kitano A, Goto M, Okubo K, Nishiyama H, Ogawa O, et al.: **Cortical organization by the septin cytoskeleton is essential for structural and mechanical integrity of mammalian spermatozoa**. *Dev Cell* 2005, **8**:343-352.
41. Hall PA, Russell SE: **The pathobiology of the septin gene family**. *J Pathol* 2004, **204**:489-505.
42. Russell SE, Hall PA: **Do septins have a role in cancer?** *Br J Cancer* 2005, **93**:499-503.
43. De Virgilio C, DeMarini DJ, Pringle JR: **SPR28, a sixth member of the septin gene family in Saccharomyces cerevisiae that is expressed specifically in sporulating cells**. *Microbiology* 1996, **142 (Pt 10)**:2897-2905.
44. Fares H, Goetsch L, Pringle JR: **Identification of a developmentally regulated septin and involvement of the septins in spore formation in Saccharomyces cerevisiae**. *J Cell Biol* 1996, **132**:399-411.
45. Tachikawa H, Bloecher A, Tatchell K, Neiman AM: **A Gip1p-Glc7p phosphatase complex regulates septin organization and spore wall formation**. *J Cell Biol* 2001, **155**:797-808.
46. Simchen G: **Are mitotic functions required in meiosis?** *Genetics* 1974, **76**:745-

753.

47. Hertz-Fowler C, Peacock CS, Wood V, Aslett M, Kerhornou A, Mooney P, Tivey A, Berriman M, Hall N, Rutherford K, et al.: **GeneDB: a resource for prokaryotic and eukaryotic organisms**. *Nucleic Acids Res* 2004, **32**:D339-343.
48. An H, Morrell JL, Jennings JL, Link AJ, Gould KL: **Requirements of fission yeast septins for complex formation, localization, and function**. *Mol Biol Cell* 2004, **15**:5551-5564.
49. Wu JQ, Kuhn JR, Kovar DR, Pollard TD: **Spatial and temporal pathway for assembly and constriction of the contractile ring in fission yeast cytokinesis**. *Dev Cell* 2003, **5**:723-734.
50. Berlin A, Paoletti A, Chang F: **Mid2p stabilizes septin rings during cytokinesis in fission yeast**. *J Cell Biol* 2003, **160**:1083-1092.
51. Tasto JJ, Morrell JL, Gould KL: **An anillin homologue, Mid2p, acts during fission yeast cytokinesis to organize the septin ring and promote cell separation**. *J Cell Biol* 2003, **160**:1093-1103.
52. Martin-Cuadrado AB, Morrell JL, Konomi M, An H, Petit C, Osumi M, Balasubramanian M, Gould KL, Del Rey F, de Aldana CR: **Role of septins and the exocyst complex in the function of hydrolytic enzymes responsible for fission yeast cell separation**. *Mol Biol Cell* 2005, **16**:4867-4881.
53. Abe H, Shimoda C: **Autoregulated expression of Schizosaccharomyces pombe meiosis-specific transcription factor Mei4 and a genome-wide search for its target genes**. *Genetics* 2000, **154**:1497-1508.
54. Mata J, Lyne R, Burns G, Bahler J: **The transcriptional program of meiosis and sporulation in fission yeast**. *Nat Genet* 2002, **32**:143-147.
55. Kinoshita M: **Diversity of septin scaffolds**. *Curr Opin Cell Biol* 2005.
56. Kinoshita M: **Assembly of mammalian septins**. *J Biochem (Tokyo)* 2003, **134**:491-496.
57. Leupold U: **Die Vererbung von Homothallie und Heterothallie bei *Schizosaccharomyces pombe*.** *C. R. Trav. Lab. Carlsberg Ser. Physiol.* 1950, **24**:381-480.
58. Sherman F, Fink G, Hicks J: **Methods in Yeas Genetics**. In *Laboratory Course Manual*. Edited by: Cold Spring Harbor Laboratory Press; 1986.
59. Egel R, Egel-Mitani M: **Premeiotic DNA synthesis in fission yeast.** *Exp. Cell Res.*

1974, **88**:127-134.

60. Petersen J, Nielsen O, Egel R, Hagan IM: **F-actin distribution and function during sexual differentiation in Schizosaccharomyces pombe**. *J Cell Sci* 1998, **111 (Pt 7)**:867-876.
61. Petersen J, Weilguny D, Egel R, Nielsen O: **Characterization of fus1 of Schizosaccharomyces pombe: a developmentally controlled function needed for conjugation**. *Mol Cell Biol* 1995, **15**:3697-3707.
62. Kurahashi H, Imai Y, Yamamoto M: **Tropomyosin is required for the cell fusion process during conjugation in fission yeast**. *Genes Cells* 2002, **7**:375-384.
63. Bahler J, Wu JQ, Longtine MS, Shah NG, McKenzie A, 3rd, Steever AB, Wach A, Philippsen P, Pringle JR: **Heterologous modules for efficient and versatile PCR-based gene targeting in Schizosaccharomyces pombe**. *Yeast* 1998, **14**:943-951.
64. Sawano A, Miyawaki A: **Directed evolution of green fluorescent protein by a new versatile PCR strategy for site-directed and semi-random mutagenesis**. *Nucleic Acids Res* 2000, **28**:E78.
65. Roy A, Levine TP: **Multiple pools of phosphatidylinositol 4-phosphate detected using the pleckstrin homology domain of Osh2p**. *J Biol Chem* 2004, **279**:44683-44689.
66. Tanaka N, Takegawa K: **Functional characterization of Gms1p/UDP-galactose transporter in Schizosaccharomyces pombe**. *Yeast* 2001, **18**:745-757.
67. Maina CV, Riggs PD, Grandea AG, 3rd, Slatko BE, Moran LS, Tagliamonte JA, McReynolds LA, Guan CD: **An Escherichia coli vector to express and purify foreign proteins by fusion to and separation from maltose-binding protein**. *Gene* 1988, **74**:365-373.
68. Casamayor A, Snyder M: **Molecular dissection of a yeast septin: distinct domains are required for septin interaction, localization, and function**. *Mol Cell Biol* 2003, **23**:2762-2777.
69. Zhang J, Kong C, Xie H, McPherson PS, Grinstein S, Trimble WS: **Phosphatidylinositol polyphosphate binding to the mammalian septin H5 is modulated by GTP**. *Curr Biol* 1999, **9**:1458-1467.
70. Audhya A, Foti M, Emr SD: **Distinct roles for the yeast phosphatidylinositol 4-kinases, Stt4p and Pik1p, in secretion, cell growth, and organelle membrane**

dynamics. *Mol Biol Cell* 2000, **11**:2673-2689.

71. Wild AC, Yu JW, Lemmon MA, Blumer KJ: **The p21-activated protein kinase-related kinase Cla4 is a coincidence detector of signaling by Cdc42 and phosphatidylinositol 4-phosphate**. *J Biol Chem* 2004, **279**:17101-17110.
72. Hama H, Schnieders EA, Thorner J, Takemoto JY, DeWald DB: **Direct involvement of phosphatidylinositol 4-phosphate in secretion in the yeast Saccharomyces cerevisiae**. *J Biol Chem* 1999, **274**:34294-34300.
73. Audhya A, Emr SD: **Stt4 PI 4-kinase localizes to the plasma membrane and functions in the Pkc1-mediated MAP kinase cascade**. *Dev Cell* 2002, **2**:593-605.
74. Mitra P, Zhang Y, Rameh LE, Ivshina MP, McCollum D, Nunnari JJ, Hendricks GM, Kerr ML, Field SJ, Cantley LC, et al.: **A novel phosphatidylinositol(3,4,5)P3 pathway in fission yeast**. *J Cell Biol* 2004, **166**:205-211.
75. Godi A, Di Campli A, Konstantakopoulos A, Di Tullio G, Alessi DR, Kular GS, Daniele T, Marra P, Lucocq JM, De Matteis MA: **FAPPs control Golgi-to-cell-surface membrane traffic by binding to ARF and PtdIns(4)P**. *Nat Cell Biol* 2004, **6**:393-404.
76. Longtine MS, Bi E: **Regulation of septin organization and function in yeast**. *Trends Cell Biol* 2003, **13**:403-409.
77. Beites CL, Campbell KA, Trimble WS: **The septin Sept5/CDCrel-1 competes with alpha-SNAP for binding to the SNARE complex**. *Biochem J* 2005, **385**:347-353.
78. Field CM, Coughlin M, Doberstein S, Marty T, Sullivan W: **Characterization of anillin mutants reveals essential roles in septin localization and plasma membrane integrity**. *Development* 2005, **132**:2849-2860.
79. Hall PA, Todd CB, Hyland PL, McDade SS, Grabsch H, Dattani M, Hillan KJ, Russell SE: **The septin-binding protein anillin is overexpressed in diverse human tumors**. *Clin Cancer Res* 2005, **11**:6780-6786.
80. Chen CR, Li YC, Chen J, Hou MC, Papadaki P, Chang EC: **Moe1, a conserved protein in Schizosaccharomyces pombe, interacts with a Ras effector, Scd1, to affect proper spindle formation**. *Proc Natl Acad Sci U S A* 1999, **96**:517-522.
81. Yen HC, Chang EC: **Yin6, a fission yeast Int6 homolog, complexes with Moe1**

and plays a role in chromosome segregation. *Proc Natl Acad Sci U S A* 2000, **97**:14370-14375.

82. Yen HC, Gordon C, Chang EC: **Schizosaccharomyces pombe Int6 and Ras homologs regulate cell division and mitotic fidelity via the proteasome**. *Cell* 2003, **112**:207-217.
83. Watkins SJ, Norbury CJ: **Cell cycle-related variation in subcellular localization of eIF3e/INT6 in human fibroblasts**. *Cell Prolif* 2004, **37**:149-160.
84. Morris C, Jalinot P: **Silencing of human Int-6 impairs mitosis progression and inhibits cyclin B-Cdk1 activation**. *Oncogene* 2005, **24**:1203-1211.
85. Akiyoshi Y, Clayton J, Phan L, Yamamoto M, Hinnebusch AG, Watanabe Y, Asano K: **Fission yeast homolog of murine Int-6 protein, encoded by mouse mammary tumor virus integration site, is associated with the conserved core subunits of eukaryotic translation initiation factor 3**. *J Biol Chem* 2001, **276**:10056-10062.
86. Bandyopadhyay A, Lakshmanan V, Matsumoto T, Chang EC, Maitra U: **Moe1 and spInt6, the fission yeast homologues of mammalian translation initiation factor 3 subunits p66 (eIF3d) and p48 (eIF3e), respectively, are required for stable association of eIF3 subunits**. *J Biol Chem* 2002, **277**:2360-2367.
87. Dunand-Sauthier I, Walker C, Wilkinson C, Gordon C, Crane R, Norbury C, Humphrey T: **Sum1, a component of the fission yeast eIF3 translation initiation complex, is rapidly relocalized during environmental stress and interacts with components of the 26S proteasome**. *Mol Biol Cell* 2002, **13**:1626-1640.
88. Bandyopadhyay A, Matsumoto T, Maitra U: **Fission yeast Int6 is not essential for global translation initiation, but deletion of int6(+) causes hypersensitivity to caffeine and affects spore formation**. *Mol Biol Cell* 2000, **11**:4005-4018.
89. Zhou C, Arslan F, Wee S, Krishnan S, Ivanov AR, Oliva A, Leatherwood J, Wolf DA: **PCI proteins eIF3e and eIF3m define distinct translation initiation factor 3 complexes**. *BMC Biol* 2005, **3**:14.
90. von Arnim AG, Chamovitz DA: **Protein homeostasis: a degrading role for Int6/eIF3e**. *Curr Biol* 2003, **13**:R323-325.
91. Chen CR, Chen J, Chang EC: **A conserved interaction between Moe1 and Mal3 is important for proper spindle formation in Schizosaccharomyces pombe**.

Mol Biol Cell 2000, **11**:4067-4077.

92. Jenkins CC, Mata J, Crane RF, Thomas B, Akoulitchev A, Bahler J, Norbury CJ: **Activation of AP-1-dependent transcription by a truncated translation initiation factor**. *Eukaryot Cell* 2005, **4**:1840-1850.
93. Woods A, Sherwin T, Sasse R, MacRae TH, Baines AJ, Gull K: **Definition of individual components within the cytoskeleton of Trypanosoma brucei by a library of monoclonal antibodies**. *J Cell Sci* 1989, **93 (Pt 3)**:491-500.
94. Sato S, Suzuki H, Widyastuti U, Hotta Y, Tabata S: **Identification and characterization of genes induced during sexual differentiation in Schizosaccharomyces pombe**. *Curr Genet* 1994, **26**:31-37.
95. Watanabe T, Miyashita K, Saito TT, Yoneki T, Kakihara Y, Nabeshima K, Kishi YA, Shimoda C, Nojima H: **Comprehensive isolation of meiosis-specific genes identifies novel proteins and unusual non-coding transcripts in Schizosaccharomyces pombe**. *Nucleic Acids Res* 2001, **29**:2327-2337.
96. Yang P, Du H, Hoffman CS, Marcus S: **The phospholipase B homolog Plb1 is a mediator of osmotic stress response and of nutrient-dependent repression of sexual differentiation in the fission yeast Schizosaccharomyces pombe**. *Mol Genet Genomics* 2003, **269**:116-125.
97. Hagan IM, Petersen J: **The microtubule organizing centers of Schizosaccharomyces pombe**. *Curr Top Dev Biol* 2000, **49**:133-159.
98. Hagan IM: **The fission yeast microtubule cytoskeleton**. *J Cell Sci* 1998, **111 (Pt 12)**:1603-1612.
99. Zimmerman S, Daga RR, Chang F: **Intra-nuclear microtubules and a mitotic spindle orientation checkpoint**. *Nat Cell Biol* 2004, **6**:1245-1246.
100. Sato M, Toda T: **Reconstruction of microtubules; entry into interphase**. *Dev Cell* 2004, **6**:456-458.
101. Pardo M, Nurse P: **Equatorial retention of the contractile actin ring by microtubules during cytokinesis**. *Science* 2003, **300**:1569-1574.
102. Sawin KE, Snaith HA: **Role of microtubules and tea1p in establishment and maintenance of fission yeast cell polarity**. *J Cell Sci* 2004, **117**:689-700.
103. Martin SG, Chang F: **New end take off: regulating cell polarity during the fission yeast cell cycle**. *Cell Cycle* 2005, **4**:1046-1049.
104. Snaith HA, Sawin KE: **Tea for three: control of fission yeast polarity**. *Nat Cell*

Biol 2005, **7**:450-451.

105. Hughes DA: **Control of signal transduction and morphogenesis by Ras**. *Semin Cell Biol* 1995, **6**:89-94.

106. Fukui Y, Yamamoto M: **Isolation and characterization of Schizosaccharomyces pombe mutants phenotypically similar to ras1**. *Mol Gen Genet* 1988, **215**:26-31.

107. Snaith HA, Sawin KE: **Fission yeast mod5p regulates polarized growth through anchoring of tea1p at cell tips**. *Nature* 2003, **423**:647-651.

108. Arellano M, Niccoli T, Nurse P: **Tea3p is a cell end marker activating polarized growth in Schizosaccharomyces pombe**. *Curr Biol* 2002, **12**:751-756.

109. Martin SG, McDonald WH, Yates JR, 3rd, Chang F: **Tea4p links microtubule plus ends with the formin for3p in the establishment of cell polarity**. *Dev Cell* 2005, **8**:479-491.

110. Bahler J, Nurse P: **Fission yeast Pom1p kinase activity is cell cycle regulated and essential for cellular symmetry during growth and division**. *Embo J* 2001, **20**:1064-1073.

111. Papadaki P, Pizon V, Onken B, Chang EC: **Two ras pathways in fission yeast are differentially regulated by two ras guanine nucleotide exchange factors**. *Mol Cell Biol* 2002, **22**:4598-4606.

112. Hirota K, Tanaka K, Ohta K, Yamamoto M: **Gef1p and Scd1p, the Two GDP-GTP exchange factors for Cdc42p, form a ring structure that shrinks during cytokinesis in Schizosaccharomyces pombe**. *Mol Biol Cell* 2003, **14**:3617-3627.

113. Bezanilla M, Wilson JM, Pollard TD: **Fission yeast myosin-II isoforms assemble into contractile rings at distinct times during mitosis**. *Curr Biol* 2000, **10**:397-400.

114. Blanco MA, Pelloquin L, Moreno S: **Fission yeast mfr1 activates APC and coordinates meiotic nuclear division with sporulation**. *J Cell Sci* 2001, **114**:2135-2143.

115. Asakawa H, Kitamura K, Shimoda C: **A novel Cdc20-related WD-repeat protein, Fzr1, is required for spore formation in Schizosaccharomyces pombe**. *Mol Genet Genomics* 2001, **265**:424-435.

Acknowledgment

I would like to present my greatest appreciation to my supervisor, Prof. Dr. Yasuhisa Fukui for his advices and encouragements to me. I would like to appreciate Dr. Hiroyuki Tachikawa, Dr. Sayoko Ihara, and all the member of my laboratory for their precise advices and fruitful discussions.

I would like to thank Dr. J. Bähler (Sanger Centre, U.K.), Dr. Y. Watanabe (The University of Tokyo, Japan), and Dr. T. Levine (University College London, U.K.), Dr. T. Yoko-o (National Institute of Advanced Industrial Science and Technology, Japan) for supplying me with resources, Dr. Aiko Hirata (Universtiy of Tokyo, Japan) for helping me with electron micrographic analysis, and Dr. J. Pringle (Stanford University, California), Dr. K. Takegawa (Kagawa University, Japan), and Dr. T. Nakamura (Osaka City University) for helpful discussions.